

Electrochemical Energy Conversion
Using
Metal hydrides Hydrogen
Storage Materials

By

Ncumisa Prudence Jonas



UNIVERSITY *of the*
WESTERN CAPE

Submitted in fulfillment of the requirements for the degree of MSc in Chemistry in the
Department of Chemistry, University of the Western Cape

Supervisor:

Dr L. Khotseng

Co-supervisor:

Dr M. Lototskyy

November 2010

DECLARATION BY CANDIDATE

I declare that *Electrochemical Energy Conversion Using Metal Hydrides Hydrogen Storage Materials* is my own work, that it has not been submitted before for any degree or examination in any other university, that all the sources I have quoted have been indicated and acknowledged as complete references.



Ncumisa Prudence Jonas

November 2010

Signed:

ACKNOWLEDGEMENTS

First and foremost I would love to thank God Almighty for blessing and keeping me till this far.

Would love to thank my mother Nokwakha Gloria Jonas, for her love, support, and patience. For always letting me live my life to the fullest, being my source of inspiration and strength. Teaching me humility, humbleness and to always put God first in everything I do.

My sincere appreciation goes to Prof V. Linkov for forwarding me the opportunity to be a student at South African Institute of Advanced Material Chemistry (SAIAMC) and for funding, would also love to thank NRF, and ESKOM for their financial support.

To my supervisor Dr L. Khotseng, I would like to express my sincere gratitude for your constant guidance, patience, and encouragement, which contributed to the fulfillment of this work. Would also love to thank my Co-supervisor Dr M. Lototskyy and mentor Dr M. Williams, this work would have not been a success without your input and invaluable instructions.

I would love to thank SAIAMC lab technician Mr Stanford Schidziva, for going an extra mile to help me finish my project and assistance with the operation of lab instruments.

To my friends Nylon 6.6, thank you for your support and always putting a smile on my face. To my colleagues at SAIAMC, would also love to thank you for your friendliness and support.

I would like to dedicate this study to my late father, Mr. Babini Jonas (will always love you dad)

ABSTRACT

Metal hydrides hydrogen storage materials have the ability to reversibly absorb and release large amounts of hydrogen at low temperature and pressure. In this study, metal hydride materials employed as negative electrodes in Ni-MH batteries are investigated.

Attention is on AB₅ alloys due to their intermediate thermodynamic properties. However, AB₅ alloys have a tendency of forming oxide film on their surface which inhibits hydrogen dissociation and penetration into interstitial sites leading to reduced capacity. To redeem this, the materials were micro-encapsulated by electroless deposition with immersion in Pd and Pt baths. PGMs were found to increase activation, electrochemical activity and H₂ sorption kinetics of the MH alloys. Between the two catalysts the one which displayed better performance was chosen.

The materials were characterized by X-ray diffractometry, and the alloys presented hexagonal CaCu₅-type structure of symmetry P6/mmm. No extra phases were found, all the modified electrodes displayed the same behavior as the parent material. No shift or change in peaks which corresponded to Pd or Pt were observed.

Scanning Electron Microscopy showed surface morphology of the materials modified with Pd and Pt particles, the effect of using different reducing agents (*i.e.*, N₂H₄ and NaH₂PO₂), and alloys functionalized with γ -aminopropyltriethoxysilane solution prior to Pd deposition. From all the surface modified alloys, Pt and Pd particles were observed on the surface of the AB₅ alloys. Surface modification without pre-functionalization had non-uniform coatings, but the pre-functionalized exhibited more uniform coatings.

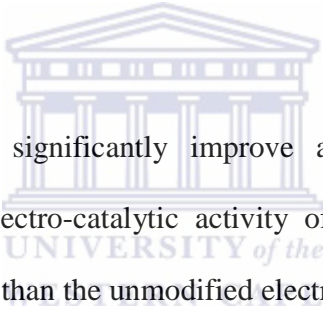
Energy dispersive X-ray Spectroscopy and Atomic Absorption Spectroscopy determined loading of the Pt and Pd on the surface of all the alloys, and the results were as follows: EDS (Pt 13.41 and Pd 31.08wt%), AAS (Pt 0.11 and Pd 0.78wt%). Checking effect of using different reducing agents N_2H_4 and NaH_2PO_2 for electroless Pd plating the results were as follows: EDS ($\text{AB}_5\text{-N}_2\text{H}_4\text{-Pd}$ - 7.57 and $\text{AB}_5\text{-NaH}_2\text{PO}_2\text{-Pd}$ - 31.08wt%), AAS ($\text{AB}_5\text{-N}_2\text{H}_4\text{-Pd}$ - 11.27 and $\text{AB}_5\text{-NaH}_2\text{PO}_2\text{-Pd}$ - 0.78wt%). For the AB_5 alloys pre-functionalized with γ -APTES, the results were: EDS (10.24wt%) and AAS (0.34wt%).

Electrochemical characterization was carried out by charge/discharge cycling controlled via potential to test the AB_5 alloy. Overpotential for unmodified, Pt and Pd modified electrodes were -1.1V, -1.24V, and -1.60V, respectively. Both modified electrodes showed discharge overpotentials at lower values implying higher specific power for the battery in comparison with the unmodified electrodes. However, Pd electrode exhibited higher specific power than Pt. To check the effect of the reducing agent the results were as follows: $\text{AB}_5\text{-N}_2\text{H}_4\text{-Pd}$ (0.4V) and $\text{AB}_5\text{-NaH}_2\text{PO}_2\text{-Pd}$ (-0.2V), sodium hypophosphite based alloy showing lower overpotential values, implying it had higher specific power than hydrazine based bath. Alloy pre-functionalized with γ -APTES, the overpotential was (0.28V), which was higher than -0.2V of the alloy without pre-functionalization, which means pre-functionalization with γ -APTES did not improve the performance of the alloy electrode.

Polarization resistance of the electrodes was investigated with Electrochemical Impedance Spectroscopy. The unmodified alloy showed high resistance of 21.6884Ω while, both Pt and Pd modified electrodes exhibited decrease 14.7397Ω and 12.1061Ω respectively, showing increase in charge transfer for the modified electrodes. Investigating the effect of the reducing agent, the

alloys exhibited the following results: (N_2H_4 97.8619 Ω and NaH_2PO_2 12.1061 Ω) based bath. Alloy pre-functionalized with γ -APTES displayed the resistance of 9.3128 Ω .

Cyclic Voltammetry was also used to study the electrochemical activity of the alloy electrodes. The voltammograms obtained displayed the anodic current peak at -0.64V to -0.65V for the Pt and Pd modified electrodes, respectively. Furthermore, the electrode which was not coated with Pt or Pd the current peak occurred at -0.59V. The Pd and Pt coated alloy electrodes represented lower discharge overpotentials, which are important to improve the battery performance. Similar results were also observed with alloy electrodes Pd modified using N_2H_4 (-0.64V) and NaH_2PO_2 (-0.65V). For the electrode modified with and without γ -APTES the over potentials were the same (-0.65V).



PGM deposition has shown to significantly improve activation and hydrogen sorption performance and increased the electro-catalytic activity of these alloy electrodes. Modified electrodes gave better performance than the unmodified electrodes. As a result, Pd was chosen as the better catalyst for the modification of AB_5 alloy. Based on the results, it was concluded that Pd electroless plated using NaH_2PO_2 reducing agent had better performance than electroless plating using N_2H_4 as the reducing agent. Alloy electrode pre-functionalized with γ -APTES gave inconsistent results, and this phenomenon needs to be further investigated. In conclusion, the alloy modified with Pd employing NaH_2PO_2 based electroless plating bath exhibited consistent results, and was found to be suitable candidate for use in Ni-MH batteries.

Table of Contents

Table of Contents

Acknowledgements

Abstract

Table of contents

List of Figures

List of Tables

Appendix

Chapter 1



Chapter 1: Introduction and Objectives of the Study	1
1.1 Background to Hydrogen Storage	1-3
1.2 Batteries	3-4
1.2.1 Rechargeable/Secondary Batteries	4-6
1.3 Motivation of the Study	7-8
1.4 Objectives of the Study	8
1.5 Research Framework and Design	9
1.6 Research Outline	9-10

Table of Contents

Chapter 2

2. Literature Review: *Electrochemical Energy Conversion Using Metal Hydrides Hydrogen Storage Material*

2.1 Introduction	11-12
2.2 Compressed Hydrogen Gas	12-13
2.3 Liquid Hydrogen	13-14
2.4 Solid State Hydrogen Storage	14-15
2.4.1 Carbon Type Material for Hydrogen Storage	16-17
2.4.2 Metal Hydrides	17-19
2.5 Classification of Hydrides	19
2.5.1 Covalent Hydrides	19-20
2.5.2 Ionic Hydrides	21
2.5.3 Interstitial Hydrides	22
2.5.3.1 Metal Alloy Hydrides	22
2.5.3.2 Metal Hydrides Intermetallic Compounds	23
2.6 Hydrogen Absorption Mechanism	24
2.7 Hydrogen Implantation in Metals	25



Table of Contents

2.7.1 Gas phase Charging	25-27
2.7.2 Electrochemical Charging	27-29
2.8 Nickel Metal Hydride Batteries (Ni-MH)	29-30
2.8.1 How Ni-MH Battery Works	31-34
2.8.2 Requirements of Metal Hydrides used in the Ni-MH Battery Industry	34-35
2.9 Intermetallic Compounds	35-36
2.9.1 AB Type Alloys	37
2.9.2 A ₂ B Type Alloys	37
2.9.3 AB ₂ Type Alloy	38-39
2.9.4 AB ₅ Type Alloy	40-43
2.9.4.1 Structure of the AB ₅ Alloy	43-45
2.9.4.2 Surface Modification of AB ₅ Alloy	46-48
2.9.5 Effect of Catalyst Deposition	49-50
2.9.6 Deposition Methods	51-54
2.9.7 Functionalization of the AB ₅ Metal Hydride Surface	54-55
2.10 Conclusion of Literature Review	55-56



Table of Contents

Chapter 3

3.1 Introduction	57
3.2 Materials and Methods	58
3.2.1 Materials	58
3.2.2 Methods	59-61
3.3 Instruments and Techniques used in the characterization of AB ₅ MH H ₂ storage alloy	61
3.3.1 X-Ray Diffractometry (XRD)	62-65
3.3.2 Scanning Electron Microscopy (SEM)	66-67
3.3.3 Energy Dispersive X-Ray Spectroscopy (EDS)	68-69
3.3.4 Atomic Absorption Spectrometry (AAS)	69-72
3.4 Electrochemical Characterization Techniques of MH alloys	73
3.4.1 Preparation of Metal Hydride Electrodes	73
3.4.2 Voltammetry	73-74
3.4.2.1 Cyclic Voltammetry	74-75
3.4.2.2 Galvanostatic Charging/Discharging	76-77
3.4.2.3 Electrochemical Impedance Spectroscopy (EIS)	77-81
3.5 Conclusion of Chapter Three	81

Table of Contents

Chapter 4

4.1 Results and Discussion	82
4.1.1 Structural Characterization of AB ₅ type alloy surface modified with Pt and Pd catalysts	82-84
4.1.2 Morphological Studies of AB ₅ MH alloy surface modified with Pt and Pd catalysts	85-86
4.1.3 Elemental Composition of AB ₅ MH alloy surface modified with Pt and Pd catalysts	86-88
4.1.4 Atomic Absorption Spectrometry Characterization of AB ₅ type alloy surface modified with Pt and Pd catalyst	88-89
4.2 Electrochemical Characterization of AB ₅ MH alloy surface modified with Pt and Pd catalyst	89
4.2.1 Galvanostatic Charge/Discharge Capacities of AB ₅ MH electrodes surface modified with Pt and Pd catalyst	90-93
4.2.2 Cyclic Voltammetry Characterization of AB ₅ type alloy surface modified with Pt and Pd catalyst	94-95
4.2.3 Impedance Characterization of AB ₅ type alloy surface modified with Pt and Pd catalyst	96-97
4.3 Summary of AB ₅ MH alloy immersed in Pt and Pd electroless plating bath derived from NaH ₂ PO ₂ reducing agent	98

Table of Contents

4.4 Effect of different reducing agents used for electroless Pd plating on the AB ₅ MH surface	99
4.4.1 Investigation of the AB ₅ _Pd Microstructure electroless plated with NaH ₂ PO ₂ plating bath	99-100
4.4.2 Determination of Pd deposits on AB ₅ MH alloy using different reducing agents	100-102
4.4.3 Total determination of Pd particles on the surface of the AB ₅ MH alloy employing AAS	102-103
4.4.4 Surface Morphological Studies of the AB ₅ MH Alloy Immersed in Pd Electroless Plating Bath Derived from N ₂ H ₄ and NaH ₂ PO ₂ Reducing Agents	103-105
4.4.5 Galvanostatic Charge/Discharge Cycles of the AB ₅ MH Alloy Immersed in Electroless Pd Plating Bath Derived from N ₂ H ₄ and NaH ₂ PO ₂ Reducing Agents	106
4.4.6 Electrochemical Activity of the AB ₅ Type Alloy Immersed in Pd Electroless Plating Derived from N ₂ H ₄ and NaH ₂ PO ₂ Based Bath	106-107
4.4.7 Impedance Analysis of AB ₅ Type Alloy Immersed in Pd Electroless Plating Bath Derived from N ₂ H ₄ and NaH ₂ PO ₂ Based Bath	108-110
4.5 Summary of Effect of Reducing Agents Used for Electroless Pd Plating on the AB ₅ MH Surface	110
4.6 Surface Functionalization in Pd Electroless Plating on AB ₅ MH Alloy using Aminosilane	111

Table of Contents

4.6.1 Structural Characterization of γ -APTES Treated AB ₅ MH Alloy	112
4.6.2 Determination of Pd Content on the AB ₅ Alloy Functionalized with γ -APTES	113-114
4.6.3 Total Determination of Pd Content on the Surface Modified AB ₅ MH Alloy Functionalized with γ -APTES Using AAS	114
4.6.4 Surface Morphologies of AB ₅ MH Alloy Functionalized with γ -APTES	115
4.6.5 Electrochemical characterization of AB ₅ MH alloy functionalized with γ -APTES using Galvanostatic charging/discharging cycles	116
4.6.6 Cyclic Voltammetry Characterization of AB ₅ _NaH ₂ PO ₂ _Pd Electrode Functionalized with γ -APTES	117
4.6.7 Impedance Characterization of AB ₅ MH Electrode Functionalized with γ -APTES	118
4.7 Summary of AB ₅ MH Alloy Functionalized with Aminosilane	119

Chapter 5

5.1 Conclusions and Recommendations	120
5.1.1 Conclusions	120-125
5.2 Recommendations	125-126

Table of Contents

Chapter 6

6.Bibliography **127-135**

Appendix **136-137**



List of Figures	Page
Figure 1.1: Hydrogen as an energy carrier linking multiple H ₂ production methods, through storage and various end users. Shaded production routes can involve substantial carbon dioxide (by-product) generation	3
Figure 1.2: Typical Diagram of Rechargeable Battery	5
Figure 2.1: Hydrogen Cycle	12
Figure 2.2: Hydrogen as Compressed Gas	13
Figure 2.3: Hydrogen as Cryogenic Liquid	14
Figure 2.4: Family Tree of hydriding alloys and complexes	15
Figure 2.5: Different types of carbon nanotubes	17
Figure 2.6: Gravimetric and Volumetric densities of various H ₂ storage options(including the weight and volume of storage tanks	18
Figure 2.7: Metal Hydrogen Interaction	24
Figure 2.8: Pressure composition isotherm for H ₂ absorption in a typical intermetallic compound on the left hand side. The solution (α -phase), the hydride phase (β -phase) and the region of coexistence of the two phases are shown. The coexistence region is characterized by the flat plateau and ends at the critical temperature T_c . The construction of the Van't Hoff plots is shown on the right hand side. The slope of the line is equal to the entropy of formation divided by the gas constants	26
Figure 2.9: Schematic representation of Ni-MH Battery cell	31
Figure 2.10: Periodic Table	35
Figure 2.11: Phase diagrams of Ti-Mn (a) and La-Ni (b) systems	39
Figure 2.12: Structure of RNi ₅ H ₆ hydride	43

Figure 2.13: Schematic process for catalyst-enhanced hydrogen storage. (OO) H ₂ ; (O) H; catalyst; HS H ₂ storage material	49
Figure 3.1: Schematic of an X-Ray Diffractometer	62
Figure 3.2: Geometrical representation of Bragg's Law	64
Figure 3.3: Basic Schematic of SEM	66
Figure 3.4: Schematic representation of an Energy Dispersive spectrometer	68
Figure 3.5: Energy diagram of an atom showing excitation to the first excited state, followed by relaxation to the ground state by the emission of an electron magnetic wave	70
Figure 3.6: Basic schematic for a typical Atomic Absorption Spectroscopy	71
Figure 3.7: Simplified block diagram of chronopotentiometric measurement device. The working, counter, and reference electrodes are denoted WE, CE, and RE, respectively	76
Figure 4.1: XRD spectrum of AB ₅ unmodified alloy	83
Figure 4.2: Diffractograms of a) unmodified, b) Pt modified and c) Pd modified AB ₅ type MH	84
Figure 4.3: SEM images of a) unmodified, b) Pt modified, and c) Pd modified AB ₅ alloy	85
Figure 4.4 a): EDS spectrum of Pd modified AB ₅ alloy	87
Figure 4.4 b): EDS spectrum of Pt modified AB ₅ alloy	87

Figure 4.5 AAS graphs of a) Pd modified and b) Pt modified AB ₅ alloys	88
Figure 4.6 a): a) Charge and b) Discharge curve of unmodified AB ₅ from the first to the sixth cycle for activation	91
Figure 4.6 b): 10 th cycle a) charge for unmodified, Pt modified and Pd modified AB ₅ alloys and b) discharge for unmodified, Pt modified and Pd modified AB ₅ alloys	92
Figure 4.7: (a – c) cyclic voltammograms for unmodified, Pt, and Pd modified AB ₅ scans from first cycle to the nth cycle, while d) shows overlay of all the cycles from the unmodified electrodes to both Pt and Pd modified	94
Figure 4.8: EIS spectra a) AB ₅ _unmodified, b) AB ₅ _Pt modified, c) AB ₅ _Pd modified	96
Figure 4.9: XRD Diffractograms of a) AB ₅ _N ₂ H ₄ _Pd and b) AB ₅ _NaH ₂ PO ₂ _Pd	100
Figure 4.10 a): EDS Spectrum of AB ₅ _N ₂ H ₄ _Pd	101
Figure 4.10 b): EDS Spectrum of AB ₅ _NaH ₂ PO ₂ _Pd	101
Figure 4.11: AAS graphs a) for AB ₅ _N ₂ H ₄ _Pd and b) AB ₅ _NaH ₂ PO ₂ _Pd	102
Figure 4.12 a): SEM image of AB ₅ _Pd (N ₂ H ₄)	104
Figure 4.12 b): SEM image of AB ₅ _Pd (NaH ₂ PO ₂)	105
Figure 4.13: a) Charge of AB ₅ _N ₂ H ₄ _Pd and AB ₅ _NaH ₂ PO ₂ _Pd and b) Discharge of AB ₅ _N ₂ H ₄ _Pd and b) AB ₅ _NaH ₂ PO ₂ _Pd	106
Figure 4.14: a) AB ₅ _N ₂ H ₄ _Pd, b) AB ₅ _NaH ₂ PO ₂ _Pd electrodes, and c) Over lay of both AB ₅ _N ₂ H ₄ _Pd and AB ₅ _NaH ₂ PO ₂ _Pd electrodes	107

Figure 4.15: EIS Spectra of a) AB ₅ -N ₂ H ₄ -Pd and b) AB ₅ -NaH ₂ PO ₂ -Pd electrodes	109
Figure 4.16: XRD Diffractogram of AB ₅ -NaH ₂ PO ₂ -Pd functionalized with γ -APTES	112
Figure 4.17: EDS spectrum of AB ₅ -NaH ₂ PO ₂ -Pd functionalized with γ -APTES	113
Figure 4.18: AAS spectrum of a) AB ₅ -NaH ₂ PO ₂ -Pd without functionalization and b) AB ₅ -NaH ₂ PO ₂ -Pd functionalization with γ -APTES	114
Figure 4.19: SEM images of AB ₅ -NaH ₂ PO ₂ -Pd functionalized with γ -APTES	115
Figure 4.20: 10 th cycle for charge and discharge for AB ₅ -NaH ₂ PO ₂ -Pd without functionalization and b) AB ₅ -NaH ₂ PO ₂ -Pd functionalization with γ -APTES	116
Figure 4.21: Voltammograms of AB ₅ -NaH ₂ PO ₂ -Pd without functionalization and AB ₅ -NaH ₂ PO ₂ -Pd functionalization with γ -APTES	117
Figure 4.22: EIS image of AB ₅ -NaH ₂ PO ₂ -Pd functionalization with γ -APTES	118
 List of Tables	
Table 2.1: a) unhydrided LaNi ₅	44
b) hydrided LaNi ₅	45
Table 2.2: Properties of Reducing Agents	53-54
Table 3.1: List of materials used in the study	58
Table 3.2: Bath Composition	59-61
Table 4.1: Total amount of Pd and Pt loading on the AB ₅ MH alloy	88
Table 4.2: Total amount of Pd loading electroless plated on the surface of AB ₅ type alloy derived from N ₂ H ₄ and NaH ₂ PO ₂ baths	102
Table 4.3: EDS data for AB ₅ -NaH ₂ PO ₂ -Pd AB ₅ type alloy with and without γ -APTES pre- functionalization	114

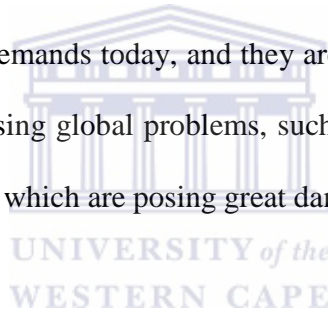
1: Chapter One

1: Chapter One

1. Introduction: *Motivation and Objectives of the study*

1.1 Background to Hydrogen Storage

The demand of energy in the world is growing as the number of the inhabitants increase. The level of life is also growing, particularly here in South Africa as a lot of industrial development is happening in urban, rural and previously disadvantaged areas. People are becoming more dependent on energy for basic needs such as hot water, lighting, heating, transport etc. Renewable energy sources such as burning wood, straw, dung and other living materials are no longer being used. Fossil fuels such as petroleum, natural gas and coal are the fuel sources which meet most of the world's energy demands today, and they are being depleted rapidly. However, their combustion products are causing global problems, such as green house effect, ozone layer depletion, acid rains and pollution, which are posing great danger for our environment.



Natural energy sources such as solar and wind power are some of the prominent renewable and carbon dioxide free energy sources and thus have attracted a lot of research interest because they are expected to resolve the shortage of fossil fuels and environmental issues related to the global warming caused by carbon dioxide[1]. However, it is necessary to have a high capacity energy storage system for their practical application, because these natural energy sources lack the power generation stability such that they are sensitive to environmental conditions such as the weather and geography [2].

Nuclear energy is also another alternative to fossil fuels. However, uranium is used as fuel and its disposal as waste is very difficult because of its high radioactivity. Thus, the waste must be

1: Chapter One

isolated for thousands of years so that uranium radioactivity can die down and not be harmful to people and the environment. It can also cause cancer, radiation damages, mutation or eventually death [3].

One of the solutions to all these problems stated above would be replacing the existing fossil fuel system with the hydrogen energy system. **Figure.1.1** illustrates the central role of H₂ as an energy carrier linking multiple H₂ production methods and various end-user applications. One of the principal attractions of H₂ as an energy carrier is obviously the diversity of production methods from a variety of resources. H₂ can be produced from coal, natural gas and other hydrocarbons by a variety of techniques, from water by electrolysis, photolytic splitting or high-temperature thermo-chemical cycles, from biomass and even municipal waste. Such a diversity of production sources contributes significantly to the energy supply. The principal drivers behind hydrogen being a sustainable energy of the future are around the need to:

1. Reduce global carbon dioxide emission and improve local air quality.
2. Ensure security of energy supply and move towards the use of sustainable local energy resources.
3. Create a new industrial and technological energy base crucial for future economic prosperity [4].

1: Chapter One

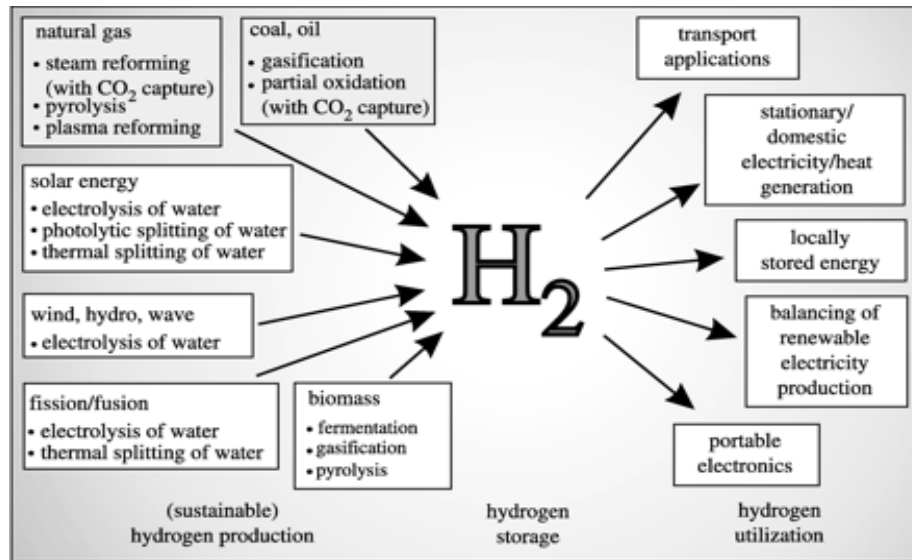


Figure 1.1: Hydrogen as an energy carrier linking multiple H_2 production methods, through storage to various end-users. Shaded production routes can involve substantial carbon dioxide (by-product) generation [4].

Hence H_2 is the most frequently discussed source, which when burnt in air produces a clean form of energy such as water. Hydrogen has attracted worldwide interest as a secondary energy carrier. This has caused many researchers to investigate about the technology of hydrogen, and how to solve the problems of production, storage and transportation. Hydrogen can be stored as gas, liquid or in form of metal hydride which can be later used as energy fuel in batteries or fuel cells. Energy storage is a very important issue that needs to be addressed in the use of fossil free fuel system, and electrochemical storage in different types of batteries is and will be an important way of intermediate storage.

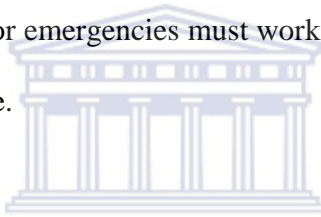
1.2 Batteries

Batteries are the most common application for storage of hydrogen, for example Ni-MH which uses metal hydrides as negative electrode in the battery cell. A battery is a device capable of converting chemical energy into electrical energy and vice versa. The chemical energy is stored

1: Chapter One

in the electro active species of the two electrodes inside the battery. The conversions occur through electrochemical reduction-oxidation (redox) or charge transfer reactions.

Batteries can be divided into primary (non-rechargeable) and secondary (rechargeable) battery systems. Primary batteries, unlike secondary batteries, their reaction cannot be reversed by running a current into the battery cell; the chemical reactants cannot be restored to their initial position and capacity. They are useful when long periods of storage are required; a primary battery can be constructed to have a lower self-discharge rate than a rechargeable battery, so all its capacity is available for useful purposes. Applications that require a small current for a long time, for example flashlight used for emergencies must work when needed, even if it has sat on a shelf for an extended period of time.



1.2.1 Rechargeable/secondary batteries

Rechargeable batteries sometimes called storage batteries or accumulators, can be used, recharged and reused. In these batteries, the chemical reaction that provides current from the battery is readily reversed when the current is supplied to the battery. They must be charged before use, they are also economical to use when their initial high cost of charging system can be spread out over many use cycles, for example in hand-held power tools, it would be very costly to replace high-capacity primary batteries every few hours of use[5].

1: Chapter One

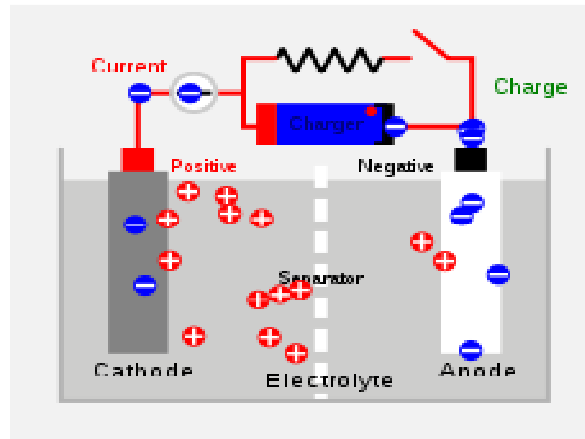


Figure 1.2: Typical Diagram of rechargeable battery [6]

From **Fig. 1.2** above, rechargeable batteries all have some common components as listed below;

Negative electrode: During discharging a reactant is oxidized and during charging a species is reduced.

Positive electrode: During discharging, a reactant is reduced and during charging a species is oxidized.

Electrolyte: Completes the circuit internally by furnishing the ions for conductance between the positive and the negative electrodes. The electrolyte can be either an alkaline solution which supplies negative ion (OH^-) or an acid solution which provides positive ions (H^+) to conduct current. Charge flows from positive to negative electrode in two manners: In an alkaline electrolyte, negative ions are created at the positive electrode and adsorbed at the negative. In an acidic electrolyte, positive ions are created at the negative electrode and absorbed at the positive. In either case, the effective flow current is the same. It is desirable to have an electrolyte with high ionic conductivity [7].

1: Chapter One

Separator: The most important function of separator is to decrease self discharge and increase current voltage efficiency. Toward that purpose, functional separators made of nonwoven fabrics or minute porous polymeric films must satisfy the following criteria: prevent any other positive or negative materials from spreading and mixing, and have a smaller contact angle with each of the electrolytes because of excellent wettability properties. Separators in most batteries are made of nonwoven fabrics that have a diameter of about 10 μ m, such as one or a combination of polyolefins, which include (PP), (HDPE), (PTFE) etc [8].

The most common application for secondary (storage) batteries is for starting, lighting, and ignition (SLI) in automobiles and engine-generator sets. In order to reach emissions reductions of 80% or more, emissions in the transport sector must be reduced by at least 25% to 75%. One of the main challenges to production of cost-effective vehicles of these kinds one needs to produce inexpensive, reliable batteries that can mimic many characteristics of internal combustion vehicles [9]. This is one of the potentially large applications of batteries.

Other secondary battery applications include uninterruptable power supplies (UPSs) for emergency and backup power, electric vehicle (traction), telecommunications, and portable tools. Secure, reliable electric power is crucial for business continuity. If the main power supply to a building or plant fails, the operator needs complete confidence in the performance and reliability of the vital emergency power system. Batteries like Ni-Cd, Ni-MH, and Li-ion rechargeable batteries are the ideal solution for power emergency, power back-up and generator starting applications.

1: Chapter One

1.3 Motivation to the study

Since the beginning of the 1990s, nickel/metal hydride (Ni-MH) batteries have been developed as a result of the demand of power sources with high energy density, high capacity, long cycle life and excellent environmental compatibility. These batteries owe this to the employment of metal hydride as a negative electrode [10, 11]. The battery's characteristic depends mainly on the physical and chemical properties of the H₂ absorbing alloy used for the negative electrode [12].

Among various kinds of H₂ storage materials, the AB₅ type rare-earth system is one of the promising candidates due to their intermediate thermodynamic properties, and they are traditionally used as negative electrode in Ni-MH batteries. However, the hydrogen storage capacity of this alloy declines drastically during cycling. In some applications where high power is needed, for example, electric vehicles, the Ni-MH battery still do not reach the ability of the Ni-Cd batteries. Therefore, the discharge kinetics of the battery should be improved [13]. Also, the AB₅ alloys have a tendency of forming oxide film on their surface which inhibits hydrogen dissociation and penetration into interstitial sites leading to reduced capacity of the battery. To redeem this, the metal hydride materials were micro-encapsulated by electroless deposition of the metal hydride materials with immersion in Pd and Pt bath.

The performance of MH electrodes such as cycle life, discharge ability are affected by many factors, for example, the composition of the alloy, the content of the binder and the conductive material in the electrode and the modification of the alloy surface. The performances are therefore affected by factors other than the corrosion stability of the alloy and the reactivity of the alloy surface for the reaction. However, it has been well established how these factors contribute to the performance of the electrodes [14]. In the investigation study on the AB₅ type

1: Chapter One

rare-earth-based H₂ storage alloys are in progress for further improvement in electrochemical characteristics and reduction in production costs.

1.4 Objectives of the Study

Metal Hydrides (MH) hydrogen storage materials have the ability to reversibly absorb and release large amounts of hydrogen at low temperature and pressure. When these metal powders absorb hydrogen to form hydrides, heat is released. Conversely, when heat is absorbed hydrogen is released from the hydride. In the absorption process, hydrogen gas molecules break down into hydrogen atoms and penetrate into the interior of the metal crystal to form a metal hydride. In the desorption process, hydrogen atoms migrate to the surface of the metal hydride, combine into hydrogen molecules and flow away as hydrogen gas, allowing the material to form the original metal structure [15]. The formation of these hydrides can be realized by both direct interaction of the metals or alloy material with hydrogen gas, and also by its electrochemical saturation with hydrogen from an electrolyte. Electrochemical saturation of the metal hydride hydrogen storage material with hydrogen using an alkaline electrolyte will be the focal point of the investigation.

The objectives of the study are as follows:

- To study the feasibility of direct transformation of low potential heat ($T < 100^{\circ}\text{C}$) into electricity, by the application of electrochemical hydrogen concentration cells with thermally managed metal hydride electrodes.
- To master basics of metal hydrides material science, including experimental technique for gas phase and electrochemical characterization of low temperature hydrogen storage materials on the basis of intermetallic hydrides.

1: Chapter One

1.5 Research frame work and design

Assumptions on which the study is based are given as follows:

- Metal Hydride hydrogen storage materials are known to be very efficient for the utilization of low grade heat. Their applications are based on the reversible hydrogen interaction with some metals and alloys to form a hydride and these reactions are exothermic.
- AB_5 intermetallic hydrides show better kinetics of hydrogen absorption/desorption and increased cycle lifetime.
- Platinum Group Metals (PGMs) exhibit catalytic properties thus the metal material (AB_5) are surface modified by them. Because they significantly improve activation, hydrogen sorption performance and also increase the electro-catalytic activity of the material.

AB_5 material will be characterized to determine their physical and chemical properties and correlation between thermodynamic and kinetic parameters of electrochemical experiments will be determined.

1.6 Research Outline

Chapter Two: *Literature Review: Electrochemical energy conversion using metal hydride hydrogen storage materials*

This chapter starts with the introduction of hydrogen, its properties and most importantly its storage. It follows with the discussion of metal hydrides, their properties, structures and applications. Attention is paid to intermetallic hydrides. Their surface modification with Platinum Group Metals and their application in Ni-MH batteries are discussed. MH can be

1: Chapter One

formed by direct interaction and electrochemical saturation of hydrogen into the metal or alloy material. Both these methods are discussed.

Chapter Three: *Experimental*

Chapter three serves as the continuation of the literature review, but it elaborates more on the characterization techniques utilized in the study. The chapter starts with the introduction of the materials and methods used. It is followed by the review and discussion of the instruments and techniques employed in the study. The principles in their operation, sample preparation and experimental parameters are also discussed.

Chapter Four: *Results and Discussion*

The chapter initiates with structural characterization studies of unmodified and modified AB₅ type alloys. The results are demonstrated and followed with appropriate discussions. The characterization is done by employing the analytical tools reviewed in chapter 3, which include XRD, SEM, EDS, and AAS. The electrochemical characterization is also done employing galvanostatic charge/discharge rates, Cyclic Voltammetry, and Electrochemical Impedance Spectroscopy.

Chapter Five: *Conclusion and Recommendations*

The research is completed with a brief discussion of the aims and objectives achieved regarding the study. Recommendations are made for future work.

2: Literature Review

2: Chapter Two

2. Literature Review: *Electrochemical Energy Conversion using Metal Hydrides Hydrogen*

Storage Materials

2.1 Introduction

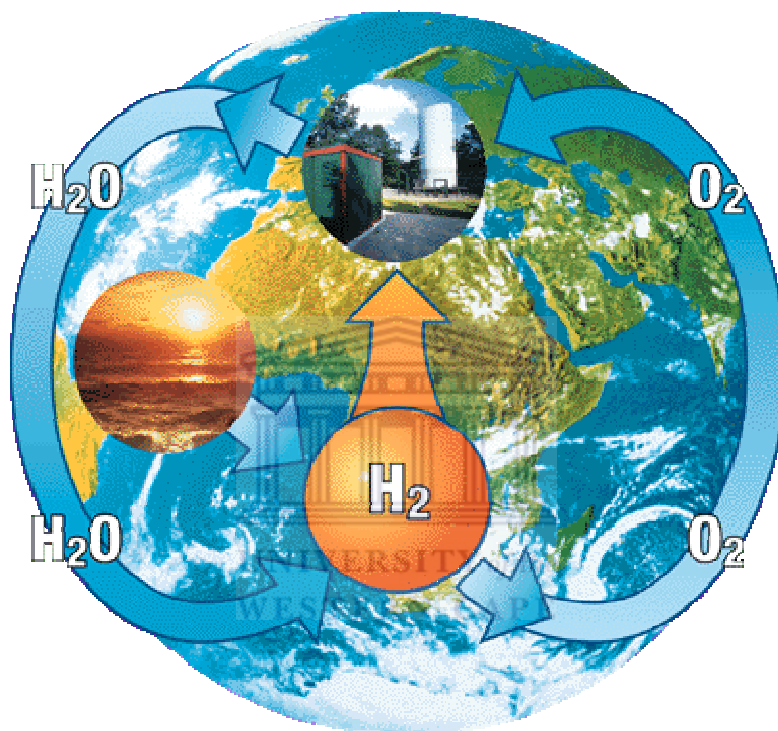


Figure: 2.1 Hydrogen Cycles [20]

H. Cavendish discovered hydrogen in 1766 [16], and concluded that water was not an element but was formed by hydrogen and oxygen, as illustrated in **Figure 2.1**. The name “hydrogen”, which means “water former” in Greek, was proposed by A.L. Lavoisier in 1783. Hydrogen is a highly reactive element; it is the first one in the periodic table, and has two isotopes; deuterium and tritium. It is the most abundant element in the universe and the third one in the earth’s crust. [16].

2: Literature Review

Hydrogen is a renewable energy carrier. Being a carrier means that it is not a direct source of electricity, but can be used to produce electricity. Unlike fossil fuels, which are naturally occurring substances, H_2 does not exist in its pure form in nature and must be extracted from other compounds. As an example, methanol, natural gas, or water can be separated to release the H_2 into its pure form to be used as fuel [17].

Hydrogen can be converted to other forms of energy in more ways and more efficiently than any other fuel, for an example, through catalytic combustion, electro-chemical conversion and hydriding, as well as through flame combustion. Hydrogen has lower buoyancy, high auto-ignition, high specific heat, and diffusivity which increase its safety [18]. Hydrogen is a non-polluting gas and it forms water as a by-product when in use [19].

The problem of storing hydrogen safely and effectively is one of the major technological barriers currently, preventing the widespread adoption of hydrogen as an energy carrier and the subsequent transition to the so-called “hydrogen economy” [21]. The conventional storage methods are compressed H_2 gas, cryogenic liquid and absorbed solid (e.g. metal hydrides). Each of these methods will be further discussed below.

2: Literature Review

2.2 Compressed H₂ Gas

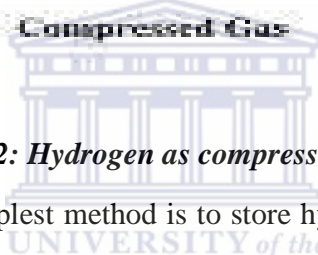
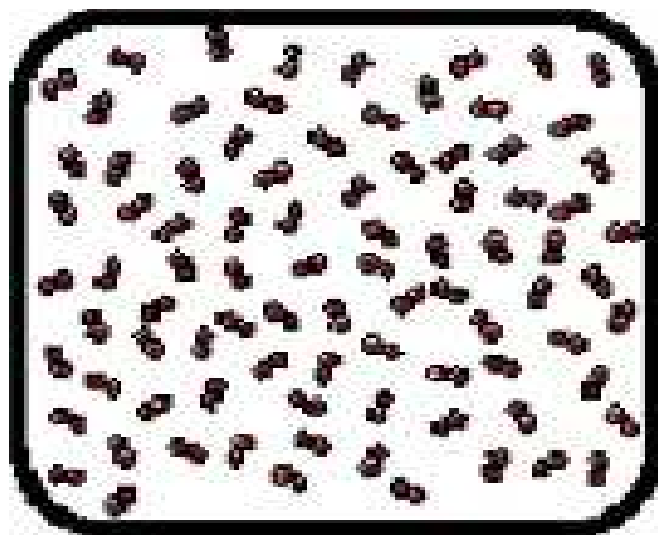


Figure 2.2: Hydrogen as compressed gas [22]

The most commonly used and simplest method is to store hydrogen in its natural form as a gas. Compressed hydrogen seems to be the best form of H₂ for fuel purposes, because in this form it can be stored in a smaller space while maintaining its energy potency. Additionally, compressed hydrogen, whilst still flammable, can be stabilized so it is less volatile, making it a good choice to power automobiles, home and office buildings [23].

The problem with storing hydrogen as compressed gas is that, energy must be consumed to reach the high pressure. The high pressure ranges from 5000 to 10 000psi. Compressed H₂ gas is not as energy intensive as liquefaction, which consumes as much as 50% of the heating value of H₂. Furthermore, compressed H₂ can be stored at ambient temperatures, unlike liquid H₂ that requires superinsulated tanks to maintain the cryogenic conditions [18]. The major setback of

2: Literature Review

storing hydrogen as a gas is that the tanks that are used to store the hydrogen can rupture which poses a safety risk, since large volume tanks are used.

2.3 Liquid Hydrogen

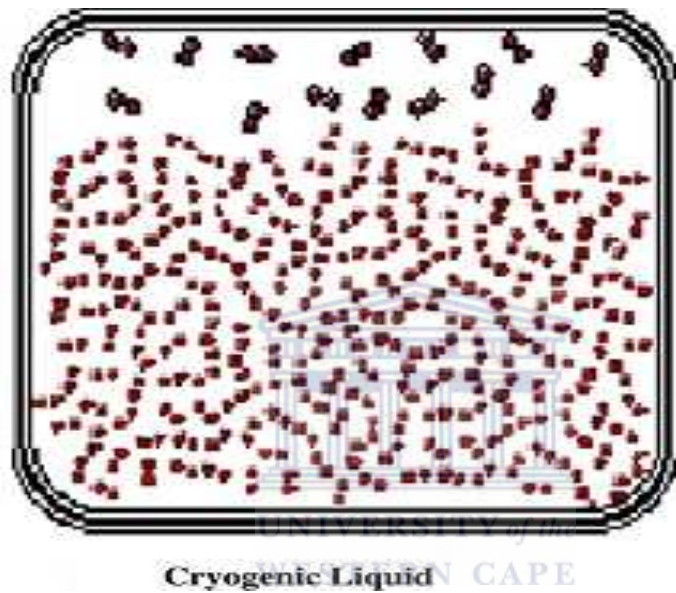


Figure 2.3: Hydrogen as cryogenic liquid[22]

The energy density of H_2 can be improved by storing hydrogen in a liquid state. Liquid H_2 must be stored in cryogenic tanks and this is a well established technique. There are three ways that heat transfer occurs from the external air to the liquid H_2 ; conduction, convection and radiation. Heat transfer increases with external surface area. As such, the majority of cryogenic tanks are spherical or cylindrical to minimize surface area (e.g. figure 2.3). However, the issues with Liquid Hydrogen (LH_2) tanks are hydrogen boil off, the energy required for H_2 liquefaction, volume, weight and tank cost. The energy requirement for H_2 liquefaction is high, typically, 30%. The energy required is much higher due to the inefficiency of regeneration at the extremely

2: Literature Review

low temperature. This provides a significant volume improvement over compressed H₂ gas. The volumetric capacity of liquid hydrogen is 0.070kg/L, compared to 0.030kg/L for 10 000psi gas tanks [18]. A considerable amount of energy is wasted on maintaining the low temperature required to keep the H₂ in liquid state. Consequently, liquid H₂ is very expensive and impractical for most automotive applications [24].

2.4 Solid State Hydrogen Storage

Hydrogen is a highly reactive element and is known to form hydrides and solid solutions with thousands of metals. This method uses alloys that can absorb and hold large amounts of hydrogen by bonding with hydrogen and forming hydrides. **Fig 2.4** shows the family tree of hydriding alloys and complexes.

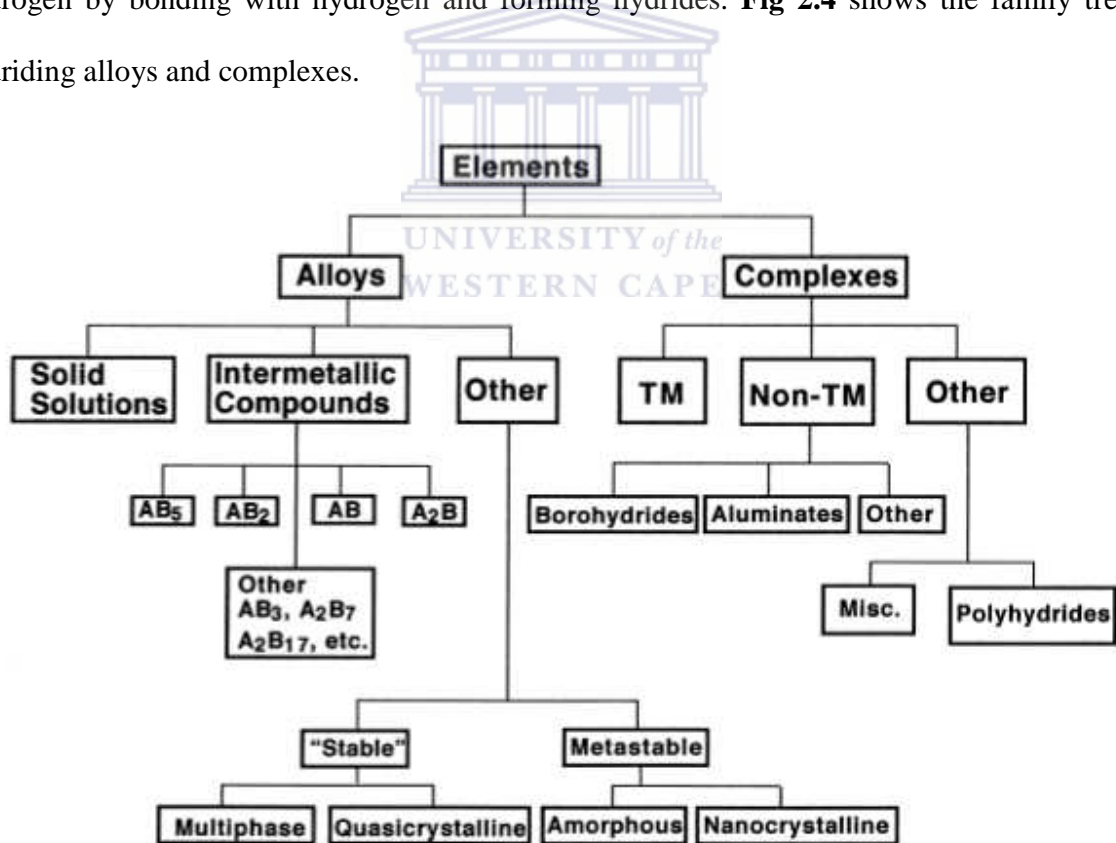


Figure 2.4: Family tree of hydriding alloys and complexes [25]

2: Literature Review

The results obtained and presented by many studies show that there are many materials that are competitive to be used in H₂ storage processes. These are materials based on carbon structures, metals and metal alloys, etc. These kinds of materials will be referred to specifically below.

2.4.1 Carbon Type Material for Hydrogen Storage

Carbon can be used as a storage medium for hydrogen. Two types of carbon will be discussed, namely, diamond and graphite. In diamond, each atom is fully coordinated symmetrically in space in all three dimensions. Graphite, on the other hand, is made up of a two-dimensional hexagonal sheet of carbon atoms, with long distance between each sheet. However, there are also other forms of carbon structures such as graphene and nanotubes that are the newest advanced carbon structures, with special properties.

Some scientists are using various approaches to shape carbon into microscopic cylindrical structures known as nanotubes. These nanotubes are microscopic tubes of carbon, two nano meters across, that store hydrogen in microscopic pores on the tubes and within the tube structure. One of the critical factors in nanotubes' usefulness as a H₂ storage medium is the ratio of stored H₂ to carbon. Carbon nanotubes have storage density (5.5wt%). They are the best current materials, having high surface area but, still require cryogenic temperatures to achieve high storage densities. Similar to the metal hydrides in their mechanism for storing and releasing hydrogen, carbon nanotubes hold the potential to store significant volumes of H₂. Nanostructured carbons include single wall, multi wall and rope type structures. While promising because of their structural and chemical versatility; these tubes have not consistently shown superior H₂ storage properties[26]. **Figure 2.5** shows different types of carbon nanotubes.

2: Literature Review

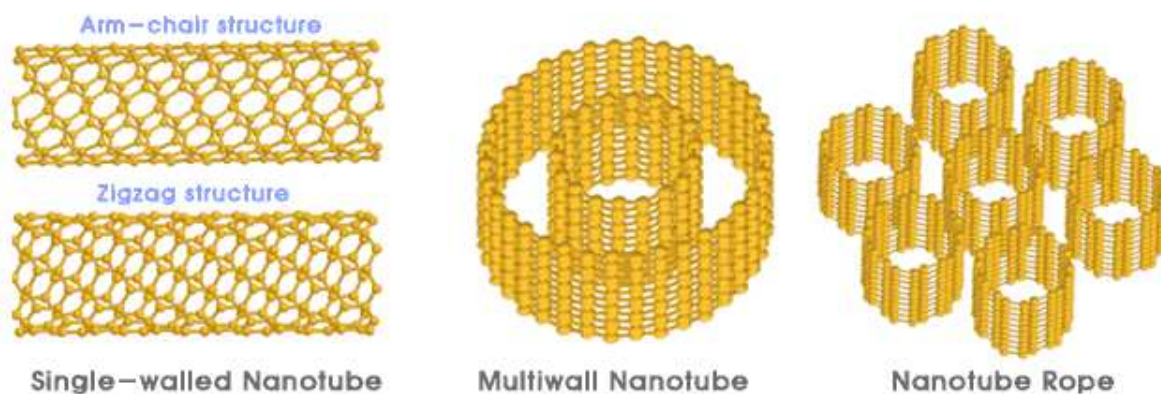


Figure 2.5: Different types of carbon nanotubes [27]

2.4.2 Metal Hydrides

A hydrogen storage alloy is capable of absorbing and releasing H_2 without compromising its own structure. These hydrogen storage alloys are known as metal hydrides which is the term used to describe compounds of metals or intermetallics compound and hydrogen that contains some kind of a metal hydrogen bond [28].

With storing hydrogen in hydride form there is possibility to control the hydrogen absorption and desorption conditions through the thermodynamic properties of the materials and this offers better security conditions. For example, metal hydrides have the lowest operating energy compared to both compressed gas and liquid hydrogen. Therefore, metal hydrides have the advantage of low operating energy, moderate pressure and temperature, and high volumetric density as compared to both compressed gas and liquid hydrogen. These metal hydrides are still behind in both gravimetric and volumetric energy densities as compared to hydrides of light

2: Literature Review

metals as shown in **Figure 2.6** below. The draw back in the application of these light metal hydrides is that their high capacities are only available at impractical high temperatures.

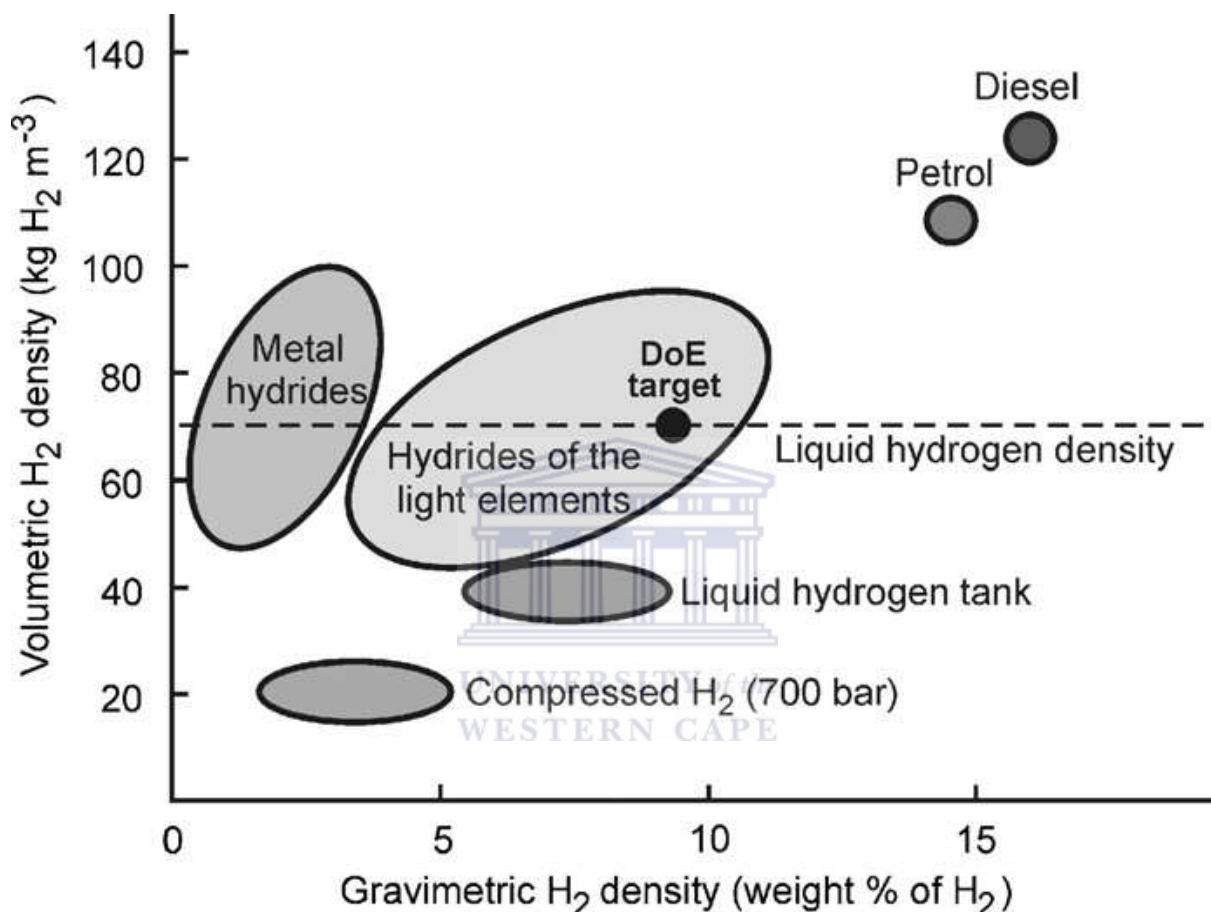


Figure 2.6: Gravimetric and Volumetric densities of various hydrogen storage options (including the weight and volume of storage tanks) [29]

In **Figure 2.6**, the gravimetric and volumetric energy densities of hydrogen chemically stored using various storage methods are displayed. One can see that neither cryogenic nor high-pressure hydrogen storage option can meet the fossil fuel energy density as the DOE target. It is becoming increasingly accepted that the solid state hydrogen storage using ionic-covalent hydrides of light elements such as lithium, boron, sodium, magnesium and aluminum (or some

2: Literature Review

combination of these elements), represents the only method enabling one to achieve the necessary gravimetric and volumetric target densities.

2.5 Classification of hydrides

Every element of the periodic table forms one or more hydrides. These compounds have been classified into three main types according to the nature of their bonding: ionic hydrides; which have significant ionic character, covalent hydrides; which include the hydrocarbons and many other compounds, and interstitial hydrides; which may be described as having metallic bonding.

2.5.1 Covalent Hydrides

They are generally formed from the metals to the right of group VIII B in the periodic table. The properties of covalent hydrides are a reflection of weak Van der Waals forces existing between covalent molecules. The common characteristics of covalent hydrides are typically: low melting and boiling points, liquid or gaseous at room temperature, and thermal instability for solid covalent hydrides [30].

Covalent hydrides encompass compounds such as AlH_3 , the boranes and the borohydrides and related derivatives, hydrocarbons, amines, amides, and ammonia complexes, etc. Where the bonding is highly localized and strong between two centres, or in the case of the boranes and borohydrides, there is often three centers, two electron bonds formed, for example, in bridging B-H-B compounds. According to the older definition of hydride, covalent hydrides cover all other compounds containing hydrogen. The more contemporary definition limits hydrides to hydrogen atoms that formally react as hydrides and hydrogen atoms bound to the metal centers. In these substances the hydride bond is formally a covalent bond much like the bond made by a

2: Literature Review

proton in a weak acid. This category includes hydrides that exist as discrete molecules, polymers or oligomers, and hydrogen that has been chemisorbed in the surface.

A particularly important segment of covalent hydrides are the so called complex hydrides which often contain discrete cation-anion pairs. The anions include borohydride or alanate, among other hydridic anions. Hydrogen may be released thermally, or in the case of sodium borohydride by hydrolysis to form sodium borate and hydrogen. Another important class of covalent hydrides are the so-called chemical hydrogen storage materials, which are discrete molecular species, usually that do not contain cation-anion pairs such as found in the complex metal hydrides.

Chemical hydrogen storage materials encompass molecules such as ammonia borane, alane, and the hydrocarbons, among many others. These molecular hydrides often involve additional ligands such as in TMEDA- AlH_3 where the tetramethylethylenediamine ligand is ligated to the alumina centre through its two nitrogen atoms, thus helping to stabilize AlH_3 . Hydride complexes occur when combinations of ligands, metal ions and hydrogen form molecules.

Hydride complexes are differentiated by whether they contain transition metals; those that are called Transition Metals (TM) hydride complexes, those that do not are called non-TM hydride complexes. The main difference between hydride complexes and Intermetallic compounds (IC) is that the bonding in hydride complexes is quite covalent, strong, and localized, whereas in intermetallic compound hydrides, hydrogen atoms reside in the interstitial sites and the multi-center bonding may be relatively weak. Complexes release hydrogen through a series of decomposition and recombination reactions. Some combinations of elements, for example, Mg and Fe, form hydride complexes but cannot form IC's; hydrogen is required for these two elements to form a stable compound (Mg_2FeH_6) [25].

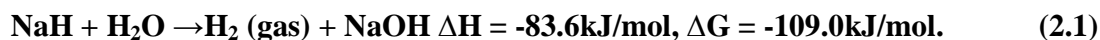
2: Literature Review

2.5.2 Ionic Hydrides

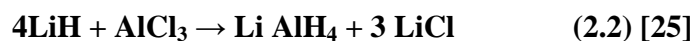
They are formed from the alkali and alkaline earth metals. The H₂ has valence of -1 in ionic hydrides, and the physical properties of these hydrides are often similar to the corresponding halides. Ionic hydrides are often also referred to as saline hydrides. Common characteristics of ionic hydrides are: high enthalpy of formation, high melting points, and electronic conductance in the molten state [30].

Most ionic hydrides exist as “binary” materials involving only two elements including hydrogen. Ionic hydrides are used as heterogeneous bases or as reducing reagents in organic synthesis. Typical solvents for such reactions are ethers. Water and other protic solvents cannot serve as a medium for pure ionic hydrides because the hydride ion is a stronger base than the deprotonated solvent anion.

Hydrogen gas is liberated in a typical acid-base reaction.



Often alkali metal hydrides react with metals halides. Lithium aluminium hydride (often abbreviated as LiAlH) arises from reactions of lithium hydride with aluminum chloride.

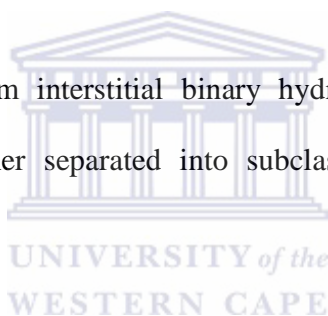


2: Literature Review

2.5.3 Interstitial Hydrides

Interstitial hydrides can exist as discrete molecules or metal clusters in which they are atomic centers in a defined multi-centered multi-electron bonds. Interstitial hydrides can also exist within bulk materials such as bulk metals or alloys at which point their bonding is generally considered metallic. The interstitial hydrides are distinct from ionic or covalent hydrides, in that way from where H atoms reside in the tetrahedral or octahedral interstices within the metal or alloy frame work; solid solution formation is common. The bonding between the metals and the hydrogen atom is highly delocalized, with multi-center, multi-electron bonding similar to that in metals occurring.

Many bulk transition metals form interstitial binary hydrides when exposed to hydrogen. Interstitial hydrides can be further separated into subclasses of metal alloy hydrides and intermetallic hydrides [25].



2.5.3.1 Metal Alloy Hydrides

The host hydrogen storage materials may consist of a solid solution alloy. These are characterized by varying composition and disordered substitution of one element for another on crystal lattice sites; they are formed by dissolving one or more minor elements into a primary element.

Solid solutions based on Pd, Ti, Zr, Nb and V form hydrogen storage materials with some attractive features such as moderate reversible storage capacities near ambient conditions, but cost and the heat released on hydrogen absorption deter the use of these materials for transport applications [25].

2: Literature Review

2.5.3.2 Metal Hydrides Intermetallic Compounds

Intermetallic compounds (IC) are characterized by homogeneous composition and crystal structure. IC's form hydrogen storage by combining a strong hydriding element **A** with weak hydriding element **B** to create a compound with the desired intermediate thermodynamic affinities for hydrogen. Hydrogen absorbs automatically into the host metal lattice as a solid solution at low concentrations and via hydride-forming metal/hydrogen bonds at higher concentrations. The host intermetallic compound elements **A** and **B** are typically present in an integer or near-integer stoichiometric relationship.

Element type **A** and/or **B** may be an ordered or disordered mixture of several metal elements. The total compositional variation has a strong impact on hydriding properties. This ability to form A_xB_y IC's containing up to 10 or more elements has been extensively studied and exploited in the commercialization of metal hydrides for hydrogen storage and Nickel-Metal Hydride battery applications. Because of their application in Ni-MH batteries, intermetallic compounds will be the main focus of this investigation, and will be further discussed. Common classifications of IC's for hydrogen storage are AB_5 , AB_2 , AB and A_2B ; $LaNi_5$, $TiCr_2$, $TiFe$ and Mg_2Ni being representative examples [25].

2: Literature Review

2.6 Hydrogen Absorption Mechanism

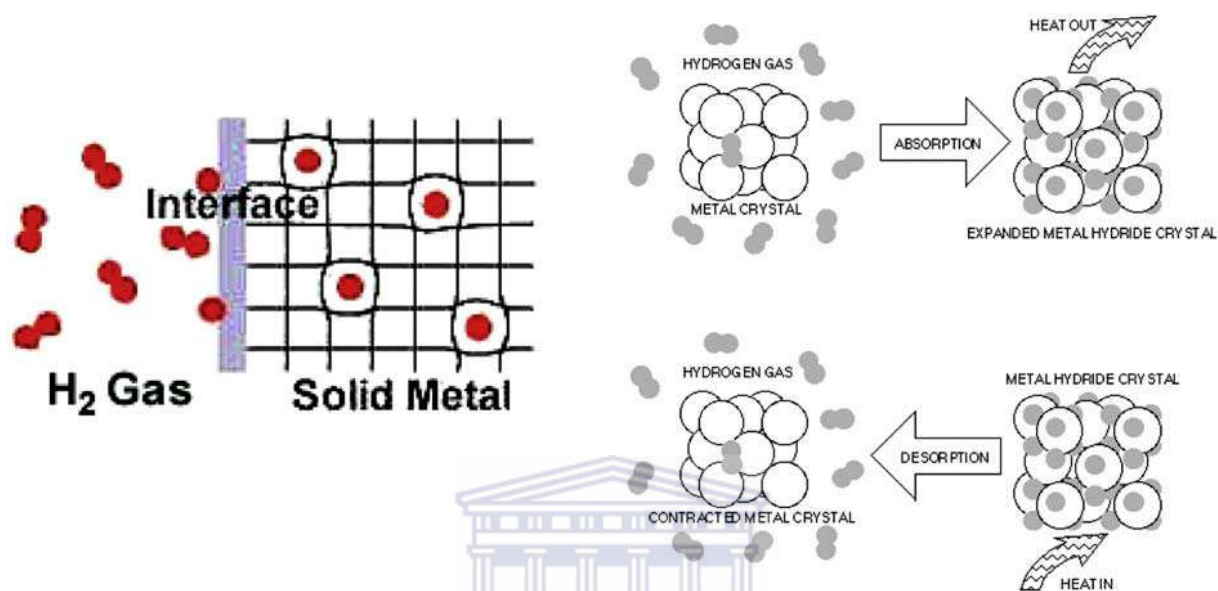


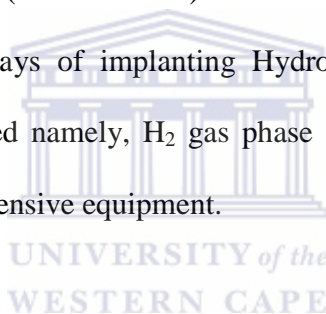
Figure 2.7: Metal hydrogen interaction [22]

The metal hydrogen system consists of a metallic material, hydrogen gas, and an interface region between them as shown in **Fig. 2.7** above. Hydrogen gas adsorbs onto the interface region. At the interface region, the molecule is dissociated into individual hydrogen atoms that are able to absorb or dissolve into the metal phase. The random dissolution of hydrogen atoms in the metal phase is known as the α -phase. Within the metallic phase, the hydrogen atoms can start to arrange themselves in a specific configuration with the metal atoms, forming the metal hydride phase called the β -phase. Where and how the β -phase is nucleated and grows is characteristic of the material [22].

2: Literature Review

2.7 Hydrogen Implantation in Metals

Molecular hydrogen gas can readily enter a molten metal surface, often added accidentally as water contained in fluxes, mould dressing and alloying additions, dissociating into the mono-atomic form on dissolution, and remaining as a mono-atomic solute on solidification. The diatomic hydrogen molecules are too large to enter the surface of a solid metal, and must be dissociated into single atoms [31]. Metal hydrides method of H₂ storage is based on the process of the reversible hydrogen absorption in hydride forming metals or intermetallic compounds with the formation of metal hydrides (MH). Hydrogen in the MH is placed in interstitials of crystal structure of the matrix of the metal (intermetallide) as individual, not associated in molecules, H₂ atoms [32]. There are several ways of implanting Hydrogen in metals, but there are two techniques that are commonly used namely, H₂ gas phase and electrolytic charging. Both are simple and require relatively inexpensive equipment.



2.7.1 Gas Phase Charging

This technique consists of simply applying hydrogen gas at appropriate temperature and pressures. The best way to understand the absorption and desorption of H₂ by metals when using the gas phase charging is via pressure composition isotherms which are performed experimentally using Sieverts apparatus.

The H₂ absorption mechanism occurs as follows. Metal hydride alloy attract and store hydrogen atoms through chemical hydriding reactions at the surface of the alloys when the surrounding temperature is relatively low. By decreasing the surrounding temperature or increasing pressure, the metal hydride alloy can be forced to absorb hydrogen, generating heat. By increasing the surrounding temperature or decreasing pressure, the metal hydride alloy can be forced to desorb

2: Literature Review

hydrogen, absorbing heat. In this manner, the reaction between metal hydride and hydrogen can be directed by controlling temperature and pressure [22]

The characteristics of these reactions can be described by the following equation:

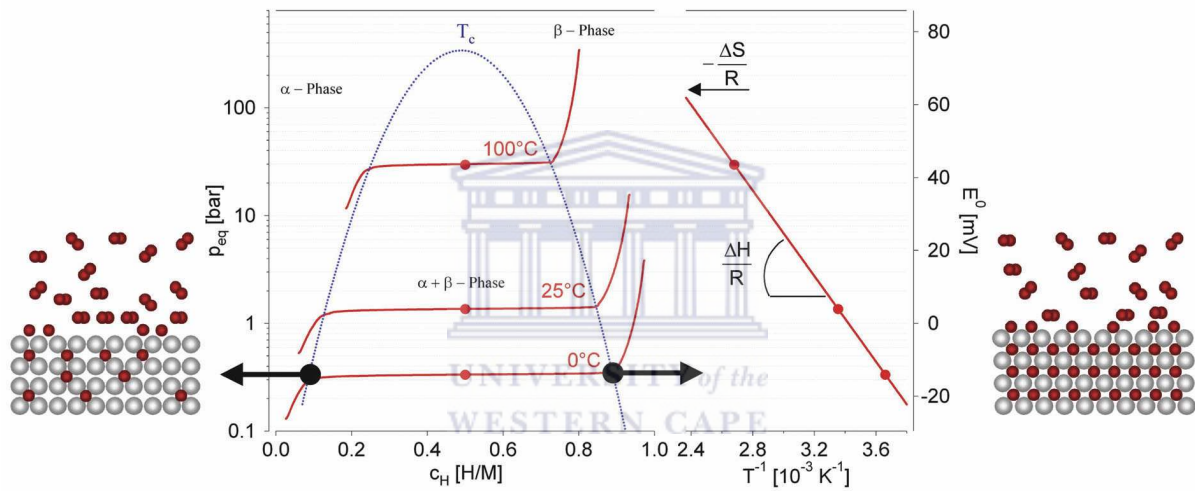


Figure 2.8: Pressure composition isotherm for hydrogen absorption in a typical intermetallic compound on the left hand side. The solution (α -phase), the hydride phase (β -phase) and the region of coexistence of the two phases are shown. The coexistence region is characterized by the flat plateau and ends at the critical temperature T_c . The construction of the Van't Hoff plot is shown on the right hand side. The slope of the line is equal to the entropy of formation divided by the gas constant [33].

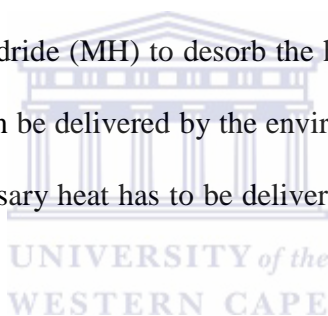
The thermodynamic aspects of hydride formation from gaseous hydrogen are described by pressure composition isotherms **Fig. 2.8**. When the solid solution and the hydride phases coexist, there is a plateau in the isotherms, the length of which determines the amount of hydrogen stored. In the pure β -phase, the H_2 pressure rises steeply with concentration. The two phases region ends in critical point, T_c , above which the transition from α - to β -phase is continuous. The

2: Literature Review

equilibrium pressure, P_{eq} , is related to the changes ΔH and ΔS in enthalpy and entropy, respectively as a function of temperature by the Van't Hoff equation:

$$\ln\left(\frac{P_{eq}}{P_0}\right) = \frac{\Delta H}{R} - \frac{1}{T} - \frac{\Delta S}{\Delta T} \quad (2.4)$$

As the entropy change corresponds mostly to the change from molecular H_2 gas to dissolved solid H_2 . It is approximately the standard entropy of H_2 ($S_0 = 130J.K^{-1}.mol^{-1}$) and is therefore $\Delta S_f = -130J.K^{-1}.mol^{-1}H_2$ for all metal- H_2 systems. The enthalpy term characterizes the stability of the metal hydrogen bond. To reach the equilibrium pressure of 1bar at 300K, ΔH should amount to significant heat evolution $\Delta Q = T.\Delta S$ (exothermal reaction) during H_2 absorption. The same heat has to be provided to the metal hydride (MH) to desorb the hydrogen (H_2) (endothermic). If the H_2 desorbs below RT , this heat can be delivered by the environment. However, if the desorption is carried out above RT , the necessary heat has to be delivered from an external source, such as combustion of H_2 [33].



2.7.2 Electrochemical charging

This technique is often called cathodic charging or electrosorption. The metal specimen is placed in an acid or alkaline for example (KOH) H_2O - based electrolyte in series with a power supply and counter electrode (for example Pt). Often a reference electrode, such as saturated Hg/HgO, is placed near a sample electrode in order to monitor the applied potential relative to a well-established electrochemical standard. If the electrons are added to the metal electrode, water is partially split according to the following reaction:



2: Literature Review

Where \mathbf{H}_{ads} is the adsorbed atomic hydrogen resulting from electrolytic water splitting. Applied cathodic potential is highly effective in driving equation (2.5) to the right, thus increasing the thermodynamic activity of \mathbf{H}_{ads} [34]. This highly active atomic \mathbf{H}_2 is then readily absorbed into the sample, often far more effectively and rapidly than by gas phase charging [35], it is very likely that the hydriding surface mechanism is more complicated process for electrochemical hydriding than for gas phase hydriding. For hydriding via gas phase, the hydrogen bond needs to be broken, and the atoms are then more or less free to enter the hydrogen storage alloy lattice. For the desorption process, adsorbed \mathbf{H}_2 is recombined to form gaseous \mathbf{H}_2 .

During the electrolytic process, an electron is transferred from the \mathbf{H}_2 storage (MH) to the water molecules during charging. After this step, the \mathbf{H}_2 atom can be adsorbed on the surface and subsequently can be absorbed into the lattice. During discharge, an electron is transferred from the hydroxyl (OH^-) ion to the alloy and adsorbed hydrogen is desorbed and forms water. The electrolytic process as such involves more sub-processes in addition to an extra barrier in the electric double layer. Electronic conductivity is also important to facilitate optimum conditions for the hydriding/dehydriding reaction. An optimum reaction rate for the electrolytic hydriding/dehydriding reaction therefore requires additional optimization compared to the gas phase reaction [30].

The rate of these reactions increases with the increase in the surface area. It can therefore be concluded that in general, the hydriding substances are used in powder form to speed up the reaction. Elements or metals with unfilled shells and sub-shells are suitable hydriding substances. Metal and hydrogen atoms form chemical compounds by sharing their electrons in the unfilled sub-shells of the metal atom and the K shell of the hydrogen atom. Ideally at a given

2: Literature Review

temperature, the charging or absorption process and the discharging or desorption process take place at a constant pressure.

Metal hydrides have found their wide spread use as rechargeable batteries in the battery industry. As mentioned in chapter one, rechargeable batteries can be divided into primary (non-rechargeable) and secondary (chargeable) systems. The most important secondary battery types are lead acid, Ni-Cd, the Ni-MH and Lithium based battery type. Ni-MH and Li-ion batteries are replacing Ni-Cd and lead acid batteries for environmental concerns and because of higher energy storage. Ni-MH will be further discussed because they are the fastest growing segment of this rechargeable market for one on one replacement of Ni-Cd batteries in electronic devices due to their higher density (both in terms of weight and volume) and good cycle life. These batteries have more environmentally acceptable chemistry than Ni-Cd batteries, owing to the absence of such hazardous materials like Pb, Cd, and Hg. It is also becoming more competitive with Li-ion batteries in terms of volumetric density, long cycle life, and inherent protection against over charge/discharge. Ni-MH use intermetallic compounds metal hydrides as the negative electrode in the battery [23, 24, 35, 36].

2.8 Nickel Metal Hydride Batteries (Ni-MH)

The development of Ni-MH batteries based on metal hydrides (MH) negative electrodes is one of the most important areas of electrochemical studies today. Batteries based on such hydride materials have some major advantages over the more conventional lead-acid and nickel-cadmium systems. The Ni-MH cell is an alkaline storage cell, similar to Ni-Cd cell, which has for some time been used for many electronic devices such as cellular phones, lap-top computers, camcorders and others. Environmental safety concerns regarding the toxicity of cadmium and the

2: Literature Review

safe disposal of Ni-Cd cells have accelerated the commercialization of Ni-MH cells. The Ni-MH also has high gravimetric and volumetric energy densities than Ni-Cd cells by approximately 30-40% if the cells are of the same size.

The Ni-MH also has the advantage of being able to replace a Ni-Cd cell virtually without a change of the existing power systems for many electronic devices because they are very similar in physical structure and have similar charge and discharge voltage characteristics. Both battery systems have a 1.2V nominal voltage and similar discharge endpoints. The charging method used in Ni-Cd batteries is compatible with that for Ni-MH batteries and there is no need to minimize the overcharge of the Ni-MH battery. Ni-MH batteries are environmentally friendly and offer more energy per unit weight or volume than Ni-Cd or lead-acid batteries [24, 37, 38]. Presently, Ni-MH is considered the most preferred rechargeable batteries of the future. The high energy density, excellent power density, and long cycle life of these batteries also make them the leading technology as the battery power source for electric vehicle (EVs) [39]. However, further improvements of the cells are needed for longer life cycle, reduced self discharge, and optimum operation at elevated temperature.

Performance of metal hydrides battery depends on the electrochemical characteristics of the metal-hydride alloy, which is used as an active electrode in the battery. Electrochemical characteristics of the alloy are life cycle, capacity, exchange current density and discharge potential. These electrochemical behaviors depend on the structure, the nature and amount of each element in the intermetallic alloy. The characteristics can be altered by designing composition of the alloy to provide optimum performance of the battery.

2: Literature Review

2.8.1 How a Ni-MH Battery Works

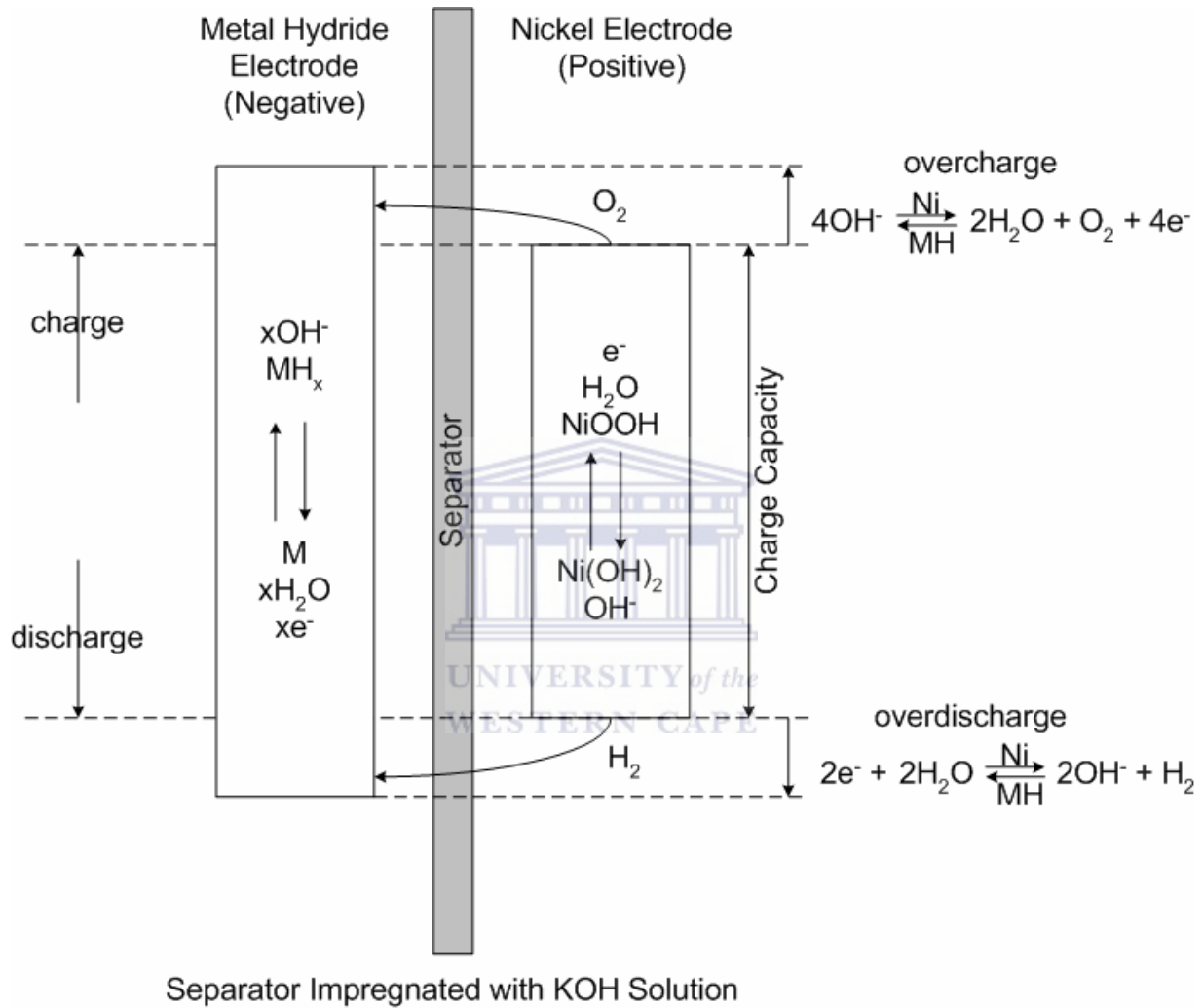


Figure 2.9: Schematic representation of Ni-MH cell [40]

As in all batteries, the Ni-MH consists of two electrodes with two connected ongoing reactions. In the Ni-MH cell, the active materials in the battery are nickel oxyhydroxide (NiOOH) and a hydride of La-Ni alloy (an AB_5 type alloy). During discharging, NiOOH gets reduced to Ni(OH)_2 and the hydride gets oxidized to its unhydrided alloy. The standard potential for the reaction at the anode is +0.490V, and that of the cathode is -0.828V. Thus, the cell voltage works out to

2: Literature Review

1.318V. The nominal voltage is 1.2V. If the cell is over charged, oxygen will evolve at the nickel electrode. However, oxygen evolved will combine with hydrogen from the metal hydride electrode to form water. This recombination reaction ensures no build up pressure in the cell, and is adopted as a safety measure. The cell must be negative limited, so there is always excess of the hydriding form of the electrode for combination with the evolving oxygen. The recombination mechanism allows the construction of sealed nickel-metal hydride batteries.

It is possible to make sealed cells which are essential maintenance free and be overcharged without creating excessive external pressures. This is done by making storage capacity of the positive nickel hydroxide electrode smaller than the negative electrode capacity. These are called positive electrode limited cells. At the end of the charging phase, there are no more accessible H₂ atoms to be removed from the positive electrode. Instead, hydrogen will be taken from the electrolyte leading to the production of oxygen molecules at the nickel oxide electrode. Sealed cells are designed with a certain amount of porosity in the separator that is not filled with the electrolyte (starved electrolyte). This will allow for gas passage, so that the oxygen produced at the positive electrode can diffuse through the separator and be recombined at the negative electrode. As long as the process works, the cell can be continuously overcharged without damage. This also facilitates the handling of the cells connected in series into a battery pack.

By a period of overcharging, the charged state of cells can be homogenized and fully charged. The reaction heat from the recombination will, however heat up the battery, which if it becomes excessive will cause it to fail. Also, if the overcharge current is high that it produces more oxygen than the recombination kinetics can combine, the oxygen pressure will increase in the cell, until the safety valve vents to release the internal pressure build up. This will lead to failure by electrolyte consumption and the separator dry out. The amount of electrolyte present in the

2: Literature Review

cell is limited in order not to fill all the porosity, which means that all small losses of the electrolyte lead to a significant reduced performance of the cell.

Generally the most common failure for Ni-MH seal cells is related to separator dry out. The normal ageing of the cell is, however also related to the dry out caused by a slow phase change and swelling of the Ni-electrode, which incorporates electrolytes in the structure and dries out the separator. This ageing process is dependent on temperature and cycling but also to a large part of the type of the Ni-electrodes used in the cell. The charging of the cell is controlled by monitoring the temperature of the cells, in order to stop or reduce the charge current when the cell starts to increase by overcharging. This temperature control can be done by indirectly using the cell itself as thermometer by monitoring the charge voltage.

The cells are charged with constant current and as they heat up, the over potential is reduced leading to a dip in the charge voltage (V). This decrease is denoted by the charger, which goes over into a low current mode. The method is usually referred to as delta V charging, which is also commonly used when charging Ni-Cd cells. The metal hydride electrode is however more effective with regard to charge acceptance leading to less marked reduction over potential upon heating necessitating a more sensitive charger to detect the voltage drop.

In contrast to other battery chemistries, the Ni-MH battery has in principle, an advantage of being able to withstand a certain amount of overcharging. When the cell is discharged and the nickel electrode is fully converted to Ni(OH)_2 , it cannot intercalate further hydrogen and the additional hydrogen will be emitted as hydrogen gas (H_2) from the positive Ni-electrode. This can be recombined again at the metal hydride electrode, helped by the match of more negative

2: Literature Review

electro active mass than positive. At high current discharging the recombination kinetics, is however, too slow to be able to cope with the emitted gaseous H_2 [41].

2.8.2 Requirements of Metal hydrides used in the Ni-MH battery industry

The discharge pressure of metal hydrides should range between (0.1 to 1)atm at room temperature to ensure that the hydrogen absorbed will be completely removed. The amount of hydrogen that a metal hydride alloy can absorb, describes the electrochemical storage capacity of the alloy and consequently the energy storage capacity of the battery. It is desired to have high-electrode capacity which has electrochemical reversibility. To obtain the capacity, the stability of the alloy should be considered. The metal to metal (M-M) chemical bond of the intermetallic alloys plays a vital role in their hydriding stability.

To ensure reversibility, the metal to hydrogen bond (M-H) strength must be between (25 to 50) $KJ.mol^{-1}$. If the bond strength is too low, hydrogen will not react with the alloy, but it will be evolved as gas. If the bond strength is too strong, the metal hydride will not absorb hydrogen reversibly. The alloy must have good oxidation and corrosion resistance in alkaline electrolyte. Most chemical elements form oxides when they react in alkaline electrolyte, and if these electrolytes are used they will oxidize and fail to store hydrogen reversibly.

In Ni-MH battery the metal hydrides operate in completely sealed environments where oxygen recombination occur on its surface. Therefore, the metal hydride must have good oxidation and corrosion resistance because cycle life depends on it. Hydrogen diffusivity in the alloy and exchange current densities must be high to ensure high discharge rate of the alloy especially during high discharge current densities. The discharge depends on mass transfer and charge transfer of the alloy. Hydrogen must migrate from the bulk in the metal to the surface of the

2: Literature Review

electrode through diffusion. Hydrogen will react with the hydroxyl ions at the metal-electrolyte interface. Hydrogen diffusivity and exchange current density of the alloy affects the rate at which energy can be stored in or removed from the battery. Exchange current density may be influenced by surface properties such as oxide thickness, electrical conductivity, surface porosity and topology, surface area and degree of catalytic activity [42].

2.9 Intermetallic Compounds

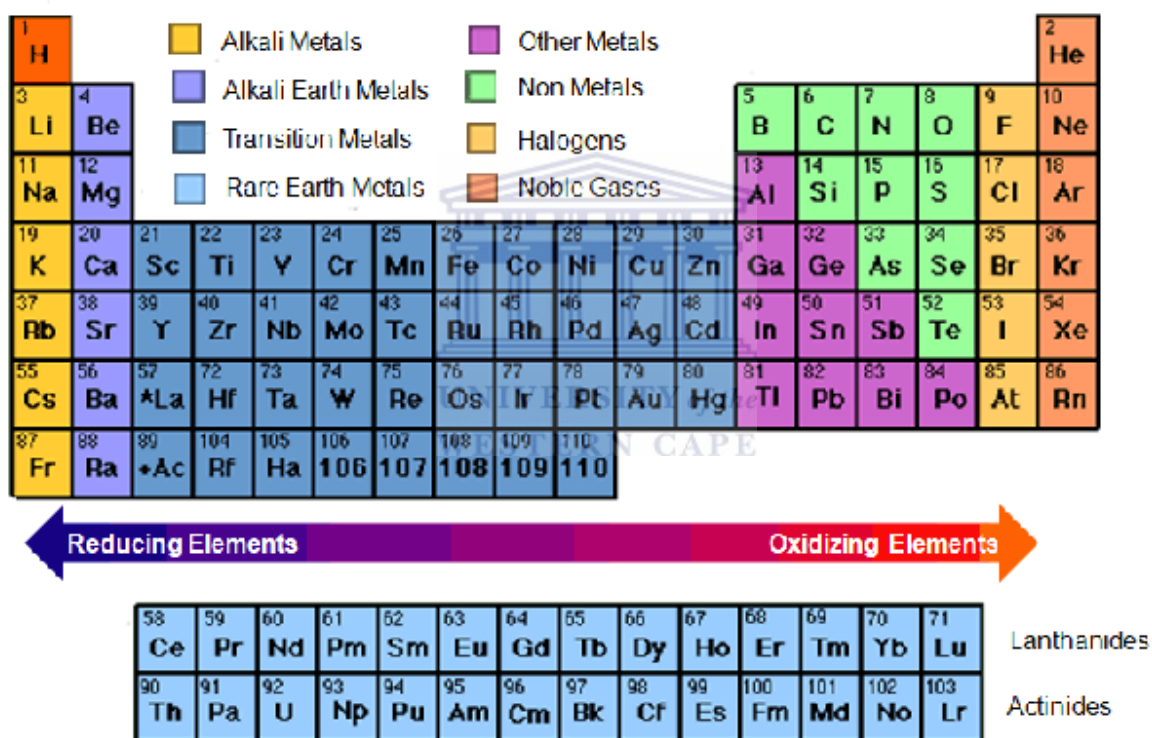


Figure 2.10: Periodic Table [43]

Different families of intermetallic compounds are classified on the basis of their crystal structures. They are formed by the combination of the elements in the side group IIA to VIA of the periodic table, having formulas like A_2B ($A=Mg$ or Ti), AB and AB_2 ($A=Ti, Zr$), and AB_5 (A is rare earth metal), etc., where B is a transition metal, mainly nickel, commonly with addition of

2: Literature Review

aluminum, cobalt, manganese, iron, chromium, etc. For the same stoichiometric formula of the metallic compound, their crystal structure may also be related to different types. For example, AB compounds have the structure of the type CsCl (non-hydrogenated) and CrB (hydrogenated), AB₂ Laves phases have the structure type MgCu, MgZn, and MgNi₂ and AB₅ have the CaCu₅ structure type. The intermetallic nature of the hydrogen storage alloy is preferred because in this case, the main conditions for effective storage of hydrogen are fulfilled:

1. The mutual position of the metallic atoms in the hydride phase is almost identical with the mutual position in the initial metallic matrix.
2. The lattice has a sufficient number of easily deformed voids suitable for accumulation of atoms in them.

In fact if these conditions are fulfilled, the intermetallic compounds absorb hydrogen reversibly and with a high rate and release hydrogen at 25-50°C. However, even the most efficient hydrogen storage alloys have certain shortcomings; high costs, high density, large hysteresis of the absorption-desorption pressure; difficult activation, low effective thermal conductivity in finely powdered state; and reduction of the working characteristics with an increase of the number of absorption-H₂ generation cycles. To eliminate the shortcomings, the intermetallic compounds, formed in the base of the hydrogen storage alloys are additionally alloyed. In the simplest case, components A or B are substituted by other elements, or both elements are substituted simultaneously [44].

2: Literature Review

2.9.1 AB Type Alloy

The first intermetallic hydride reported in detail was of the AB type, $ZrNiH_3$. However $ZrNiH_3$ had a high hysteresis and required about 300°C for a desorption pressure of 1atm, and as such was never really very practical for room storage applications. Early works on AB type hydrogen storage alloy were restricted to TiFe. There are two stable intermetallic compounds formed by the Ti-Fe system, TiFe (hydride-forming) and $TiFe_2$ (does not form hydrides). The application of TiFe in Ni-MH batteries has been limited because of easy deterioration of its hydrogen absorption /desorption by trace amounts of gas impurities including O_2 and H_2O . In recent years, more AB type hydrogen storage alloy consisting of Ti, Zr, and Hf on the A side and Fe, Ni, Al, Co, Mn, or Sn on the B side has been investigated. The substitution of Ni or Fe could improve the activation performance and discharge capacity. Nevertheless, the electrochemical properties of this system of alloys are unsatisfactory and, the AB family is rather sensitive to the surface damage from trace impurities present in commercial purity H_2 , and is obviously little used anymore [45].

2.9.2 A_2B type alloy

Examples of A_2B compounds that are historically important for hydrogen storage purpose include Ti_2Ni , important in early Ni-MH battery work, and Mg_2Ni , the earliest of the “the lightweight” hydride. Mg_2Ni forms the hydride Mg_2NiH_4 (3.6%wt H_2) by direct and reverse reaction with hydrogen gas around 300°C . Unlike all the intermetallic hydrides discussed above, Mg_2NiH_4 is not really interstitial metallic hydride but rather a transition metal complex. Perhaps this resulted in the failure of several studies aimed at reducing the dissociation temperature of Mg_2NiH_4 to much lower than 300°C temperatures. This type also had little practical use [46].

2: Literature Review

2.9.3 AB₂ type alloy

AB₂ hydrides are based on the AB₂ Laves phases which form under certain conditions of the **A/B** metal atom size-ratios and d-electrons concentration. For the Laves phases that form useful hydrides, **A** is usually a group IVA elements (mostly Ti and or Zr) and **B** is one or more transition elements in the range of V and Cu (with special emphasis on V, Mn and Cr). First studied in the 1960's, the AB₂ hydrides were the subject renewed efforts that started in the mid 1970s. Like the AB₅ hydrides, numerous substitutions can be made for both **A** and **B** elements in the AB₂ hydrides to control absorption/desorption pressure.

Unlike the AB₅ intermetallics, which almost always have very narrow homogeneity regions (**Figure 2.11a**; LaNi₅), the AB₂ intermetallic often show significant ranges of stoichiometry (**Figure 2.11b**; TiMn₂). In fact, most AB₂ intermetallics in applications are multicomponent and probably off-stoichiometric. Multiphase, disordered alloys based on at least one AB₂ phases have been promoted for Ni-MH battery. AB₂ intermetallic system is of great interest since it possesses a higher energy density than the AB₅ system. Besides AB₅ type, only the AB₂ type has reached commercialization in rechargeable batteries.

The AB₂ alloys have higher storage capacity and plateau with higher slope than the AB₅, and are known to have slower kinetics. AB₂ alloy crystallizes in Laves phase structure which can be hexagonal (MgZn₂ or MgNi₂ structure types) or cubic (MgCu₂ structure type). Nickel substitution on the B site is favorable not only to increase the pressure but also to its catalytic effect on the H₂ dissociation. For larger substitution the capacity falls down. The main drawback of these types of compounds is the surface passivation by titanium and / or zirconium oxides which reduce the kinetics and slow down the activation. In order to improve the kinetics and

2: Literature Review

reduce the activation period different surface treatment like surface coating or fluorination were employed. The fluorination was the most efficient treatment to improve the activation process by dissolving Zr or Ti and precipitating catalytic Ni particles [47].

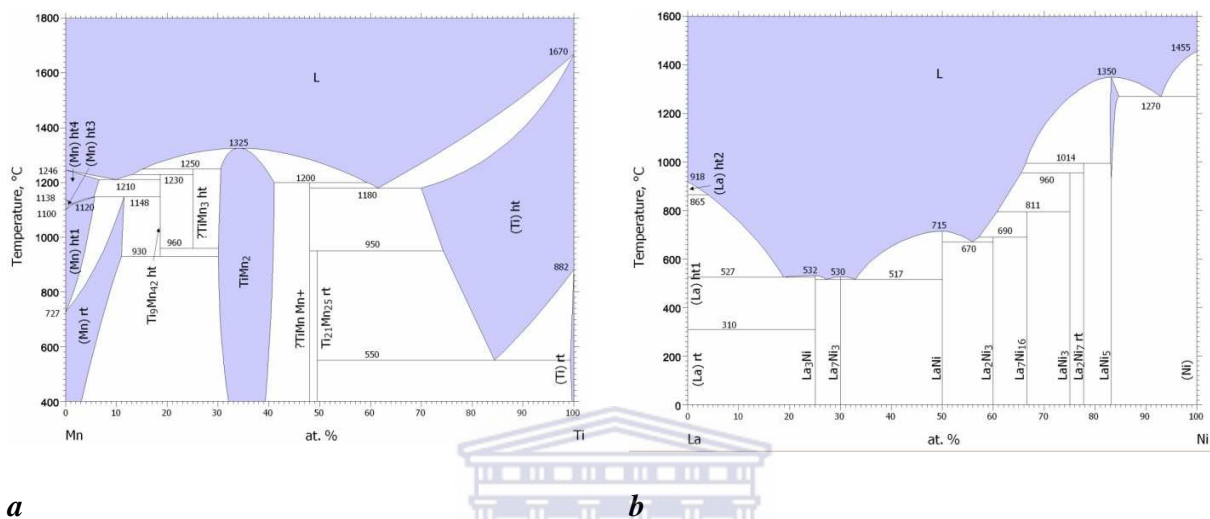


Figure 2.11: Phase diagrams of Ti–Mn (a) and La–Ni (b) systems [48-49]

Conventionally, both AB₅ and AB₂ types of alloys have been used for metal hydride electrodes. They meet almost all of the above requirements of the metal hydrides to be used in Ni-MH batteries. However, for hydrogen storage applications, the alloy formulations are complex. From the time period that metal hydrides were researched on for hydrogen storage there has been great interest in these alloys for nickel/metal hydrides batteries. The reason is that the nickel/metal hydride batteries has performance characteristic practically identical to nickel/cadmium batteries. In practical terms, all batteries, use AB₅ alloys and not AB₂ alloys even though the latter have higher specific energies and energy densities. The AB₅ alloys have longer cycle life, high exchange current densities, higher charge/discharge rates and better performance at higher and lower temperatures than 25°C. They show intermediate thermodynamics properties. The main attention is paid to these intermetallics.

2: Literature Review

2.9.4 AB₅ type alloy

Development of first practical hydrogen storage alloys AB₅ type intermetallic began as a typical accidental laboratory experiment. The outstanding hydrogen sorption properties of rare-earth AB₅ intermetallics were discovered in Philips Laboratories in Eindhoven, Netherlands in about 1969 in a program to develop a new permanent magnet alloy [50]. **A** is a rare earth metal like lanthanum, or commonly misch metal, which is a mixture of rare earth elements, mainly lanthanum, cerium, neodymium, and praseodymium. **B** is a transition metal, mainly nickel, commonly with additions of aluminum, cobalt, and manganese.

AB₅ intermetallic compounds are most used materials for negative electrodes in Ni-MH batteries. As early as the 1970s, it was reported that LaNi₅ could be utilized as a negative electrode material in Ni-MH batteries. However, in such applications LaNi₅ exhibits too high equilibrium pressure and too short cycle life time to be of practical interest for commercial batteries. The short cycle life time, i.e. the dramatic capacity loss during cycling, is probably due to the oxidation of Lanthanum to La(OH)₃ and a formation of Ni particles. This is compensated by substitution of Ni by other transition metals [51].

The A site substitution in AB₅ alloys has one practical reason, namely, the low cost of misch metal in comparison to the pure rare earth metals. However, changes in the misch metal composition (resulting from both the ore composition and the manufacturing technology) can result in a serious deterioration of the battery performance. These problems show also the economy of the misch metal production, dictated by a growing market for individual rare earth elements (for example, cerium as a catalyst in automotive applications or neodymium in permanent magnets). For these reasons, composition of the misch metal in the battery alloys

2: Literature Review

needs to be adjustable, without sacrificing the electrode performance. Understanding and controlling the effects of rare earth composition is therefore important for the real-life performance of the batteries.

When misch metal based Ni-MH batteries were being developed, the metallurgical grade misch metal was used as this was cheaper than lanthanum. Since then, the developments have mainly taken place using misch metal as the **A** component in the **A.B** alloy. The misch metal has a typical composition of 20-30% lanthanum, 40-50% cerium, 10-20% neodymium and 5-10% praseodymium. Rare earth elements, replacing lanthanum in the LaNi_5 structure, substantially change the thermodynamic properties of the alloy. In particular, the equilibrium hydrogen pressure markedly increases as a result of the **A** site substitution with cerium, praseodymium or neodymium. A too high plateau pressure (resulting from commercial grade misch metal) can also contain small amounts of other metals. The most common are some of samarium.

From the point of view of kinetics of hydrogenation, alloys containing cerium are the best. This means that a higher plateau pressure (and consequently lower stability of the hydride), corresponds directly to better kinetics of hydrogenation. These apparently contradicting effects of the **A** site composition in LaNi_5 -based alloys underline the importance of optimization of the misch metal composition. One clear improvement resulting from the **A** site substitution is that the presence of neodymium or cerium enhances corrosion resistance of the alloys.

The effect of various substitutions for the **B** side Ni in LaNi_5 have been studied by Ratnakumar et al, the results show that cycle life improves with ternary alloy substitution in the order $\text{Mn} < \text{Ni} < \text{Cu} < \text{Cr} < \text{Al} < \text{Co}$. This means that Co has the optimum effect. Hydrogen storage capacity of AB_5 alloy decreases drastically during cycling, and alloy pulverization and oxidation have been

2: Literature Review

reported as the important causes for this capacity decrease by Willems [41]. Alloy pulverization is the breaking of the metal hydride alloy particles during cycling. This is believed to be a result of the continuous lattice expansion/contraction during cycling. Many investigators have shown that the cycling stability of the LaNi_5 could be improved by partial substitution of nickel by silicon, aluminum, manganese, cobalt and other elements [30, 43, 51, 52].

However, substitutions lower the reversible capacity leading to a decrease in energy density. They also do not provide the necessary corrosion resistance towards the alloy. Cobalt substitutions have been shown by B.S Haran et al. to be most beneficial to the performance of the metal hydride as a battery electrode [53]. Apart from reducing the volume expansion, previous investigators have found the formation of $\text{Co}(\text{OH})_2$ during cycling which had beneficial effects on the alloy cycle life [54]. Sn improves cycle life and the kinetics of H_2 absorption/desorption, with only a slight reduction in specific capacity. Fe has similar features to Co because it also causes the alloy to have long cycle life and easy activation and low polarization during discharge.

Research on AB_5 alloys has concentrated on modifying the alloy composition by alloying it with various elements. The purposes of these modifications were as follows:

1. To enhance the corrosion stability of the alloy, especially under electrochemical cyclic charging/discharging;
2. To decrease the plateau pressure to enable the reversible charging at ambient conditions of pressure and temperature;
3. To increase the hydrogen storage capacity; and

2: Literature Review

4. Increase the rate at which the hydrogen can be stored or withdrawn from the alloy while maintaining satisfactory electrochemical parameters.

If the lattice is pre-expanded by introducing substitutional elements prior to hydriding, the volume changes during hydriding will be lower. One of the main tasks of a substitution element is therefore to pre-expand the lattice prior to hydrogenation to minimize the lattice stress, decreasing the cracking of the alloy during cycling [55]. These are widely used as negative electrodes in rechargeable Ni-MH batteries because of their beneficial kinetic properties, reasonable cost, and long cycle lives.

2.9.4.1 Structure of the AB₅ Alloy

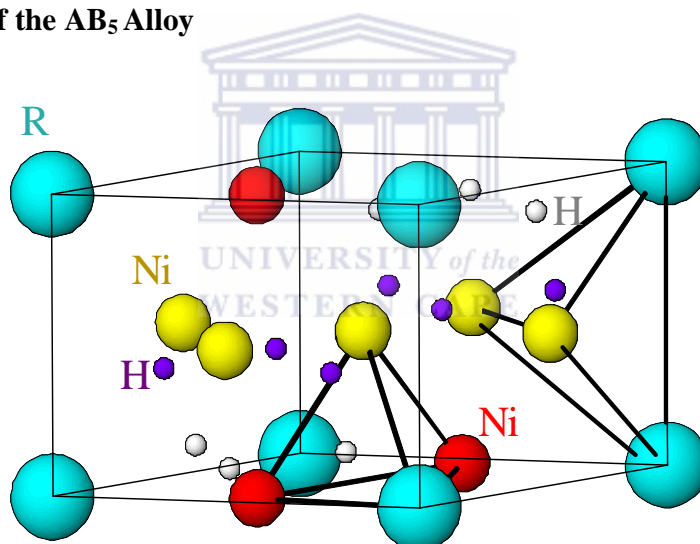


Figure 2.12: Structure of RNi₅H₆ hydride

In the figure above (structure of RNi₅H₆ hydride) these sites are shown as two kinds of tetrahedra one of which (bottom) contains one R and three Ni atoms, and another (right) – two R and two Ni atoms.

2: Literature Review

Intermetallic compounds tend to crystallize into a hexagonal, CaCu₅-type, structure. Two different methods for determination of structure parameters in hydrogen storage alloys used are, X-ray and neutron diffraction [41]. The first one is used to determine positions of metal atoms, and the second mainly for the determination of positions of hydrogen (deuterium) atoms in the MH.

LaNi₅ [54]:

Space group: *P6/mmm* (#191)

Cell parameters: $a = 5.015 \text{ \AA}$, $c = 3.982 \text{ \AA}$

Atom coordinates:

Table 2.1 a): Unhydrided LaNi₅ alloy

Site	Elements	Wyckoff symbol	x/a	y/b	z/c	Occupancy
La	La	1a	0	0	0	1
Ni1	Ni	2c	1/3	2/3	0	1
Ni2	Ni	3g	1/2	0	1/2	1

2: Literature Review

LaNi₅H₆ [55]:

Space group: $P31m$ (#157)

Cell parameters: $a= 5.336 \text{ \AA}$, $c= 4.259 \text{ \AA}$

Atom coordinates:

Table 2.1 b): Hydrided LaNi₅ alloy

Site	Elements	Wyckoff symbol	x/a	y/b	z/c	Occupancy
La	La	1a	0	0	0	1
Ni1	Ni	2b	1/3	2/3	0.98	1
Ni2	Ni	3c	0.499	0	0.496	1
H1	H(D)*	3c	0.47	0	0.092	1
H2	H(D)*	6d	0.1890	0.8640	0.4930	0.42

* - deuterium was used instead of hydrogen because deuterium is characterized by better neutron scattering and, therefore, by better quality of the pattern.

Furthermore, the formation of AB₅ hydride (LaNi₅ typical example) is accompanied by the accommodation of the hydrogen atoms into the tetrahedral interstitial sites that cause expansion of the metallic matrix (by ~20% for LaNi₅) and its slight distortion, but the symmetry of the metal atoms remains the same (hexagonal). Also the partial substitution of Ni for Co results in a smaller lattice expansion upon hydrogenation and, therefore, in less decrepitation of the material in the course of the hydrogenation / dehydrogenation. The latter is used in the electrochemical applications, so that usually battery AB₅ alloys contain significant amounts of Co (Ni substitution from the B-side).

2: Literature Review

2.9.4.2 Surface Modification of AB₅ Alloys

AB₅ alloy is the first one that has been studied extensively as an electrode material in Ni-MH batteries, because of its easy reaction with hydrogen at normal temperature. The AB₅ hydrogen storage alloy must have high capacity, long cycle life, and rapid absorption/desorption properties, low pressure hysteresis, low cost, environmentally friendly and minimal effects of over charge/discharge. The mostly used metal hydride electrode LaNi₅ (AB₅) type intermetallic alloy, suffers from power oxidation resistance which reduces the cycle life of the alloy. When a hydrogen absorbing alloy is used as negative electrode for a battery, there is a problem that the constituent elements are corroded by the electrolyte and oxygen gas generated from the positive electrode. This corrosion of the alloy leads to such problems of loss of capacity balance between the positive and negative electrodes and poisoning the positive electrode by dissolving ions from the alloy, particularly under such conditions such as charge-discharge cycling at high temperatures and continuous over charging [56]

Microencapsulation or surface coating of metal hydride alloys with various metals like (Cu, Ni, Pd, Co) has shown to be effective for improving electrode properties such as discharge capacity, cycle life and rate capacity [57]. This technique protected the electrode from oxygen produced at the nickel electrode during charging/discharging in addition to improving the current collection and protecting the alloys from degradation due to the electrolyte. However, coating with nickel, copper, palladium increases the dead weight of the electrode and reduces the net energy density. On the other hand, cobalt encapsulation leads to superior electrodes with increased capacity and cycle life.

2: Literature Review

Studies on electroless cobalt coating for microencapsulation of metal hydrides by Haran et al. [58] have shown the beneficial effects of cobalt on cycle life of AB₅ alloys. However, they did not consider the role of Co on alloy protection and improvement of the cycle life of the alloy. Durairajan et al. [58] have checked the role of Co on alloy protection and improvement of cycle life, and they have shown that Co coated alloys have a protective Co(OH)₂ layer over them and also show that there were no alloy oxidation, which clearly states that Co coating protects the alloy from corrosion. The only disadvantage is that cobalt is expensive and substantially increases the cost of the battery.

Another attempted improvement method done was fluorination treatment of the metal hydride particles, which was found to be beneficial to the cycle life of the alloy. The metal hydride alloy, which has rare-earth components, was placed in fluorinated environment to have fluorine coat the alloy, and rare-earth fluorides were formed at the surface of the alloy in preference to surface oxides/hydroxides. This surface coating was found to be chemically stable in the cell environment and increased the cycle life of the cell; however environmental concerns disadvantaged the use of the fluorine [59].

With all the improvements, the metal hydride still has poor electrochemical activity which reduced the charge/discharge properties of the alloy. The possible solution was found by Philips [60] who found that manipulation of the stoichiometry of the base alloy, the high electrocatalytic intermetallic compounds could be precipitated at the grain boundaries. These alloys enhanced the charge/discharge process within the alloy. The elements found to produce this effect were molybdenum, which formed the MoNi₃ intermetallic, and aluminum which formed AlNi₃. All these techniques stated above, improved either the discharge capacities or cycle life of the battery to varying degrees, yet each technique has its advantages and disadvantages. For

2: Literature Review

example, the microencapsulation technique requires high concentration of metal that does not take part in the storage of hydrogen, thus increasing the unit weight of the electrodes, while full coatings of other metals and metal oxides add to the cost of the electrode price. There are also safety issues associated with the use of fluorine [61].

Still low cost electrodes, rapid charge/discharge characteristics and oxidation resistant properties of the alloy needed improvement. Matthey technology found the process which improves the charge/discharge of the alloy and also protects the alloy from over charging/discharging which reduces the life time of the alloy. The solution is the deposition of the platinum group metals (PGMs) on the surface of the alloy which is the main focus of this study. The presence of the PGMs in the surface of the alloy enables the hydrogen to pass rapidly through the surface of the metal hydride alloy to the bulk, while still maintaining the hydrogen activity even after extensive exposure to the oxidizing environment [62]. The presence of the PGMs in the surface of the alloy enhances hydrogen absorption/desorption processes. The presence of both ruthenium and palladium shows rapid charge/discharge times to be obtained, as well as high resistance in deactivation even after long exposure to air.

It also improves the electrolytic charging/discharge characteristics of the AB₅ metal hydride electrode component in Ni-MH rechargeable batteries. Catalytic properties of PGMs in many aspects of physical science and engineering have been long appreciated. Palladium is a binary H₂ storage material which meets nearly all the ideal storage criteria. In addition to catalyzing H₂ dissociation in many reactions, it forms intermetallic hydrides. Recently, palladium has been used to modify the electrode surface it has been found to enhance discharge capacity [63].

2: Literature Review

2.9.5 Effects of catalyst deposition

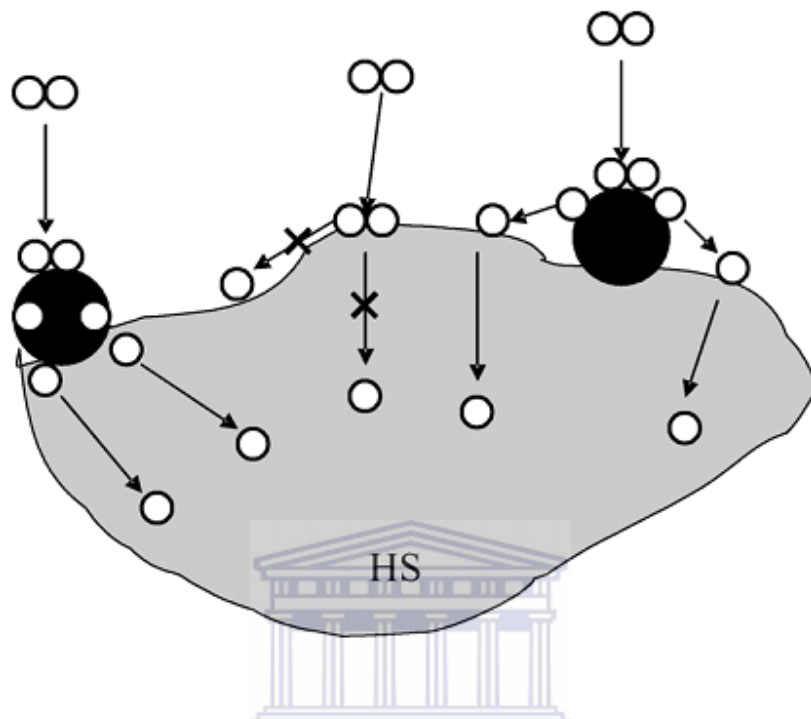


Figure 2.13: Schematic process for catalyst- enhanced H_2 storage. (OO) H_2 ; (O) H; ● catalyst; (HS) H_2 storage material [64]

Figure 2.13: shows schematic process for hydrogen storage with and without catalysts.

Generally, H_2 absorption by H_2 storage material is divided into the following steps:

1. H_2 molecules diffuse to the surface of the hydrogen storage materials.
2. H_2 molecules absorb onto the surface of hydrogen storage material.
3. H_2 molecules dissociate into hydrogen atoms on the surface of the hydrogen storage materials and the hydrogen atoms react with H_2 storage materials, or H_2 molecules directly react with hydrogen storage material.
4. H_2 atoms diffuse into the bulk material.

2: Literature Review

If the diffusion of the hydrogen molecules into the bulk material is considered as a fast step, the H_2 absorption is mainly determined by the materials ability to adsorb/dissociate the hydrogen molecules and to react with the H_2 molecule or atoms, and by the rate of H_2 diffusion into the bulk material.

Metal hydride materials form oxide films on their surfaces which inhibit hydrogen dissociation and penetration into the interstitial sites of the materials as mentioned earlier. Therefore, catalyst may be used to assist the adsorption and dissociation of H_2 molecules. Noble metals or Platinum Group Metals (PGMs) as known, such as Pd, Pt, or Ru which have strong ability to adsorb and dissociate H_2 , may be used as catalyst for hydriding/dehydriding on the H_2 storage material. With the aid of the PGM catalysts, the mechanism for H_2 uptake changes.

Because the catalyst has strong ability to adsorb hydrogen, H_2 molecule prefers to adsorb onto the catalyst surface. H_2 molecules dissociate into H atoms on the catalyst surface, and the dissociated hydrogen atoms spillover onto the surface of the hydrogen storage material. Finally, the dissociated H atoms react with the hydrogen storage material to form hydride or the intermediate catalyst hydride and the intermediate catalyst hydride react with the hydrogen storage material to form hydride and catalyst. Therefore, the catalytic effect of a catalyst is determined by its ability to adsorb/dissociate the H_2 molecule or react with hydrogen. The different catalytic effect of Pd, Pt, or Ru on the hydrogen uptake/release of the hydrogen storage material can be ascribed to the different ability of the catalyst to adsorb or dissociate or react with the hydrogen molecule [64].

2: Literature Review

2.9.6 Deposition Methods

The deposition of precious metals either chemically or electrochemically plays an important role in the development of technologies where these metals are used. Particularly, this is true in the area of electrodeposition as each method with different operating parameters such as temperature, pH and current density likely to produce different kinds of deposition structures. As PGMs are known to be good catalysts for various chemical and electrochemical reactions, the production of such catalytic surfaces with a range of particle sizes and surface area are of prime importance.

Electrochemical deposition is a versatile technique by which a thin desired metallic coating can be obtained by chemically reducing the metal ion or its complex on-to the surface of another metal by simple electrolysis of an aqueous solution containing the desired metal ion or its complex. Electroless deposition is a method of obtaining a desired coating by chemically reducing the metal ion or its complex on to the substrate in a controlled fashion.

These two processes distinctively differ in their reduction approaches. In the electrochemical method, reduction takes place by supplying current externally and the sites for the anodic and cathodic reactions are separated. For chemical deposition method, electrons required for the reduction are supplied by a reducing agent and the anodic/cathodic reactions are on the inseparable work piece. Moreover, these reactions proceed only on catalytically active surfaces, that is, newly coated metallic surfaces should be catalytically active enough to promote redox reactions. All the PGMs are catalytically active and can be deposited. Deposits obtained from both chemical and electrochemical processes have many applications [65]:

2: Literature Review

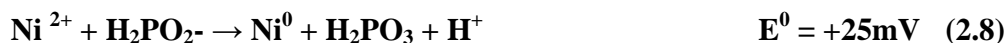
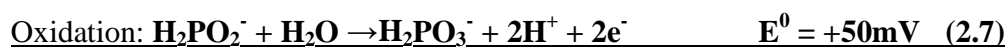
- Resistance against corrosion of underlying layers,
- Offer low resistance for the electrical contacts,
- Catalytic surfaces for the electrodes for chemical reaction.

Chemical deposition will be fully discussed, because it was employed in the investigation. The chemical deposition of a metal has an electrochemical mechanism, both oxidation and reduction (redox), reaction involving the transfer of electrons between reacting chemical species. The oxidation of the substance is characterized by the loss of electrons, while reduction is distinguished by gain of electrons. Further, oxidation describes an anodic process, whereas reduction indicates cathodic action.

The simplest form of chemical plating is the so called metal displacement reaction. Chemical plating displacement yield deposits limited only to a few micron in thickness, usually 1-3 μ m. Hence, chemical plating via the displacement process has few applications. In order to continually build the deposits by chemical means without consuming the substrate, it is less essential that a sustainable oxidation reaction be employed as an alternative to the dissolution of the substrate.

The deposition reaction must occur initially and exclusively on the substrate and subsequently continue to deposit on the initial deposit. The redox potential for this chemical process is usually more positive than that for metal being deposited by immersion. The chemical deposition of nickel by hypophosphite meets both the oxidation and redox potential criteria without changing the mass of the substrate:

2: Literature Review



Equation (2.8) is the sum of the oxidation and reduction equations [66].

Electroless deposition can also be defined as an autocatalytic process of depositing a metal in the absence of an external source of electrical current. The deposition is achieved by the incorporation of a reducing agent in the bath. The process is autocatalytic and proceeds on the newly formed catalytic active surface. The method has significant practical importance in modern technologies, the battery technologies and etc [67]. **Table 2.2** gives properties of various reducing agents used in electroless plating.

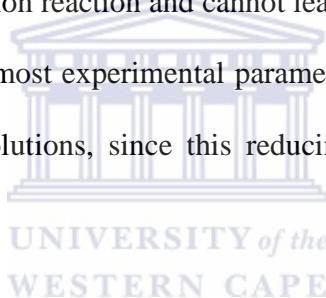
Table 2.2: Properties of Reducing Agents [68]

Reducing agent (no. of electrons available)	Representative chemical equation in the text	Redox potential at (vs. NHE) (V)
Sodium hypophosphite (2)	5	-1.40
Hydrazine (4)	2 (or 3)	-1.16
Dimethyl amine borane (DMAB) (6)	10	-1.20
Diethyl amine borane (DEAB) (6)	10	-1.10

2: Literature Review

Sodium borohydride (8)	8	-1.20
------------------------	---	-------

In the investigation Hydrazine and Hypophosphite were utilized as reducing agents for the deposition of both Pt and Pd on the alloy surfaces. Hydrazine is a powerful reducing agent that works both in acidic and alkaline media. It can reduce the higher valent metal ions to lower valent one or to zero valent state depending on the conditions of the reaction. Hydrazine is a stronger reducing agent in alkaline medium compared to acidic medium [67]. The main problem encountered is the limited stability of their baths towards time; they quickly decompose through a progressive homogeneous reduction reaction and cannot lead to industrial applications. Coating purity requires dictated choice of most experimental parameters. For example, use of hydrazine implies high pH value for the solutions, since this reducing agent is efficient only in basic conditions [69].



Hypophosphite is mainly used for Electroless Ni plating. With this method, a durable nickel-phosphorus film can coat objects with irregular surfaces. The metal usually gives to electroless deposits good mechanical and/or low temperature behavior. In addition, the film possesses a good surface hardness and abrasion resistance. Studies on hydrazine and hypophosphite baths showed that baths based on hypophosphite as reducing agent perform better in terms of stability and deposit quality [67].

2.9.7 Functionalization of the AB₅ MH surface

The surface modification is usually carried out by the Electroless deposition technique using multiple procedures which includes the steps of substrate surface cleaning, sensitization/activation, and autocatalytic reduction in a plating bath. This is a costly and time

2: Literature Review

consuming exercise, and the preparation of the uniform coatings is not guaranteed. Furthermore, the oxide layer, on the surface of the material inhibits interaction with PGM precursor ions in solution. Finally, PGM (e.g. Pd) colloidal particles have poor adhesion to the substrate because of the absence of chemical conjunction. This results in the decomposition of the plating bath as the PGM activation nuclei leach out into the solution [70].

An approach could be adopted to modify the MH prior deposition of PGM by the alteration of the surface chemical state (functionalization). This can be realized by the treatment of the substrate material with an aqueous solution of aminosilane. Water soluble aminosilane (for example, γ -aminopropyltriethoxysilane or γ -APTES) are known to improve adhesion on adsorbents (for example, based on alumina, silica, etc) in chromatographic studies and were identified as promising functionalizing agents, due to their commercial availability, high branching capacity, high flexibility, ability to polymerize, hydrophobicity, and ability to improve control of interfacial chemistry. The process is fully discussed in paper by M. Williams et al. [70].

AB₅ alloys (unmodified, Pt and Pd modified using reducing agents hydrazine and hypophosphite, and functionalization with APTES will be compared in the investigation).

2.10 Conclusion of Literature Review

The literature review shows that one of the challenges facing the world today is the depletion of fossil fuels and environmental concerns to the harmful emission of these fuels. The current interest in hydrogen is primarily due to the facile production of H₂ from various renewable sources of energy and environmental friendliness. Storage of H₂ is the only hindrance to H₂ application as the energy source. Conventional storage mediums, Pressurized H₂ gas take great

2: Literature Review

deal of volume and condensed H_2 is too expensive to produce and maintain. There are safety issues concerning their application. From the literature review one can see that MH store hydrogen in solid form under moderate temperature and pressures, which gives them safety advantage; they are the best suitable option for hydrogen storage.

Electrochemical storage in different types of batteries is and will be an important way of intermediate storage of the energy. Ni-MH batteries are the perfect example of electrochemical storage because they employ metal hydrides as negative electrode in the battery. Attention was paid to AB_5 intermetallics, because, they are conventionally used in the battery and they have intermediate thermodynamic storage capacities. The drawback of AB_5 is that, it forms oxide films on the surface which hinders dissociation and penetration of H_2 in the interstitial sites, which reduces its storage capacity.

Electroless deposition of PGMs on the surface of the materials significantly improve activation and hydrogen sorption performances, also increases the electro-catalytic activity. The performance of these MH alloy is affected by numerous factors such as kinetics of the processes taking place at the metal-electrolyte interface and the H_2 diffusion within the bulk of the metal alloy particles. The hypothesis of the investigation is the development of prototype battery competitive in electrochemical performance to conventional Ni-MH batteries. AB_5 intermetallic hydrides have been chosen as the ideal material for the reasons mentioned above. The physico-chemical properties influencing their electro-activity and their characterization will be studied. Analytical tools utilized in the characterization study are discussed and reviewed in detail in *Chapter three*. The principles in their operation, sample preparation and experimental parameters are also discussed.

3: Experimental

3: Chapter Three

3.1 Introduction

After the preparation of MH alloys, their characterization is the rational step proceeding to their application. The MH alloys are subjected to special characterization challenges; and the purpose of elaborating MH electrodes using various electrochemical techniques can be summarized as follows:

- Characterize the cycle life behavior; that is to understand how the corrosion processes deteriorates the metal hydride forming alloy.
- Characterize kinetics of electrodes; understand model process and sub-processes involved in the hydrogen absorption/desorption process. It is of great importance to understand how different substitution elements act during this process, and how to apply systematic search for applicable catalysts.
- Characterize the hydrogen diffusion in the H₂ storage alloy in the electrode and understand the influence of the H₂ storage alloy composition.
- Characterize the transport of ions in the porous electrode structure and understand the influence of the electrode construction and using this knowledge to maximize heat, electrons and ion flow rates in the electrode [30].

The characterization of the physical and chemical properties of the alloys forms a starting point for the optimization, in order to achieve cost-reduction and high electrocatalytic performance of the alloy. This chapter is dedicated to designing the experimental approach to the characterization of AB₅ MH alloys.

3: Experimental

3.2 Materials and Methods

3.2.1 Materials

The materials used in this study and their suppliers are listed in table 3.1

Table 3.1: List of materials used in the study

Material	Supplier
AB ₅ (DH ₄)	Guangzhou Research Institute for Non-Ferrous Metals
Vulcan XC-72	CABOT CORPORATION
KOH	KIMIX
Hydrochloric Acid (HCl)	KIMIX
Nitric Acid (HNO ₃)	KIMIX
Platinum 1000ppm	B & M Scientific
Palladium 1000ppm	B & M Scientific
Polytetraflouroethylene (PTFE)	ElectroChem. Inc.

3: Experimental

3.2.2 Methods

Commercial AB₅ hydriding alloy material obtained from Guangzhou Research Institute for Non-Ferrous Metals, China with composition ([La, Ce, Nd, Pr][Ni, Co, Al, Mn]₅ with trade mark DH₄ was employed as the parent material for this study. As mentioned in *Chapter 2*, AB₅ MH's have a tendency to naturally form oxide on their surfaces, which inhibits H₂ dissociation and penetration into the interstitial sites of the material, which reduces the capacity of the material. To redeem this, Matthey technology found the process which improves the charge/discharge of the alloy and also protects the alloy from over charging/discharging, which reduces the life time of the alloy. And the process is the deposition of the platinum group metals (PGMs) on the surface of the alloy material [62]. The MH alloys were microencapsulated by Dr M. Williams employing a method used by D. Barsellini et.al [71]. The alloy powder particles were coated with Pd and Pt by electroless deposition using reducing agents such as hypophosphite, hydrazine. The conditions of the bath are given in **table 3.2**.

Table 3.2 Bath composition

Reagent	Formula	Palladium bath [67]	Nickel bath [72]	Copper bath [73]	Function
Palladium Chloride	PdCl ₂	0.2g/100mL	-	-	Metal Salt Precursor
Chloroplatinic acid	H ₂ PtCl ₆ .6H ₂ O	0.2g/100mL	-	-	Metal Salt Precursor

3: Experimental

Hydrochloric acid	HCl (32%)	0.4mL/100mL	-	-	Competing agent
Ammonia hydroxide	NH ₄ OH (28%)	16mL/100mL	-	-	Complexing agent
Ammonium Chloride	NH ₄ Cl	2.7g/100mL	-	-	Bath Stabilizer
Sodium Hypophosphite	Na ₂ PO ₂ .H ₂ O	1g/100mL	0.5g/100mL	3.5g/100mL	Reducing agent
Nickel Chloride Hexahydrate	NiCl ₂ .6H ₂ O	-	0.15g/100mL	-	Metal salt precursor
Disodium ethylenediamine tetra acetic acid	Na ₂ EDTA	-	1.5g/100mL	-	Complexing agent
Nickel sulphate hexahydrate	NiSO ₄ .6H ₂ O	-	1.2g/100mL	0.16g/100mL	Metal salt precursor/catalyst
Sodium citrate	Na ₃ C ₆ H ₅ O ₇ .2 H ₂ O	-	0.1g/100mL	2.5g/100mL	Complexing agent
Copper Sulphate	CuSO ₄	-	-	1g/100mL	Metal Salt precursor

3: Experimental

Boric Acid	H ₃ BO ₃	-	-	3.5g/100mL	Bath stabilizer
pH	-	9.8 ± 2.0	9.0	10	-
Temperature (°C)	-	50	50	70	-
Plating rate (μm/hr)	-	2.5	-	-	-

3.3. Instrument and Techniques used in the Characterization of AB₅ MH H₂ Storage Alloy

In the characterization and evaluation of H₂ storage capacity, H₂ absorption/desorption kinetics and cyclic stability of MH and other H₂ storage materials, the following techniques have been proven to be useful, and will be used to investigate the properties of the AB₅ MH H₂ storage alloy.

- X-Ray Diffractometry (XRD)
- Scanning Electron Microscopy (SEM)
- Energy Dispersive X-ray Spectroscopy (EDS)
- Atomic Absorption spectroscopy (AAS)

Electrochemical characterization of Metal hydrides

- Cyclic Voltammetry (CV)
- Chronopotentiometry, and
- Electrochemical Impedance Spectroscopy (EIS)

3: Experimental

3.3.1 X-Ray Diffractometry

X-Ray Diffractometry (XRD) is a rapid analytical technique primarily used for phase identification of a crystalline material and can provide information on unit cell dimensions. It is one of the most important non-destructive tools to analyze all kinds of matter ranging from fluids, to powders and crystals. For the purpose of this study, XRD was used to investigate the crystalline structure, particle size and lattice parameters of the sample material.

In the XRD the analyzed material is finely ground, homogenized and average bulk composition is determined and it is based on constructive interference of monochromatic X-rays and a crystalline sample. The X-rays are generated by the cathode ray tube, filtered to produce monochromatic X-rays, collimate to concentrate, and direct towards the sample. **Figure 3.1** shows a schematic diagram of an x-ray diffraction.

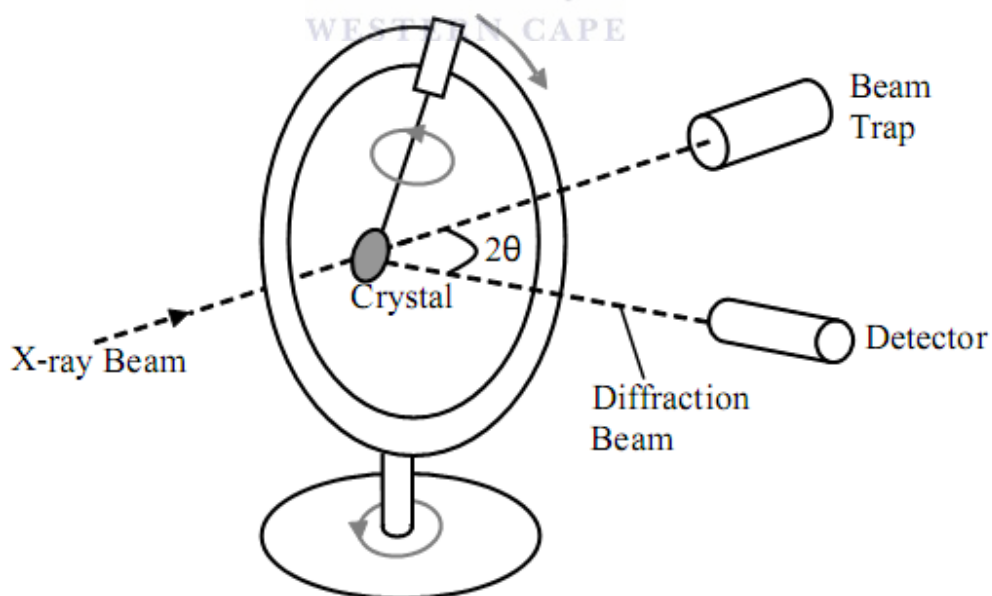


Figure 3.1: Schematic of an X-ray Diffractometer [74]

3: Experimental

The interaction of incident rays with the sample produces constructive interference (and a diffracted ray) when conditions satisfy the Bragg's law

$$n\lambda = 2d \sin \theta \quad (3.1)$$

Where n is any integer

λ wavelength of the beam

d spacing between diffraction planes

θ incident angle

This law relates the wavelength of electromagnetic radiation to the diffraction angle and the lattice spacing in a crystalline sample. These diffracted X-rays can then be detected, processed and counted. By scanning the sample through a range of 2θ angles, all possible diffraction directions of the lattice should be attained due to the random orientation of the powder material [75].

The peaks in an x-ray diffraction pattern are directly related to the atomic distance which can be explained using geometry **Figure 3.2**.

3: Experimental

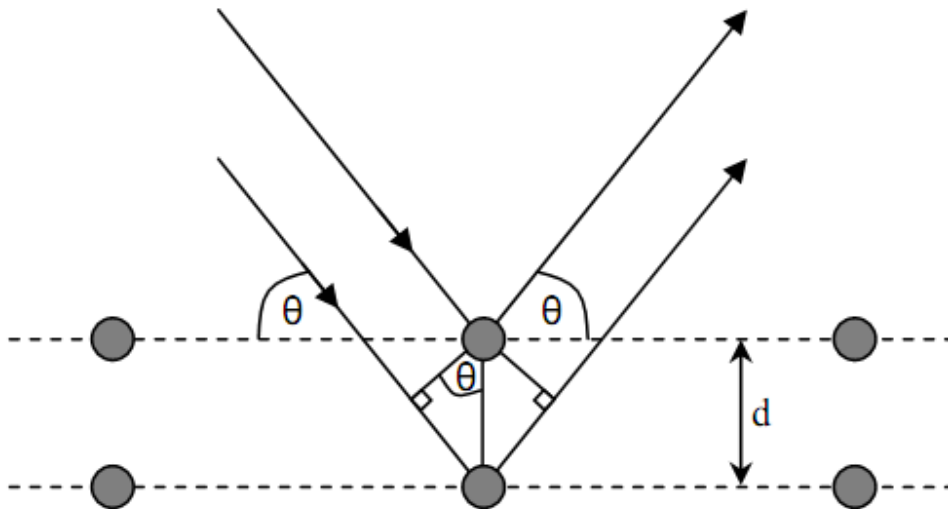


Figure 3.2: Geometrical representation of Bragg's Law [76]

In a diffraction pattern from a crystal lattice, a number of reflections are generated, each one being associated to a lattice plane (identified by the Miller indices $\mathbf{h, k, l}$), and occurring at an angular position (2θ) depending on the related interplanar spacing ($d(\mathbf{hkl})$), and on the x-ray wavelength (λ), as defined by the Bragg's Law as stated above. A diffraction pattern contains a lot of structural information: like the angular position of the reflections is related to the size and shape of the unit cell (repeating unit cell of crystal) while intensities reflect the lattice symmetry and the electron density (practically the position and types of atoms) within the unit cell. Diffractograms are unique for different materials, and can be quantitatively used as material identification [77].

XRD can also be used quantitatively for the determination of average particle size by using the Scherrer equation, given as:

$$D = \frac{0.9\lambda}{\beta \cos \theta} \quad (3.2)$$

Where D is the particle size

3: Experimental

0.9 is the shape factor

λ is the x-ray wavelength, typically 1.54\AA

β is the peak width at half peak height in radians,

θ is the angle of reflection

Lattice parameter (a_0) can be calculated using the following equation:

$$a_0 = d[(h^2 + k^2 + l^2)]^{1/2} \quad (3.3)$$

Where hkl are Miller indices, d is the interlinear spacing determined using Bragg's Law.

In the XRD analysis dry metal hydride alloy sample were mounted in the plastic sample holders and the surface was flattened to allow maximum X-ray exposure. The experiments were conducted using the Siemens D8 Advance (Brukes AXS) X-Ray Diffractometer. The operational parameters were as follows:

Table 3.3: XRD Operational Parameters

Tube	Copper K-Alpha
Detector	PSD Vantec-1, Gas Detector with 1600 chambers
Monochromator	None
Generator Operation	40kV and 40mA
X-Ray source	Cu $K\alpha$ ($\lambda K\alpha_1 = 1.5406\text{\AA}$)
Current (mA)	40
Scan range (2θ)	20-100

3: Experimental

3.3.2 Scanning Electron Microscopy

Scanning Electron Microscopy (SEM) is a type of electron microscope that images the sample surface by scanning it with high energy beam of electrons in a raster scan pattern. The electrons interact with the atoms that make up the sample producing signals that contain information about the samples surface topography, composition and other properties such as electrical conductivity. The types of electrons produced by SEM include secondary electrons, back-scattering electrons (BSE), characteristic x-rays, light, specimen current and transmitted electrons [78].

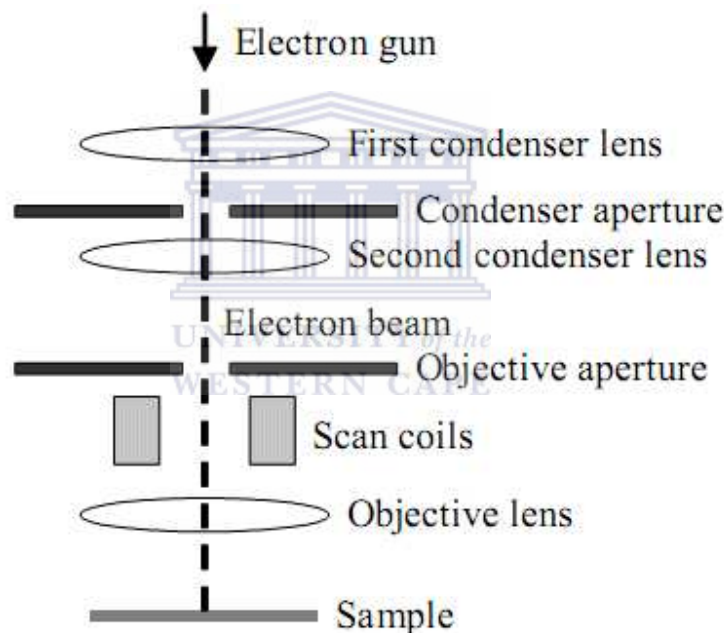


Figure 3.3: Basic schematic of a typical SEM [79]

In SEM, an electron beam is scanned across a samples surface. When the electrons strike the sample, a variety of signals are generated, and it is the detection of specific signals which produces an image or a sample's elemental composition. Secondary electrons are emitted from the atoms occupying the top surface and produce an interpretable image of the surface. The

3: Experimental

contrast in the image is determined by the sample morphology. A high resolution image can be obtained because of the small diameter of the primary electron beam.

Backscattering electrons are primary beam electrons which are reflected from the atom solid. The contrast in the image produced is determined by the atomic number of the elements in the sample. The image will therefore show the distribution of the chemical phases in the sample, and the resolution in the image is not as good for the secondary electrons as the backscattering. Interaction of the primary beam in the sample causes shell transitions which result in the emission of an X-ray. The emitted X-ray has an energy characteristic of the parent element. Detection and measurement of the energy permits elemental analysis Energy Diffraction Spectroscopy (EDS) [80].

All the prepared sample materials were characterized using scanning electron microscopy (NOVA NANO SEM230 FEI, working distance = 51-49mm, accelerating voltage = 15.0-16.7kV). Carbon glue was spread on the stub and the sample was mounted. No sputter coatings were required as the sample was electron-conductive. Samples were fitted in the vacuum chamber of the microscope and analysis was conducted.

3: Experimental

3.3.3 Energy Diffraction Spectroscopy

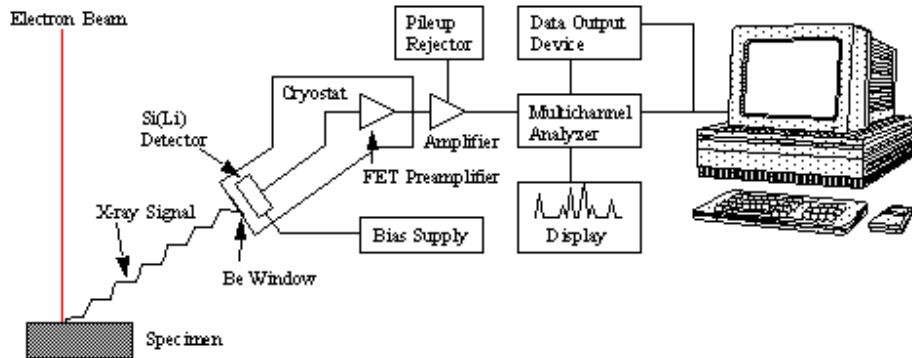


Figure 3.4: Schematic Representation of an energy-dispersive spectrometer [81]

Energy Diffraction Spectroscopy (EDS) is an analytical technique used for elemental analysis or chemical characterization of the sample. It is one of the variations of X-Ray Fluorescence (XRF). As a type of spectroscopy, it relies on the investigation of a sample through interactions between electromagnetic radiation and matter, analyzing x-rays emitted by the matter in response to being hit with charge particles [82].

The technique utilizes a SEM, a type of high magnification microscopy in which the sample is bombarded by electrons. The resultant pattern of the electrons reflection by the sample is used to generate a detailed three dimensional appearing surface view. At the heat of the energy dispersive spectroscopy are X-rays. During electron bombardment, electrons are also ejected from the surface atom of the sample. The resulting electron vacancy is filled by a higher energy electron. To maintain the energy balance of the atom, some energy must be released. The energy is released as X-rays; the released X-rays are gathered by a detector positioned above the sample. Because the energy of the X-rays will vary, depending on the element from which they were released, analysis of the X-ray spectrum can permit the various elements comprising a sample to

3: Experimental

be identified. The X-ray spectrum is graphically displayed as a series of peaks. The pattern of peaks is a fingerprint of the specific elements in a specimen [83].

Energy Dispersion Spectroscopy was employed to determine how much of the Palladium and Platinum have been loaded in the surface-modified AB₅ alloy material (Real time(s) = 65.09, Livetime (s) =60.00. The same SEM instrument was employed for the EDX results. Different readings with EDS were performed on each of the AB₅ alloys and the average was taken.

3.3.4 Atomic Absorption Spectroscopy (AAS)

Flame atomic absorption spectroscopy is a very common technique for detecting metals and metalloids in solid and aqueous samples. It is very reliable and simple to use. The technique is based on the fact that ground state metals absorb light at specific wavelengths [80, 84]. All atoms and their components have energy. Unless excited in their most stable state; their ground states they do not have the energy. The application of energy such as thermal or electromagnetic radiation can change energy state of an atom, increasing it to an excited state.

In theory, there are infinite numbers of excited states, however, the higher the excited state the lower the number of atoms from a given population that have enough energy to reach each level [85]. These energy states are not continuous but separated by discrete energy gaps known as quantum transitions. The transition from the ground state (E_0) to the first excited state (E_1) requires atoms to absorb energy ($\Delta E_{0 \rightarrow 1}$) to relax from the excited state an equivalent amount of energy must be emitted (**Fig. 3.5**). Every element has specific ΔE that they will absorb and emit which correspond to specific wavelengths of electro-magnetic spectrum.

3: Experimental

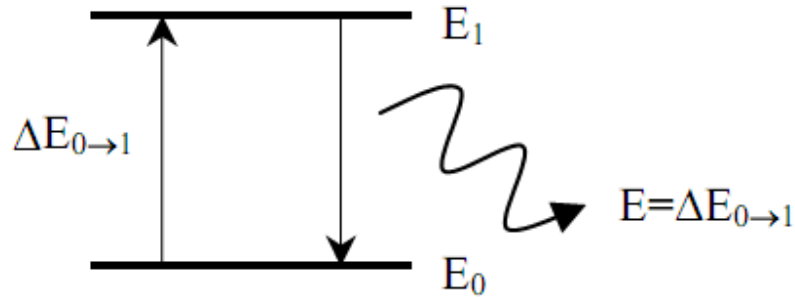


Figure 3.5: Energy diagram of an atom showing excitation to the first excited state followed by relaxation to the ground state by the emission of an electro-magnetic wave

The relationship between energy transition and wavelength (λ) is described by **Equation (3.4)** where **h** is the Planck's constant [86].

$$\Delta E = \frac{h\nu}{\lambda} \quad (3.4)$$

A flame atomic absorption spectrometer consists of a hollow cathode lamp, a nebulizer, the flame, a monochromator and a photomultiplier tube **Fig. 3.5** [87]. The hollow lamp uses a cathode made of element of interest with a low internal pressure of an inert gas. A low electrical current is used to excite the elements causing it to emit a few spectral lines of characteristic wavelength, providing a constant and intense analytical line for the analysis. Samples are introduced into the instrument through the nebulizer and are vaporized in the acetylene flame. The flame destroys any molecules and breaks down complexes creating the atomized form of elements. The total absorbance is stated by Beer Lambert's Law **Equation (3.5)** where **A** is the measured absorbance, ϵ is a wavelength-dependent absorptivity coefficient, **b** is the path length, and **c** is the analyte concentration.

$$A = \epsilon bc \quad (3.5)$$

3: Experimental

The light then passes through a monochromator in order to remove scattered light of other wavelengths from the flame and is detected using a photomultiplier tube. The analyte concentration is determined from the amount of absorption. Concentration measurements are usually determined from a working curve after calibrating the instrument with standards of known concentration.

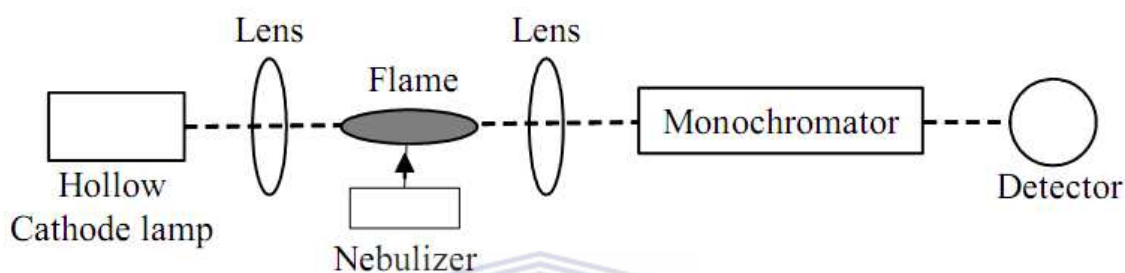


Figure 3.6: Basic Schematic for a typical Atomic Absorption Spectroscopy [88]

To determine the total amount of Palladium and Platinum in the surface modified AB₅ sample Atomic Absorption Spectrometry was employed. The samples were obtained by digesting in aqua regia. The aqua regia was prepared using 3:1 (HCL: HNO₃). The samples were digested by taking 1g sample mix with 50ml aqua regia and digested at 50°C, stirred at 300rpm for 30min, filtered twice and made up to the mark with ultra pure water in 100ml volumetric flask. Standard Preparation was done using commercial stork solution for both Pd and Pt.

AAS; Philips PU9100 instrument was employed and operational parameters were as follows:

1. Palladium

- λ = 247.6 nm
- Band-pass = 0.2nm
- Lamp current = 12mA

3: Experimental

2. Platinum

- λ = 265.9 nm
- Band-pass = 0.5
- Lamp current = 12mA

3.4 Electrochemical Characterization techniques of MH alloys

The majority of heterogeneous catalyst applied in everyday research and application are powdered materials that cannot directly be used in electrochemical measurements. By using composite electrodes where the catalyst is mixed with a binder and graphite, it is possible to make electrochemical composite like carbons, minerals and metal placed on conductive and non-conductive supports [89]. Application of binders has a dual effect on the results of the measurement.

On the one hand, it is impossible to prepare an electrode without a binder, while on the other hand this binder can cover some fraction of metal particles, or mover, too large amount of binder can create pellet areas that are non-permeable for the solution. A Teflon-bound electrode technique with graphite addition and a number of modifications was chosen in the present study. The main disadvantage of this technique is the possibility to measure the surface area metals on non-conductive support, which is a typical case in heterogeneous catalysis. It is necessary to mention that graphite can very easily stick to parts of the press. In order to prevent this, platinum mesh was used in between the press and the graphite [90].

The composition of the alloy investigated was $\text{La}_{0.4} \text{Ce}_{0.48} (\text{Nd}, \text{Pr})_{0.16} \text{Ni}_{3.34} \text{Co}_{0.64} \text{Al}_{0.63} \text{Mn}_{0.58}$ confirmed by M. Williams et.al [70]. The MH electrodes were prepared using a method used by Barsellini et.al [71].

3: Experimental

3.4.1 Preparation of Metal Hydride Electrodes

1. 0.150g MH powder + 0.150g teflonised Vulcan XC-72 (33wt% PTFE)
2. Mixed powder sandwiched between two nickel mesh disks
3. Apply pressure as follows:
5 tons – 10 minutes
10 tons – 30 minutes

The carbon black and the polytetrafluoroethylene were grinded using an agate mortar and pestle and the mixture was sandwiched between two nickel mesh discs. The sandwich was pressed using a die in a presser 5tons for 10min and 10tons for 30min without vacuum as mentioned above. Electrochemical measurements were done in a three electrode cell in 6mol.L^{-1} KOH, with Ni mesh counter electrode and an Hg/HgO reference electrode. Electrochemical investigations were performed with an Autolab PGSTAT 30 (Eco Chemie BV, Netherlands) at room temperature. For all the electrochemical methods, the samples preparation was the same, unless stated otherwise. The KOH electrolyte was deaerated by N_2 -bubbling. Before any measurements were taken the electrode was activated during 20 charge/discharge cycles.

3.4.2 Voltammetry

Voltammetry is a category of electroanalytical methods used in analytical chemistry and various industrial processes. The term voltammetry is used to describe the process of measuring the current passed through an electrolytic system as a function of applied voltage. This technique is used in many methods where information about the analyte is determined from the measurement of this current as a function of applied potential under polarization of the indicator or working electrode.

3: Experimental

Voltammetry is widely used by inorganic, physical and biological chemists for non-analytical measurements such as fundamental studies of oxidation-reduction processes in various electrolytes, adsorption processes on surface, and electron-transfer mechanisms at chemically modified electrode surfaces and pharmaceutical applications. If a potential is applied across two electrodes immersed in an electrolyte, a current is generated due to the reduction of the analyte at an electrode surface.

In practice the voltage is scanned and the resulting current presented as a curve relating current to applied voltage. The applied potential must reach a value that is sufficient to initiate the redox reaction which results in the initiation or an increase in the current flowing through the cell, a process that has been defined as electrolysis. The electrochemical reactions can be completely controlled by varying the applied potential.

Generally, the electrodes used in voltammetry are either milli-electrodes, having surface area of less than a few square millimeters or microelectrodes having surface area of less than a square micrometers [91]. There are a number of voltammetry techniques employed in analytical chemistry which, among others, include linear scan voltammetry, pulsed voltammetry, cyclic voltammetry, stripping voltammetry, chronoamperometry and polarography. We will refer particularly to chronopotentiometry, cyclic voltammetry, and electrochemical impedance spectroscopy since they are employed in the investigation.

3.4.2.1 Cyclic Voltammetry

Cyclic voltammetry is widely used as an electroanalytical technique in electrochemistry and many other fields such as inorganic chemistry, organic chemistry and biochemistry. CV is

3: Experimental

performed using a potentiostat, which consists of the necessary electric circuits, a working electrode, a reference electrode and counter electrode and an electrolyte [92].

In cyclic voltammetry, the electrode potential is ramped linearly versus time. This ramping is known as the experiment's scan rate (V/s). The potential is measured between the reference electrode and the working electrode and the current is measured between the working electrode and the counter electrode. This data is then plotted as current (i) vs. potential (E). The forward scan produces a current peak for any analyte that can be reduced (or oxidized depending on the initial scan direction) through the range of the potential scanned.

The current will increase as the potential reaches the reduction potential of the analyte, but then falls off as the concentration of the analyte is depleted close to the electrode surface. If the redox couple is reversible, then when the applied potential is reversed, it will reach the potential that will re-oxidize the product formed in the first reduction reaction, and produce a current of reverse polarity from the forward scan.

This oxidation peak will usually have a similar shape to the reduction peak. As a result, information about the redox potential and electrochemical reaction rates of the compounds is obtained [93]. CV is a popular technique in electrochemical studies in general and specially to obtain information about the kinetics and mechanism of the electrode reaction. CV is used in this study in the analysis of metal electrodes, and in the determination of the electrochemically-active surface area of metal hydride pellet electrodes. It is also used in the study of electrode surface reactions, the behavior of electrochemically-active species, and to investigate the quality of the electrocatalysts. The alloy electrodes were cycled at 1mV/s between -0.4 and -1.3V.

3: Experimental

3.4.2.2 Galvanostatic Charging and Discharging

In the situation of galvanostatic experiments a controlled, constant current is applied to the working electrode and the resulting working electrode potential is measured. This technique is also called a chronopotentiometric technique, as the voltage is recorded in time. The experimental set up for these types of experiment is schematically depicted in Figure 3.7.

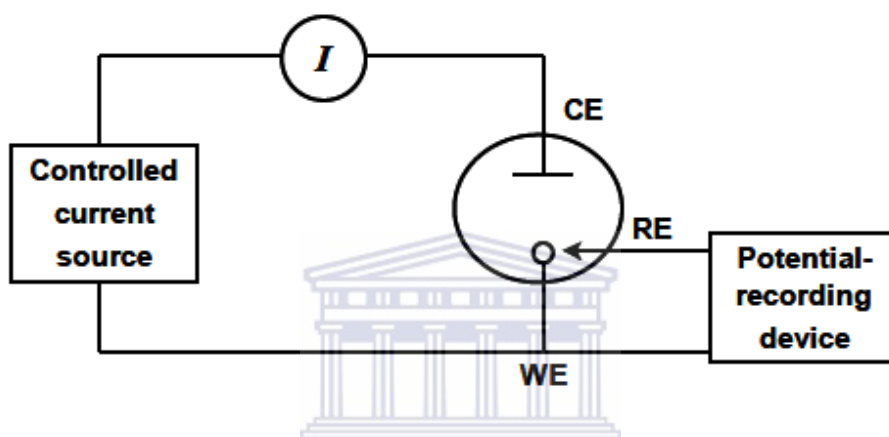


Figure 3.7: Simplified block diagram of chronopotentiometric measurement device. The working, counter, and reference electrode are denoted as WE, CE and RE, respectively [94].

The current applied to the electrode causes reactants at the electrode surface to react. The potential of the working electrode changes to value characteristic of the electrochemical reaction that is occurring. Galvanostatic experiments provide a means of gain information about the charge and discharge capacities of electrode material. For example, as the discharge current is constant in time, the multiplication of the applied current and the charging time will yield exact amount of charge transferred during a particular potential response of the working electrode. This allows, for the fact that, for example, the H_2 concentration in a hydride forming compound can be precisely tuned, as ideally one electron is transferred per H_2 atom stored [95].

3: Experimental

Chronopotentiometry was employed to electrochemically test the sample electrodes by charge and discharge rates. The electrochemical testing of the electrode was carried out by charging the electrode with a cathodic current 300mAh/g and discharged with an anodic current of the same magnitude to the cut off potential -7mV vs Hg/HgO. Five minutes breaks were given in-between the charge/ discharge cycles.

3.4.2.3 Electrochemical Impedance Spectroscopy (EIS)

Impedance Spectroscopy is widely recognized as a versatile technique to obtain detailed information on ion and electron transport [96]. Impedance spectroscopy is also called AC Impedance or just Impedance Spectroscopy. The usefulness of impedance spectroscopy lies in the ability to distinguish the dielectric and electric properties of individual contributions of components under investigation. Impedance characterization can be used to provide information on the overall reaction rate as well as a rate and the significance of the sub-processes. This provides important information about the kinetics and the reaction mechanism.

Impedance analysis of the metal hydride electrode is an established characterization technique. Furthermore, the EIS technique provides non-destructive methods for investigating the electrochemical properties of the electrode, as all data are obtained with minimum polarization (i.e. change in the state of charge) of the electrode. EIS is one of the most sensitive electrochemical techniques, but is usually not sufficient to solve all the questions which exist with regards to kinetics. Like any other electrochemical techniques impedance spectroscopy cannot be regarded as a 'stand-alone' method for model identification because the response of a system to a periodic perturbation does not provide a direct measure of the governing physical

3: Experimental

phenomena. Impedance characterization of metal hydride electrodes generally makes use of equivalent circuits for interpretation of data [97].

EIS can also provide time dependent information about the properties, but also about ongoing processes such as corrosion or the discharge of batteries, and for example, the electrochemical reaction in fuel cells, batteries or any other electrochemical process.

Advantages of EIS Technique

1. Useful on high resistance materials such as paint and coatings
2. Time dependent data is available
3. Non-Destructive
4. Quantitative data available
5. Use service environments



Disadvantages of EIS Technique

1. Expensive
2. Complex data analysis for quantification

Impedance characterization can be used to provide the following information:

- The overall reaction rate
- The rate of sub processes. An important characteristic of this technique is that the kinetic contribution from sub processes can to a certain extent be separated and evaluated independently. This provides important information about the reaction mechanism; and
- The rate of the overall reaction and the various sub processes as a function of the state of charge

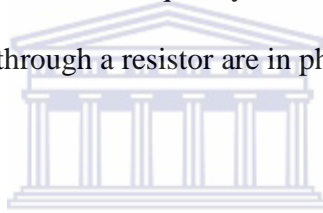
3: Experimental

The concept of electrical resistance is a common one in scientific research. It is the ability of a circuit element to resist the flow of electrical current. Ohm's Law defines resistance in terms of ratio between Voltage **E** and Current **I**.

$$\mathbf{R} = \frac{\mathbf{Et}}{\mathbf{It}} \quad (3.6)$$

The relationship is limited to only one circuit element the ideal resistor. An ideal resistor has several simplifying properties:

- It follows Ohm's law at all current and voltage levels
- Its resistance value is independent of frequency
- AC current voltage signals through a resistor are in phase with each other



The real world contains circuit elements that exhibit much more complex behavior. These elements force us to abandon the simple concept of resistance. In its place we use impedance, which is a more general circuit parameter. Like resistance, impedance is a measure of the ability of a circuit to resist the flow of electrical current. Unlike resistance, impedance is not limited by the simplifying properties listed above.

Electrochemical Impedance Spectroscopy is usually measured by applying an AC potential to an electrochemical cell measuring the current through the cell. Suppose that we apply a sinusoidal potential excitation, the response to this potential is an AC current signal, containing the excitation frequency and its harmonics. EIS is normally measured using a small excitation signal of 10 to 50mV. The excitation signal expressed as a function time, has the form

3: Experimental

$$E_t = E_0 \sin(\omega t) \quad (3.7)$$

E_0 is the potential time E_0 is the amplitude of the signal, and ω is the radial frequency. The relationship between radial frequency ω (expressed in radians/seconds) and the frequency f (expressed in hertz) is: $\omega = 2\pi f$.

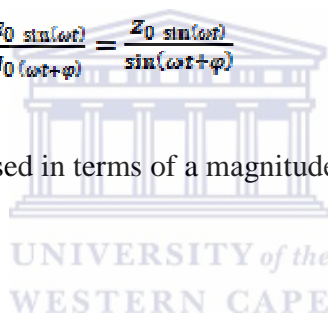
In a linear system, the response signal, I_t , is shifted in phase (δ) and has a different amplitude,

$$I_0 : I_t = I_0 \sin(\omega t + \varphi) \quad (3.8)$$

An expression analogous to Ohm's law allows us to calculate the impedance of a system as:

$$Z = \frac{E_t}{I_t} = \frac{E_0 \sin(\omega t)}{I_0 \sin(\omega t + \varphi)} = \frac{Z_0 \sin(\omega t)}{\sin(\omega t + \varphi)} \quad (3.9)$$

The impedance is therefore expressed in terms of a magnitude (modulus) $|Z|$, and a phase shift, φ



Using Euler relationship,

$$\exp(j\varphi) = \cos \varphi + j \sin \varphi \quad (3.10)$$

It is possible to express the impedance as a complex function. The potential is described as,

$$E_t = E_0 \exp(j\omega t) \quad (3.11)$$

And the current response as,

$$I_t = \exp(j\omega t - \varphi) \quad (3.12)$$

3: Experimental

The impedance is the represented as a complex number,

$$Z_{(\omega)} = \frac{E}{I} = Z_0 \exp(j\varphi) = Z_0 (\cos \varphi + j \sin \varphi) \quad (3.13) [98]$$

EIS in the investigation was utilized in combination with other characterization methods (CV) to obtain more thorough understanding of change in kinetic properties of MH electrodes with charge discharge cycling. A frequency range from 10kHz to 0.1mHz using amplitude 5mV for the whole frequency range, six frequencies per decade was employed for the EIS investigation; applying a computer controlled AUTOLAB PGSTAT 30 coupled with Frequency Analyzer (FRA) for running the Impedance studies. Electrochemical impedance measurements were conducted on a fully charged hydride electrode.

3.5 Conclusion

A series of analytical techniques were employed in the investigation for the characterization of the AB₅ MH alloy material. These analytical tools addressed the minimum set of physical and chemical properties identified in the literature review. The chapter initiated with the investigation of structural properties of the MH using fundamental characterization techniques. XRD to characterize the microstructure and the lattice parameters, SEM surface morphologies, EDS the total amount of the PGM deposited on the alloy surface and AAS to compare with EDS. Electrochemical characterization started with galvanostatic charging and discharging to test the stability of the alloy. CV and EIS measurements were utilized to check the activity of the alloy. The chapter shows the methods and techniques used in experimental approach designed to characterize the AB₅ MH alloys. The results of the experimental task that were conducted for evaluating the characterization tools discussed in chapter 3 are presented in Chapter 4.

4: Chapter Four

4.Chapter Four

4.1 Results and Discussion

4.1.1 Structural Characterization of AB₅-type MH Alloy Surface Modified with Pt and Pd Catalysts

Investigation on the AB₅ type H₂ storage material are in progress in order to further improve the material in electrochemical characteristics. The investigation initiates with structural characterization studies of modified and unmodified AB₅ electrodes. The electrochemical properties are correlated with structural study of the AB₅ MH electrodes. The chapter evaluates the investigation of structural properties of such electrodes using the experimental task formulated in the literature review of chapter two and methodologies given in chapter three.

Electroless deposition of PGMs on the surface of the materials removes the oxide increase, and also improves catalytic activity of the alloy which significantly improves the performance of the MH alloy. Electroless deposition of Pt and Pd catalysts was done using sodium hypophosphite based electroless plating bath. The effect of the PGMs on the morphology and kinetic properties of the AB₅ alloy were investigated. Comparing the findings, the catalyst with better performance between Pt and Pd was chosen, and used as a suitable catalyst for AB₅ MH alloys modification.

X-ray Diffractometry was used to characterize the microstructure and measure the lattice parameters of the metal hydride alloys with and without platinum or palladium. The X-Ray spectra was analyzed by the powder cell 2.4 software in order to calculate the lattice parameters and also perform phase identification on the MH alloy. The lattice parameters were calculated by the standard procedure in the software and all the visible peaks were used. The results show that

4: Chapter Four

the alloy presents hexagonal CaCu_5 -type structure of symmetry $P6/mmm$. No extra phases were observed evidencing that the structure is a single phase, as shown in **Figure 4.1**. The lattice parameters were measured and found to be $a=4.9966$ and $c=4.0473$.

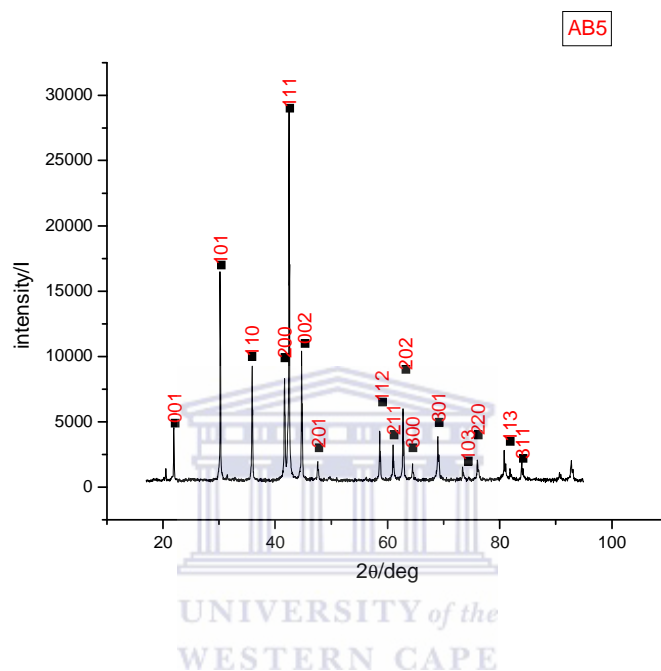


Figure 4.1: XRD Spectrum of AB₅ unmodified alloy

Figure 4.2 shows diffraction patterns for AB₅_unmodified, AB₅_Pd_modified and AB₅_Pt_modified alloys. All the diffraction patterns of the AB₅-type MH alloy, surface modified by Pd and Pt coatings utilizing NaH_2PO_2 -based bath showed that the crystal symmetry was the same in these materials as in the master alloy. This can be seen by comparing **Figure 4.2** a), b), and c). These diagrams also show that the position of the diffraction peaks for the modified material did not change significantly. The lattice parameters are also the same.

4: Chapter Four

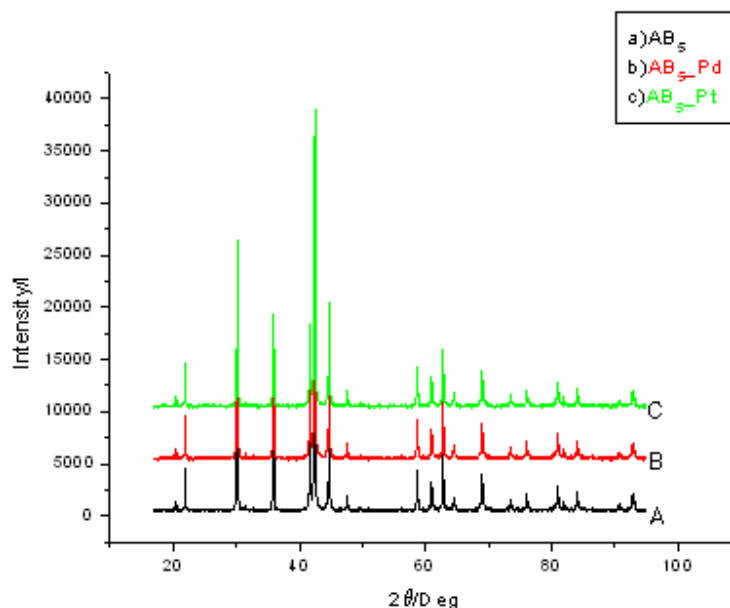


Figure 4.2: Diffractograms of a) unmodified, b) Pt modified and c) Pd modified AB_5 type MH

The measured XRD patterns did not show the presence of crystalline Pd which allows for the deduction of the amorphous nature of the Pd coating, and is due to the inclusion of phosphorus into the metal coating. Utilization of hypophosphite as reducing agent results in the incorporation of phosphorus or boron into the deposits [68]. In addition, the absence of peaks corresponding to the deposited Pd particles may result from the relatively low surface loadings of the metal on the surface of the AB_5 type intermetallic. As can be seen from the results, Pt modified alloy also exhibited the same behavior as Pd modified. This may be of consequence, because of similarities between chemical properties of the two metals.

4: Chapter Four

4.1.2 Morphological Studies of AB₅ MH Alloy Surface Modified with Pt and Pd Catalysts

Scanning Electron Microscopy (SEM) was used to investigate morphology of the AB₅ MH alloy. SEM is more powerful as compared to ordinary microscope. The combination of higher magnification, large depth of focus, greater resolution, and ease of sample observation makes SEM one of the basic research tools [99]. The surface morphologies of the unmodified and surface modified AB₅ type intermetallic are shown in **Figure 4.3**. The unmodified alloy was composed of relatively smooth surfaces.

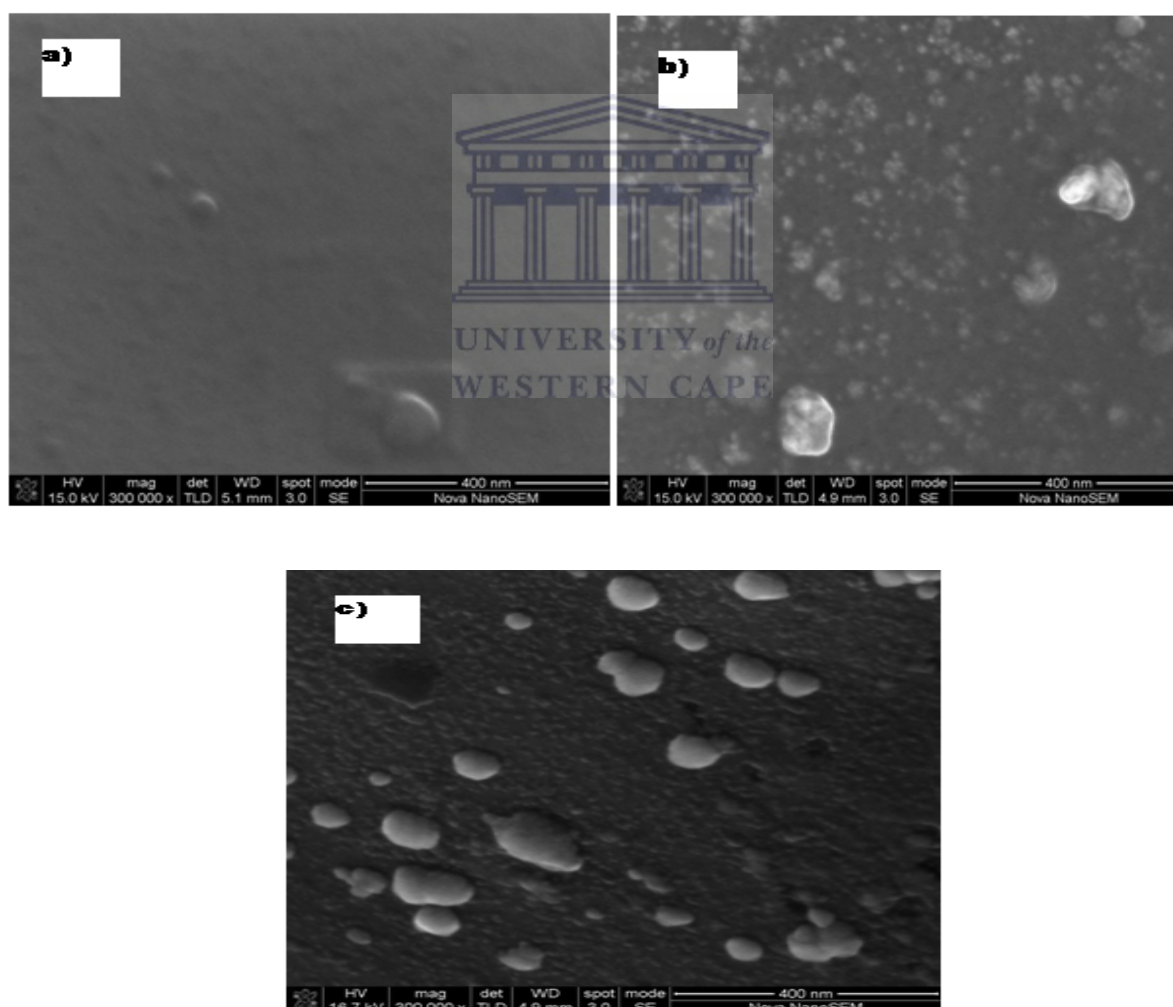


Figure 4.3: SEM images a) unmodified AB₅, b) Pt-modified AB₅, and c) Pd-modified AB₅

4: Chapter Four

Figure 4.3 b) and c) show the change in the surface morphology of both AB₅ particles, with immersion in the Pd and Pt electroless deposition bath. The figure shows that the modified electrodes can be clearly observed compared to the unmodified AB₅ alloy, given in **Figure 4.3** a). No palladium or Platinum particles were observed on the surface of the unmodified parent alloy. A rich coating of Pd **Figure 4.3** c) can be clearly observed with the palladium modified AB₅ compared to the Pt surface particles observed on AB₅ modified with Pt **Figure 4.3** b). This is of consequence because Pt has higher density than Pd being 21.45 g/cm³ and 12.02g/cm³ respectively, which means since Pd is light when coating the material, can cover nearly double the area for a given thickness. The difference in densities of these group metals can be exploited by choosing a light metal [65].

4.1.3 Elemental Composition of AB₅ MH Alloy Material Surface Modified with Pt and Pd Catalysts

The elemental composition of the AB₅ MH alloy was determined by Energy Dispersive X-Ray Spectroscopy (EDS) following the procedure given in Section 3.2.3. The elemental composition study of the parent material unmodified AB₅ alloy was conducted to compare the elemental state of the AB₅ alloys before and after modification in order to determine whether there is significant change in AB₅ composition. **Figure 4.4** a) and b) shows the presence of Pd and Pt catalyst on the surface of the AB₅ MH alloy. In this study, EDS was also used in the quantitative determination of the surface loading of the deposited metals (Pt and Pd).

4: Chapter Four

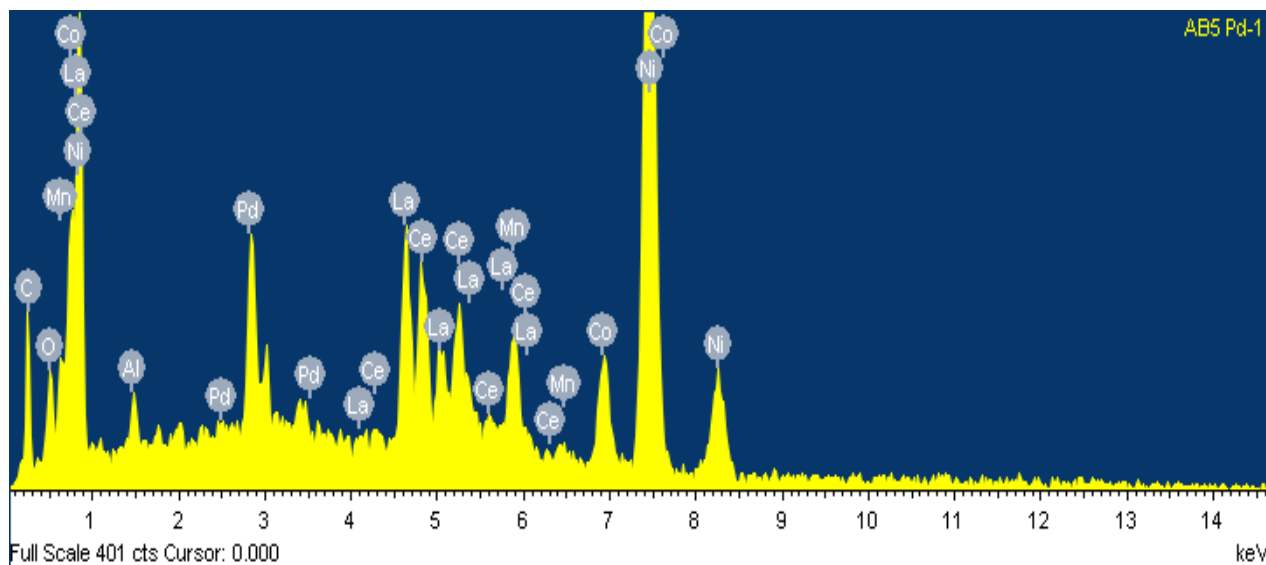


Figure 4.4 a): EDS spectrum of Palladium modified AB₅

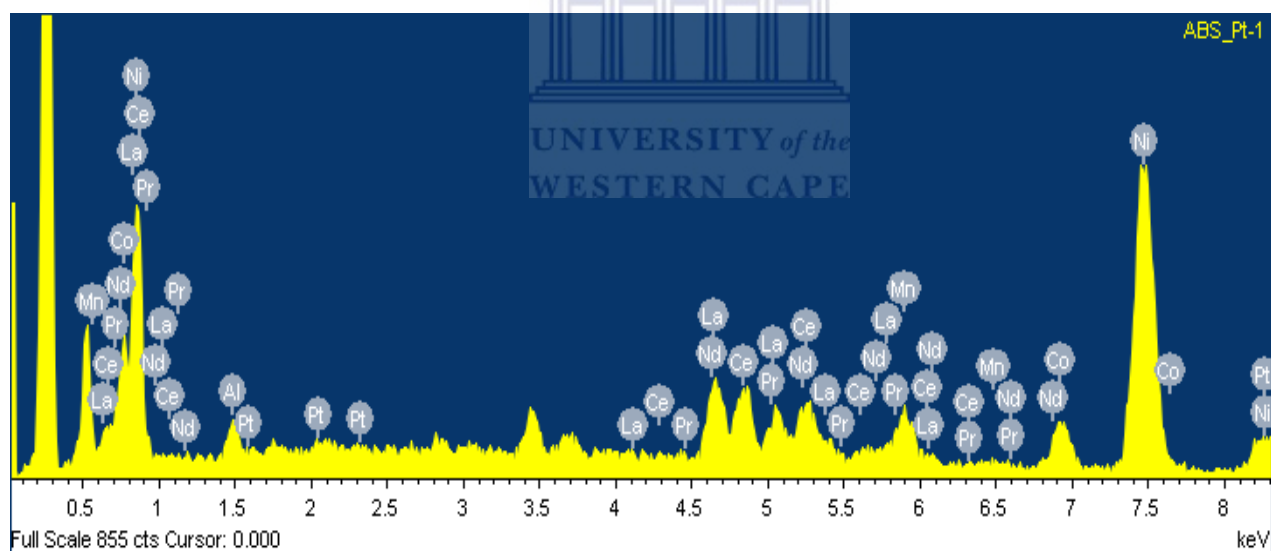


Figure 4.4 b): EDS spectrum of Platinum modified AB₅

Several readings with EDS were performed on each of the AB₅ modified alloys and the average was taken. The total amount of the loading is shown in **table 4.1** below:

4: Chapter Four

Table 4.1: Total Amount of Pd and Pt loading on the AB₅ MH Alloy Surface

Element	Weight %	Atomic %
Palladium	31.08	1.95
Platinum	13.41	1.23

4.1.4 Atomic Absorption Spectrometry (AAS) Characterization of Pt and Pd Modified AB₅ type Alloy

AAS was used in the investigation to determine the total elemental content of the deposited layers (Pd and Pt) on the AB₅ alloy as a function of unit weight of the surface modified samples.

The samples were prepared following the procedure given in Section 3.2.4.

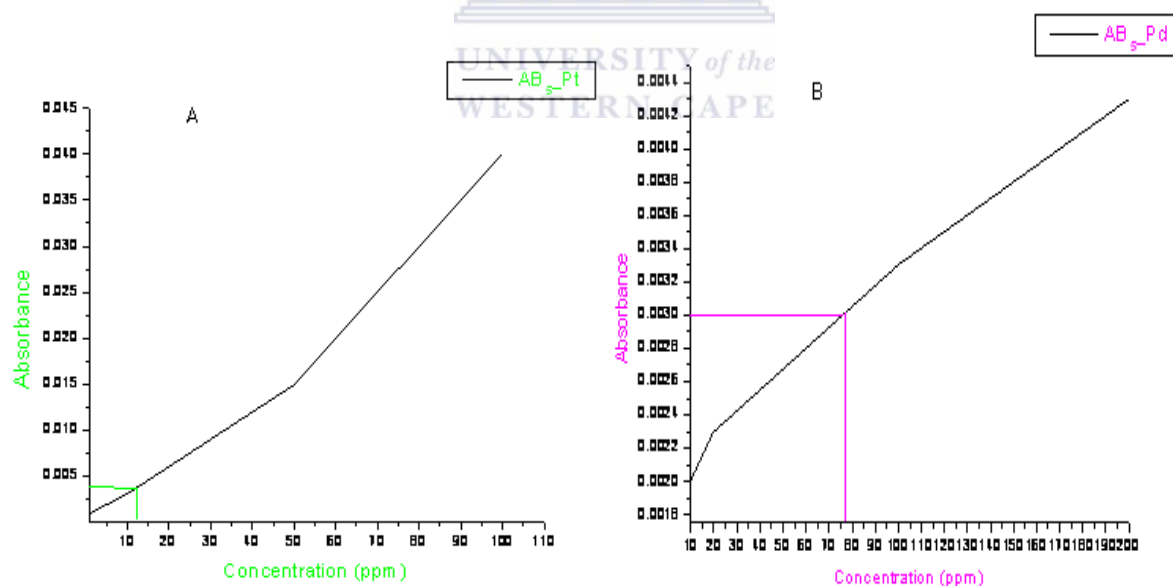


Figure 4.5: AAS graphs a) Pd modified AB₅ and b) Pt modified AB₅

4: Chapter Four

The results were obtained (see Appendix A1) and extrapolated; and **Figure 4.5 a)** shows the total amount of Pd in the AB₅ sample ranged from 75ppm to 80ppm. The results were converted to weight percent, and were found to range between 0.75wt% to 0.80wt%. **Figure 4.5 b)** shows the total amount of Pt in the AB₅ sample ranged from 10ppm to 12ppm, and also converted to weight percent and were found to range between 0.10wt% to 11wt%. These results are in agreement with results obtained with Energy Dispersive X-ray spectroscopy (EDS), as Pd is more than Pt on the surface of the AB₅ electrodes.

4.2 Electrochemical characterization of AB₅ MH electrodes surface modified with Pt and Pd Catalysts

It is well known that Pt and Pd are excellent catalysts for the electrochemical H₂ reaction and become very stable in alkaline solution. For the AB₅ type alloys, it has been demonstrated that the presence of amorphous Pd coatings improves the cycle lifetime and high rate discharge ability of MH electrodes [65]. Since H₂ absorption on amorphous Pd powder are negligible [100], the enhancement in the electrode performance has been explained on the basis of the electrocatalytic effect of Pd coating on the kinetics of the charge transfer process at the electrode surface, which is the rate determining step in the overall hydriding/dehydriding process. In the investigation, the effect of the addition of polycrystalline Pd and Pt powders into the hydride forming metal alloys electrode on the activation and cycle stability was investigated employing charge/discharge galvanostatic techniques, Cyclic Voltammetry and Impedance Spectroscopy.

4: Chapter Four

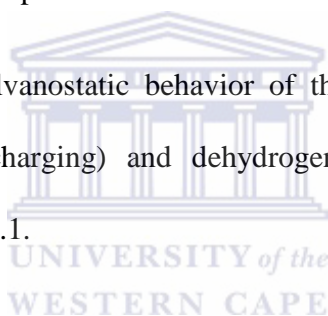
4.2.1 Galvanostatic Charge/Discharge Capacities of AB₅ MH electrodes surface modified with Pt and Pd catalysts

The activation of the alloy plays a fundamental role in absorption electrodic process, since it defines the reaction rate of the hydrogen with the metal and the incorporation to its structure.

During activation, several different processes occurred [101, 102], such as:

- ❖ Reduction of surface oxides that interfere with hydrogen
- ❖ Reduction of particle size due to the cracks produced by the volume increase
- ❖ Changes in the chemical composition and /or surface structure of the metal

To accurately investigate the Galvanostatic behavior of the AB₅ alloy electrodes, the alloy electrodes were hydrogenated (charging) and dehydrogenated (discharging) following the parameters stated in section 3.3.3.2.1.



4: Chapter Four

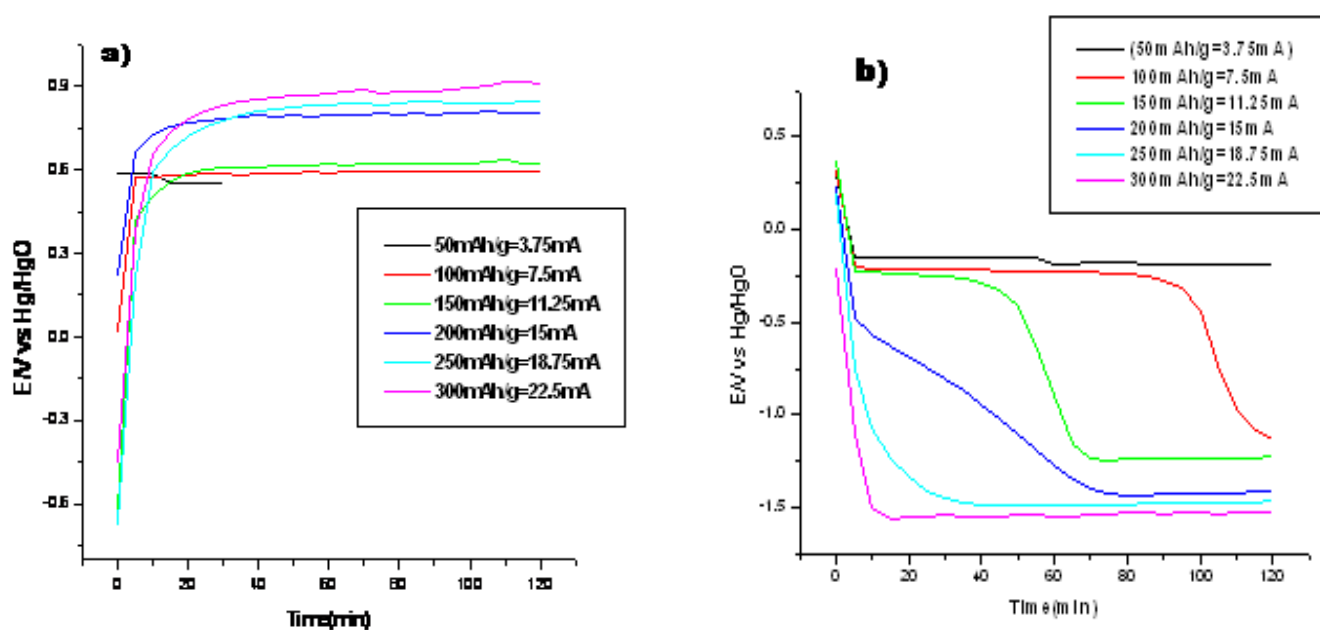


Figure 4.6: a) Charge of Unmodified AB₅, b) Discharge curve of Unmodified AB₅ from the first to the sixth cycle for activation

To investigate the effect of metal catalyst addition on the overpotentials related to the hydriding/dehydriding processes, the charge/discharge profiles of the alloy electrodes with different metal catalyst content were analysed. First, the MH electrodes were subjected to charge/discharge cycles for activation. Activation reactions (charge/discharge) of the electrode were charged from smallest capacity 50mAh/g to highest 300mAh/g, the sixth cycle as shown in **Figure 4.6** a) and b). The highest capacity was employed for the subsequent charge/discharge cycles.

4: Chapter Four

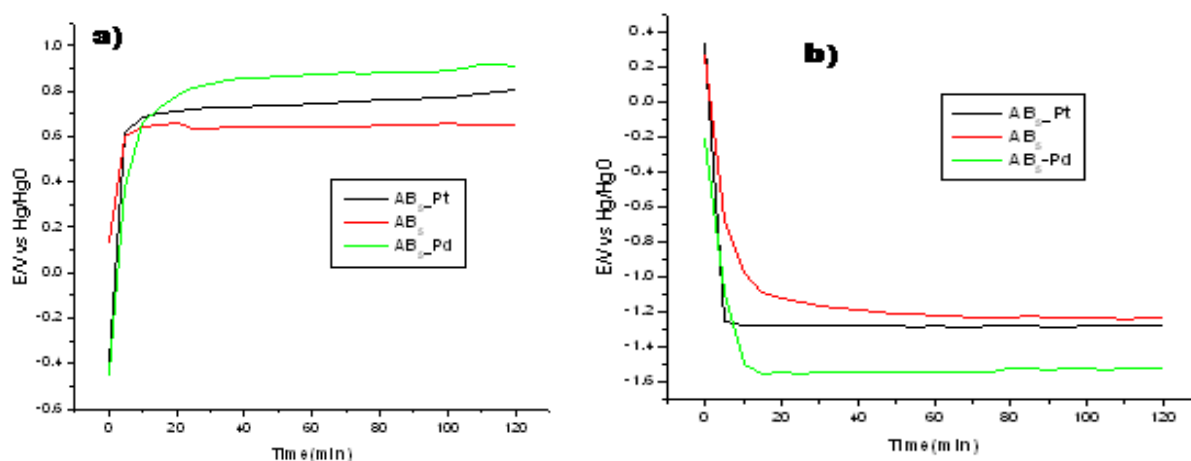


Figure 4.6 b): 10th cycle of a) Charge for AB₅ unmodified, AB₅-Pt modified, AB₅-Pd modified b) discharge AB₅ unmodified, AB₅-Pt modified, AB₅-Pd modified

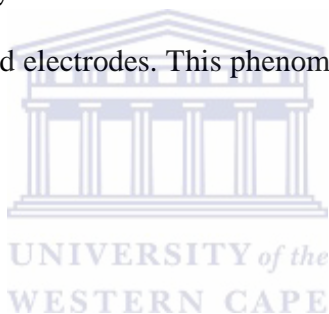
The electrochemical testing and effect of metal catalyst addition on charge/discharge overpotentials of MH electrodes was carried out, following the procedure given in section 3.3.2.1. **Figure 4.6** a) and b) shows charge/discharge potential versus time profiles obtained for the three electrodes at the 10th cycle. In each case, well defined charge/discharge plateaus are observed. The MH electrode without metal catalyst addition shows a high charge overpotential. For the Palladium modified electrode, the discharge potentials presents lower values (i.e. more negative) implying a smaller discharge overpotential or higher specific power for the battery. These improvements were also observed by other authors Visitin et.al [100], Barsellini et.al [101], and Ambrosio et.al [103]. Similar behavior was also observed for Platinum modified electrode Ambrosio et.al [103].

The initial high charge overpotentials of the MH electrodes may be attributed to a surface oxide film, formed during metal alloy exposure to air. Thus, the metal catalyst surface, either enhances H₂ evolution on the catalyst surface, either promotes the fast reduction of the surface oxides as a

4: Chapter Four

consequence of a reducing atmosphere, or the H_2 atoms produced during the charge process on the catalyst surface are quickly transformed to the alloy particles and absorbed through the oxide film. Hence, the global hydriding/dehydriding processes in the catalyst added electrodes are favoured by the initial decrease in the charge/discharge overpotentials, leading to higher discharge capacity values even for the first charge/discharge cycles. In turn, the metal catalyst surface enhances H_2 entrance induces volume changes that produces pulverization of the metal particle and subsequent decrease in diffusion overpotentials during charge/discharge cycling.

In this respect, it must be noted that all these processes become significant after many cycles for MH electrodes without metal catalyst additives while less than 10 cycles are required for the full activation of the catalyst additivated electrodes. This phenomenon was also observed by Visintin et al. [104].



4: Chapter Four

4.2.2 Cyclic Voltammetry Characterization of AB₅ Type Alloy Surface Modified with Pt and Pd Catalysts

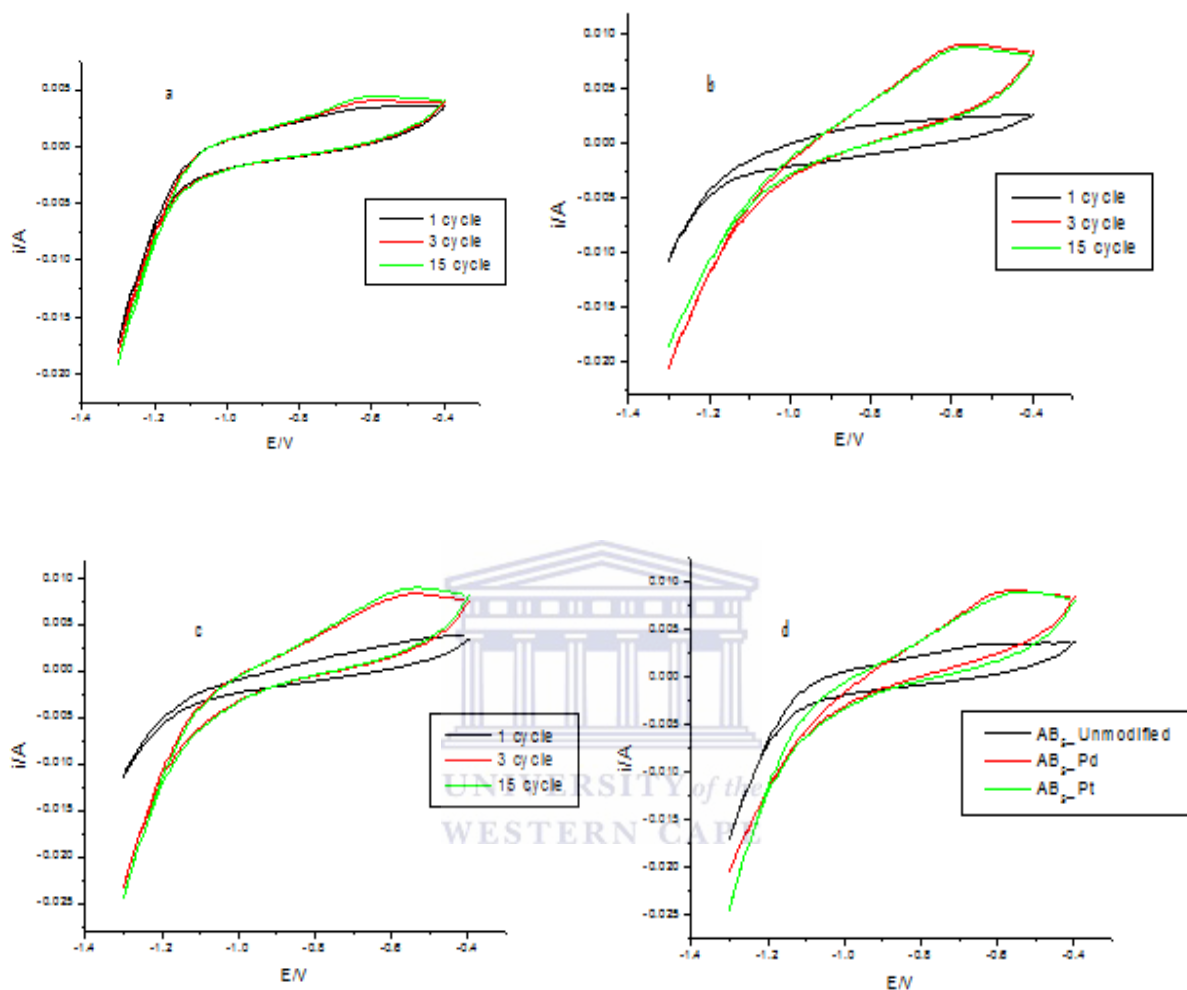


Figure 4.7: (a – c) Show cyclic voltammograms of AB₅_Unmodified, AB₅_Pt, AB₅_Pd scan from first cycle to the 15th cycle, while d) shows overlay of all the cycles from the unmodified electrodes to both Pt and Pd modified electrodes

The alloy electrodes were cycled at 1mV/s between -0.4 and -1.3V. At low scan rates, hydrogen in the interior of the alloy has sufficient time to diffuse into the powder surface. The diffused H₂ at the surface also participates in the charge transfer reaction [105].

4: Chapter Four

From the entire scans the electro-reduction current peak was not observed, because there are no oxides present on the surface of the electrode. Prior the voltammograms were taken, the electrodes were activated by charge/discharge cycling controlled via the potential. Only, the current peaks related to the hydrogen electrode reaction could be detected. During the forward scanning, a broad anodic peak related to the electro-oxidation of absorbed hydrogen was observed. As the number of the reduction-oxidation cycles increases, the hydrogen electro formation occurs earlier, and correspondingly the H₂ electro-oxidation current peaks also increases. These processes, as can be seen from **Figure 4.7** (d) are further favored when the pellet electrodes are modified with platinum or palladium.

The activation effect by potential cycling can be attributed to the reduction of the surface oxides which increases the reaction surface area. Otherwise, the reaction surface area also increases during activation procedure due to the continuous expansion and contraction of the metal alloy surface produced by the formation of the hydride phase and the subsequent dehydriding processes. The position of the broad anodic current peak corresponding to the dehydriding reaction can be represented by the following equation:



Equation 4.1 reflects the overpotential and provides information about the effect of palladium and platinum on the reaction kinetics. Thus, the voltammograms in **Fig.4.7** (a) to (d) show that the anodic current peak at -0.64 to -0.65V for the Pt and Pd modified electrodes, respectively. Furthermore, the electrode which was not coated with Platinum or Palladium the current peak occurs at -0.59V.

4: Chapter Four

4.2.3 Impedance Characterization of the AB₅ type Alloy surface modified with Pt and Pd catalysts

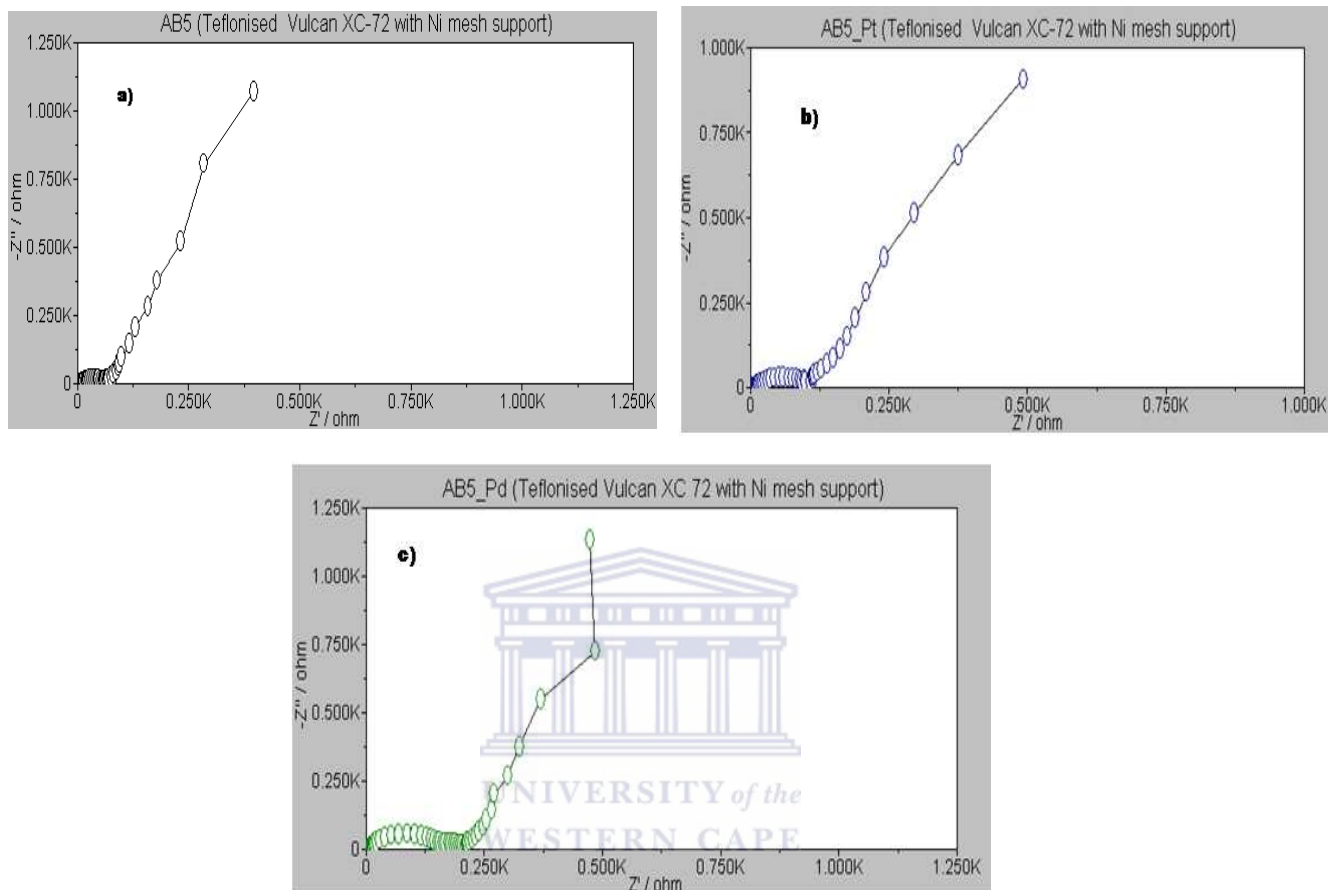


Figure 4.8: Shows EIS spectra a) AB₅_unmodified, b) AB₅_Pt modified, c) AB₅_Pd modified

Figure 4.8 Compares the results for different alloys at the fully discharge state. Almost the same behavior was observed for all electrodes. The EIS images show that all three electrodes have the same depressed semicircles, this may occur because the electrodes have high porosity. At high frequencies the plot start as a semicircle and, as the frequency decreases, it changes to a straight line. According to some researchers S. Cheng et al. [107] the semicircle in high frequency range is attributed to the contact resistance between the hydrogen storage alloy and to the current collector between the alloy particles. The intercept at high frequency region is directly related to the electrolyte resistance. The slope of the straight line is related to the diffusion of protons in the

4: Chapter Four

electrode and is called Warburg diffusion; this is in agreement with literature [107]. **Figure 4.8** a) the semicircle is highly depressed giving high resistance 21.6884Ω . This behavior has been attributed to the presence of a passive film oxide on the particle surface in the discharged material. **Figure 4.8** b) and c) show that the semicircle in high frequency regions for the platinum and palladium modified electrode increased as compared to the unmodified electrode, because the resistance decreased b) 14.7397Ω and c) 12.1061Ω respectively. This behavior occurs because the contact resistance decreased after surface modification, due to the fact that the modified alloy electrodes show less resistance.

These facts may be explained by the improvement of the morphology of the alloy surface. By removing the oxide layer which naturally form on the surface by depositing Pt or Pd on the surface of the electrode, this causes the contact resistance between the alloy particles and the current collector to decrease, and it significantly increases the conductivity of the alloy surface, resulting in a lower contact resistance of the alloy, these findings for the semicircle are similar to Deng et.al [106].

The charge transfer is also reduced by the modification of alloy surface with Pt or Pd since they remove the oxide film on the alloy surface, which helps with the absorption and diffusion of hydrogen in the alloy lattice. The easier the charge transfer process the lesser the reaction resistance. These results correspond to the values acquired practically. The resistance obtained from the impedance data was used to calculate the overpotentials and the results were as follows: a) unmodified electrode 0.4879V , b) Platinum modified electrode 0.3316V and c) Palladium modified electrode 0.2724V . These results are in agreement with the results obtained for the charge/discharge potentials. The lower the overpotentials the higher the specific power of the battery. Both Palladium and Platinum improve the performance of the alloy electrode.

4: Chapter Four

4.3 Summary of AB₅ MH with immersion in Pt and Pd on NaH₂PO₂ based electroless plating bath

Pd and Pt deposition was carried out on the surface of the MH alloy, by electroless deposition using NaH₂PO₂ as reducing agent. The film microstructure was characterized by XRD, SEM, EDS, and AAS techniques. The electrochemical behaviour of the prepared electrodes was studied with galvanostatic charge/discharge cycles, CV and EIS. Based on the results, it was concluded that electroless plated Pd and Pt MH alloy electrodes had better performance compared to unmodified AB₅ MH electrode. However, Pd shows more interesting results compared to Pt.

The Pd and Pt coated alloy electrodes represented lower discharge overpotentials, which is important to improve the battery performance. The main impedance feature of the MH electrodes was related to the charge transfer step of the hydriding/dehydriding processes. It was found that the catalytic activity of charge/discharge is improved with Pd and Pt deposition, a factor exclusively related to a higher active area of the coated layer, since the values of the apparent activation energy are higher for the coated samples. From these findings it was also concluded that Pd catalyst had better performance than Pt.

4: Chapter Four

4.4 Effect of Different Reducing Agent Used for Electroless Pd Plating on the AB₅ MH Surface

The improvement of hydrogen storage alloys by palladium treatment is caused by H₂ spill-over and reverse hydrogen spill-over. The deactivation of the H₂ storage alloy is due to the oxidation of the alloy surface, which prevents the dissociation of molecular H₂, a key step for the H₂ to be absorbed by the alloy. After Pd treatment, the Pd particles adhere to the Pd surfaces of the alloy. Molecular H₂ can be dissociated on the Pd surfaces, and then the dissociated H₂ atoms are split-over to the alloy surface and absorbed by the H₂ storage alloy. Because Pd remains un-oxidised and unaffected by the exposure to air, the Pd treated alloys have outstanding durability for hydrogen storage and release [108].

The hydrogen spill-over effect is identified as a means of enhancing the catalytic activity towards the H₂ dissociation process. Enhancements in the catalytic activity with the H₂ spill-over are due to the increase in the active surface area of the Pd catalyst on the alloy surface. The phenomenon is dependent on the catalyst loadings, catalyst dispersion, active surface area between the catalyst and the surface of the support material [107].

4.4.1 Investigation of AB₅_Pd Microstructure Electroless Plated with N₂H₄ and NaH₂PO₂ Based Bath

The influence of the type of reducing agent (*i.e.*, N₂H₄ and NaH₂PO₂) on the morphological and kinetic properties of the AB₅ alloy, surface modified with Pd was investigated by studying the crystallinity, Pd dispersion and hydrogen kinetics.

The alloys were characterized through XRD analysis. The corresponding diffractograms were shown in **Figure 4.9**. The presence of CaCu₅-type intermetallic was confirmed using the XRD,

4: Chapter Four

following experimental procedure stated in section 3.3.1. Both AB₅-type alloys surface modified by Pd coatings derived from N₂H₄ and NaH₂PO₂ electroless plating baths, showed that the material contained more or less unchanged lattice constants. These diagrams also confirm that the position of the diffraction peaks for the modified material did not change significantly.

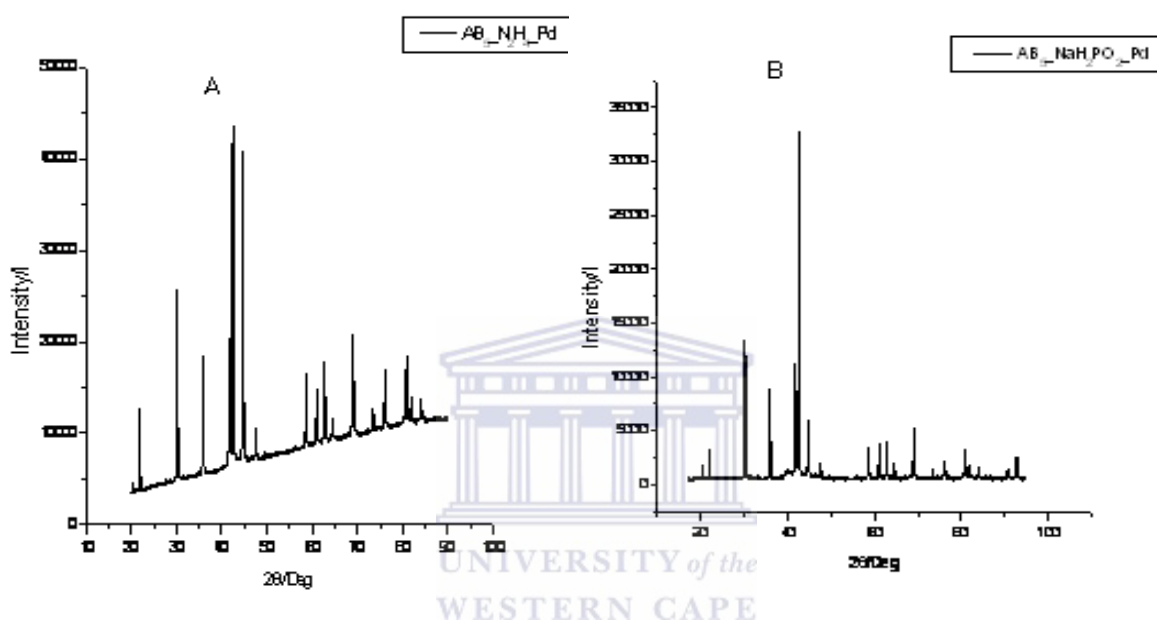


Figure 4.9: XRD Diffractograms of a) AB₅-N₂H₄-Pd and b) AB₅-NaH₂PO₂-Pd

The measured XRD patterns did not show any presence of additional peaks or change in peak position. The Pd content on the surface of the modified powders may have been very small (less than 1wt%). The observation was also established by Zaluski et al. [109].

4.4.2 Determination of Pd Deposites on AB₅ MH Alloys Using Different Reducing Agents

The determination of Palladium on the surface modified AB₅ MH alloy with application of N₂H₄ and NaH₂PO₂ as reducing agents was determined by EDS, following the procedure given in section 3.2.3. The Pd deposition study of the surface modified AB₅ alloys was conducted to

4: Chapter Four

compare the effect of using different reducing agents for the modification of the MH alloys. That is to quantitatively determine the surface loading of the deposited metals with Pd. **Figure 4.10 a)** and b) demonstrate the images of the modified AB₅ type alloy with Pd catalyst, using N₂H₄ and NaH₂PO₂ reducing agents respectively.

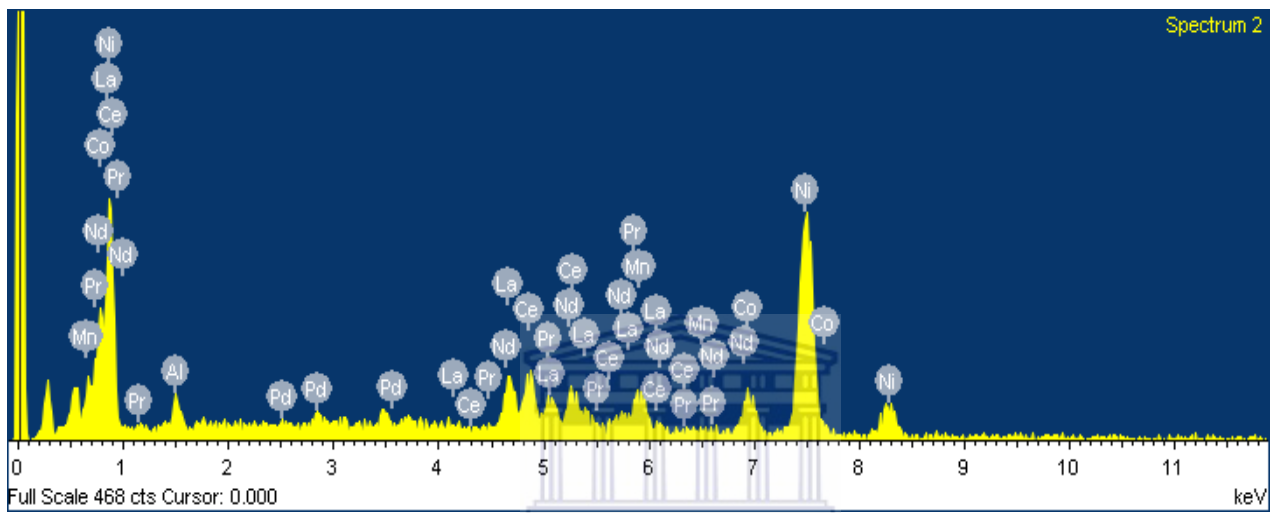


Figure 4.10 a): Shows EDS Spectrum of AB₅_N₂H₄_Pd

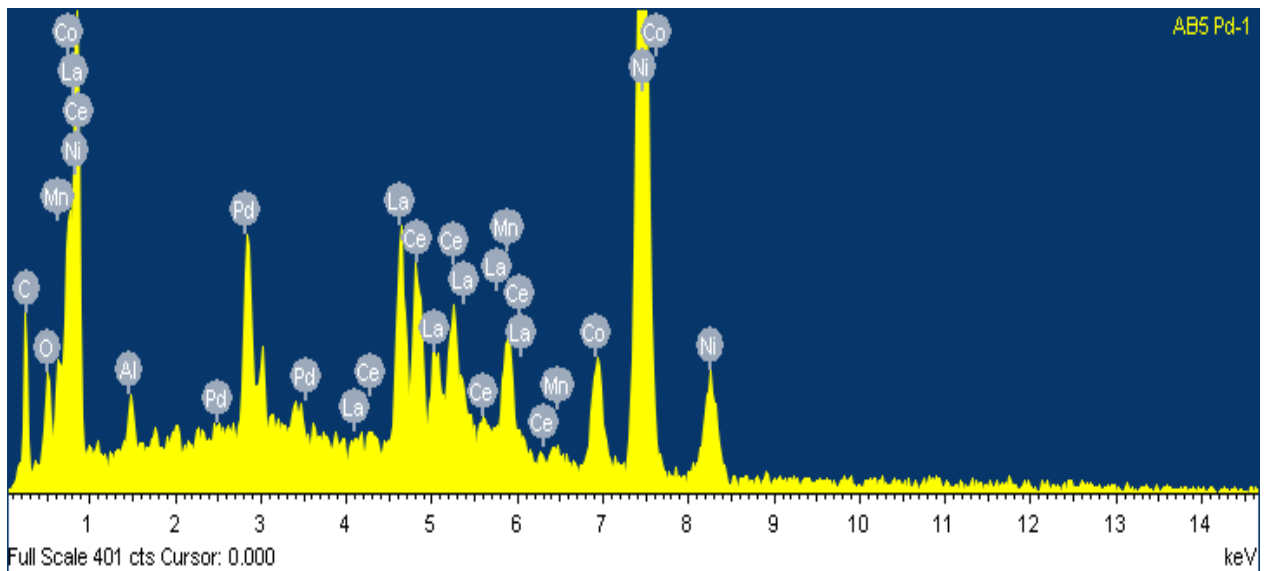


Figure 4.10 b): Shows EDS Spectrum of AB₅_NaH₂PO₂

4: Chapter Four

Table 4.2: Exhibits the total loading of AB₅ metal hydride alloy deposited using different reducing agents (N₂H₄ and NaH₂PO₂). Several readings were taken and they were averaged to give the results shown in the table below. It can be seen that Pd plating using N₂H₄ based bath had very low weight percent compared to the Pd plating employing NaH₂PO₂ based bath. The results corresponds to Riedel's findings, which demonstrate that baths based on hypophosphite as reducing agent perform better in terms of stability and deposit quality [67] compared to hydrazine.

Table 4.2: Total Loading of Pd on AB₅ MH Alloy Deposited in N₂H₄, NaH₂PO₂

Element	Reducing agent	Weight%	Atomic%
Pd	N ₂ H ₄	7.57	0.54
Pd	NaH ₂ PO ₂	31.08	1.95

4.4.3 Total Determination of Pd Particles on the Surface of the AB₅ Type Alloy Employing AAS

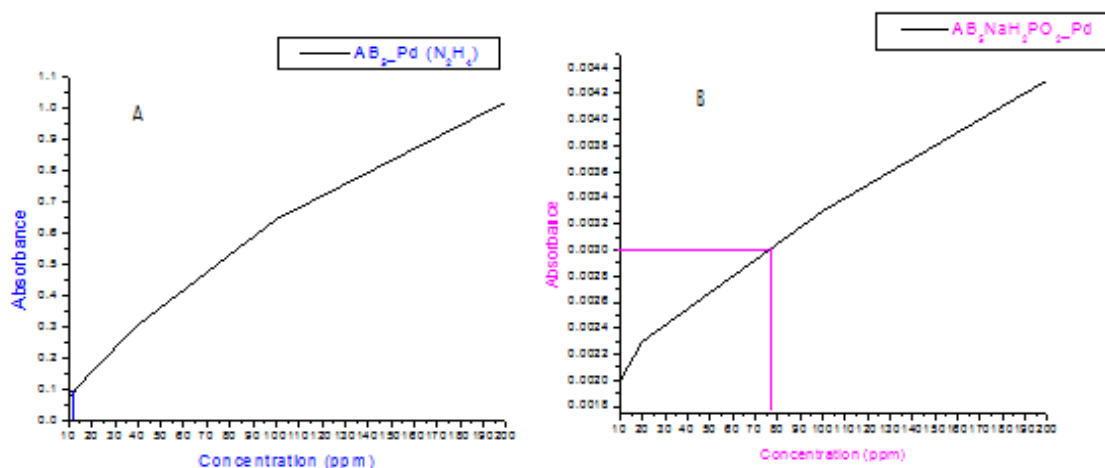


Figure 4.11: Shows AAS graphs a) for AB₅-N₂H₄-Pd and b) AB₅-NaH₂PO₂-Pd

4: Chapter Four

The results were obtained and extrapolated (see Appendix A2); **Figure 4.11 a)** shows the total amount of Pd in the AB₅ modified in N₂H₄ electroless plating bath (0.10 to 0.15wt%). **Figure 4.11 b)** shows the total amount of Pd in the AB₅ modified in NaH₂PO₂ electroless plating bath (0.75 to 0.80wt%). As seen from the results, very small amounts of Pd were detected for the AB₅ alloy modified in N₂H₄ electroless plating bath, compared to AB₅ alloy modified in NaH₂PO₂ electroless plating bath.

4.4.4 Surface Morphological Studies of the AB₅ MH Alloys Immersed in Pd Electroless Plating Bath Derived from N₂H₄ and NaH₂PO₂ Based Baths

Direct determination of the Pd particles distribution on the surface of the AB₅ MH alloy was conducted using SEM. **Figure 4.12 a)** show micrographs collected for the AB₅-type alloys surface modified using N₂H₄ electroless plating based baths. Crystalline Pd layers on the AB₅-type alloy surface were found to be discontinuous. The Pd particle had a fairly good dispersion on the surface of the AB₅-type alloy. Very small Pd particles were observed for the N₂H₄ based electroless bath. The Pd particles formed agglomerates on the surface of the alloy. This behavior was similar to observations made by Pratt et al, but they observed large agglomeration of the deposited Pd coatings on certain faces of AB₅ alloy particles [110].

4: Chapter Four

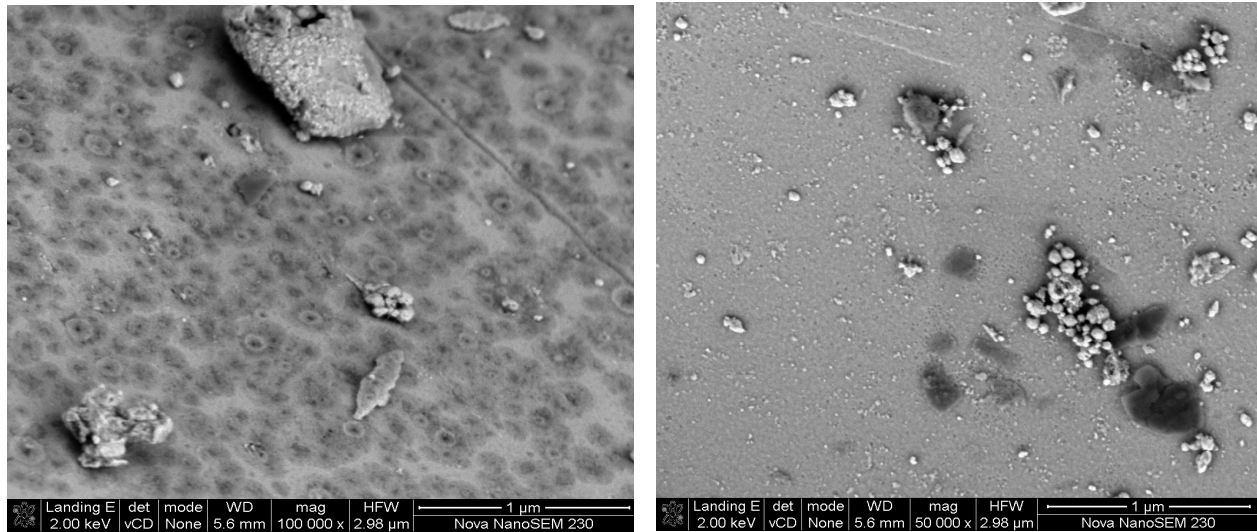


Figure 4.12 a): Shows SEM images AB₅_Pd (N₂H₄)

Palladium particles were observed on the surface of the AB₅-type alloy surface modified in NaH₂PO₂ based electroless plating bath **Figure 4.12 b)**. Pd particles had fairly good dispersion upon deposition derived from NaH₂PO₂ based electroless plating bath. The dispersion was denser on the alloy surface, even better than that of the sample surface modified in N₂H₄ based electroless plating bath. Pd coatings were also found to be discontinuous for the sample surface modified in NaH₂PO₂ based electroless plating bath. This phenomenon was stated by Doyle et al. [111], saying that 80-100% of surface modified alloy particles may house discontinuous metal coatings after PGM depositions.

4: Chapter Four

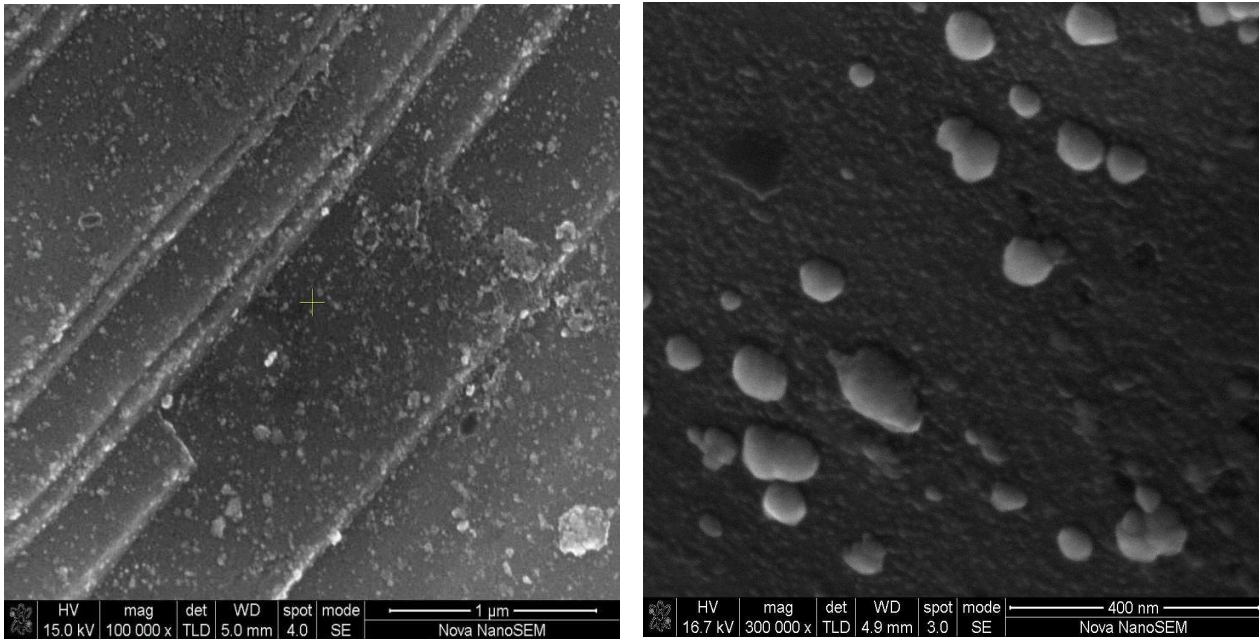


Figure 4.12 b): Shows SEM images of $AB_5_Pd (NaH_2PO_2)$



4: Chapter Four

4.4.5 Galvanostatic Charge/Discharge Cycles of the AB₅ MH Alloy Immersed in Electroless Pd Plating Bath Derived from N₂H₄ and NaH₂PO₂ Baths

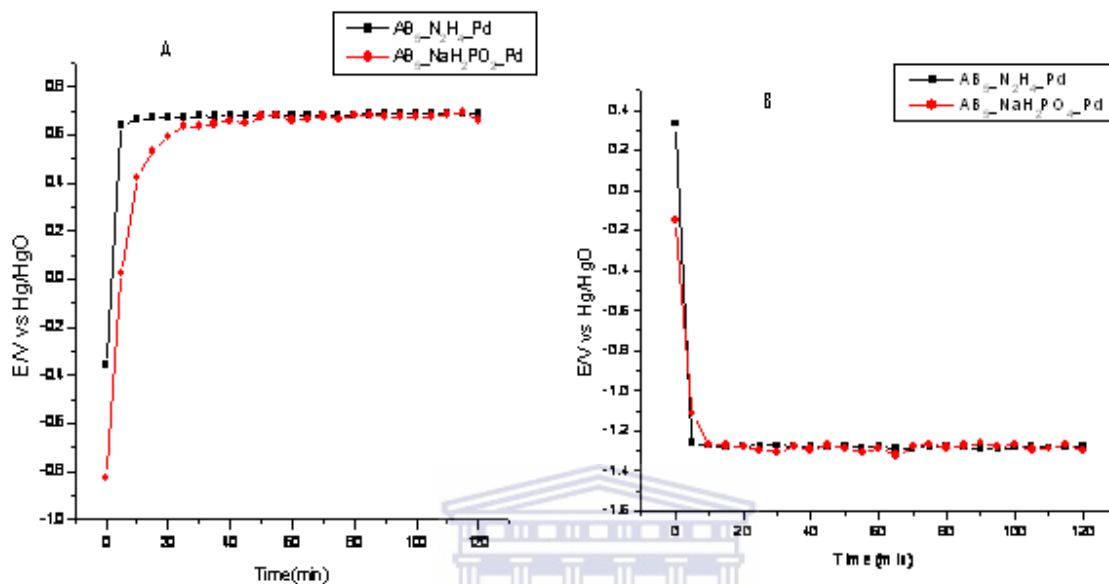


Figure 4.13: Shows a) Charge of AB₅-N₂H₄-Pd and AB₅-NaH₂PO₂-Pd and b) Discharge of AB₅-N₂H₄-Pd and b) AB₅-NaH₂PO₂-Pd

Discharge capacity of the electrode was determined using galvanostatically charge. **Figure 4.13** a) and b) show charge/discharge potential versus time profiles obtained for the two electrodes at the 10th cycle. In each case, well defined charge/discharge plateaus are observed. The MH electrode surface modified in N₂H₄ based electroless plating bath shows high charge overpotential, compared to the alloy electrode surface modified in NaH₂PO₂ based electroless deposition bath. For the Palladium modified electrode immersed in NaH₂PO₂ based bath, the discharge potentials presents lower values (i.e. more negative) implying a smaller discharge overpotential or higher specific power for the battery.

4: Chapter Four

4.4.6 Electrochemical activity of the AB₅-type alloy immersed in Pd electroless plating bath derived from N₂H₄ and NaH₂PO₂ reducing agents

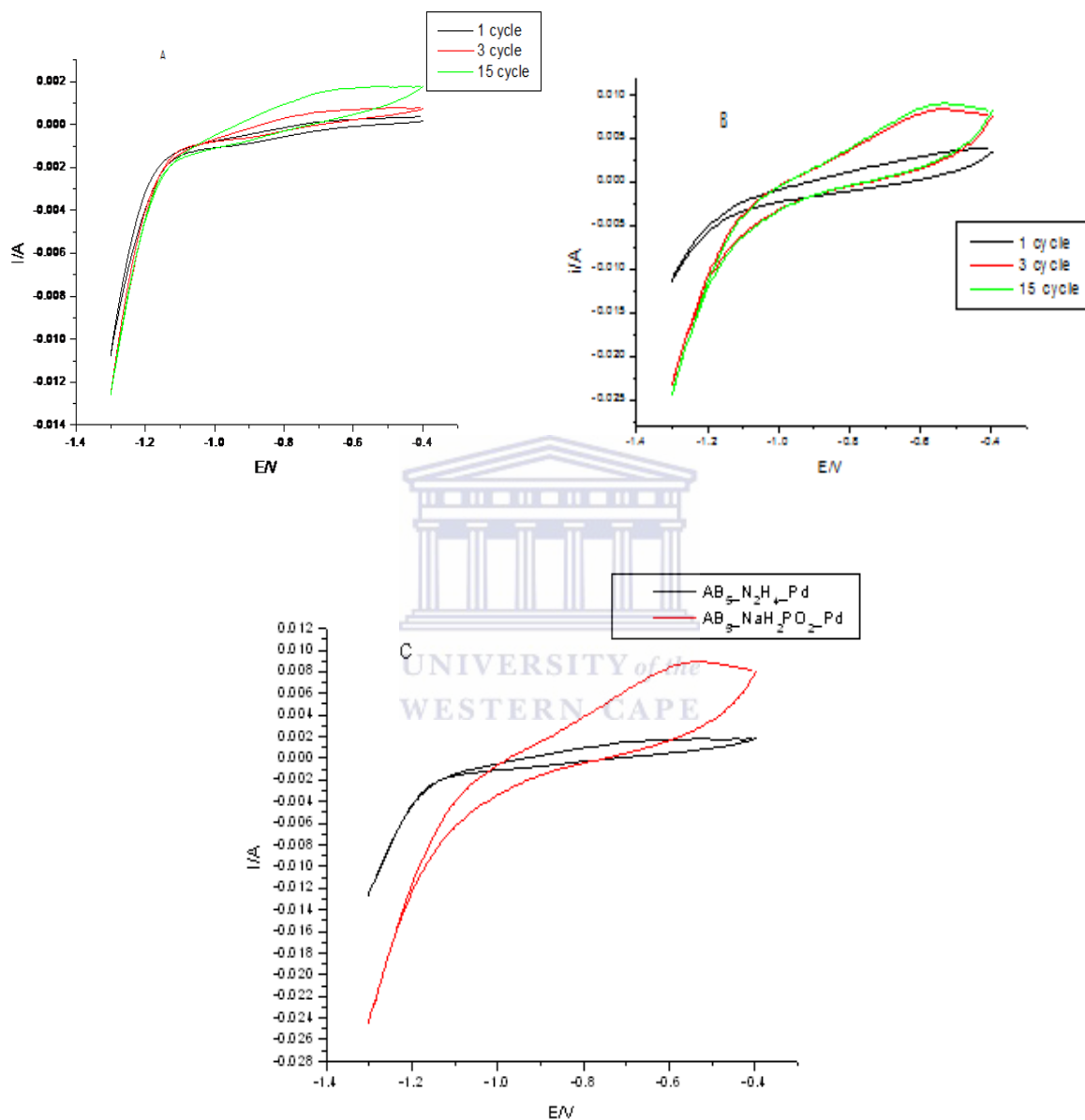


Figure 4.14 a) AB₅-N₂H₄-Pd, b) AB₅-NaH₂PO₂-Pd, and c) Overlay of both AB₅-N₂H₄-Pd and AB₅-NaH₂PO₂-Pd

4: Chapter Four

The alloy electrodes were cycled at 1mV/s between -0.4 and -1.3V. Similar voltammograms were observed similar to earlier findings, where different PGM catalysts (Pt and Pd) were compared. All the voltammograms (**Figure 4.14** a) and b)), exhibited that no electro-reduction current peak was observed, because there were no oxides present on the surface of the electrode, since the CV was applied after the activation of the electrode. Only, the current peaks related to the hydrogen electrode reaction could be detected.

In anodic branch, anodic peaks were observed at around -0.64 ~ -0.65V vs Hg/HgO for the two electrodes as can be seen in **Figure 4.14** c). However, the peak was higher for NaH₂PO₂ based electroless plating bath than that of N₂H₄ based electroless plating bath modified MH electrode. Both N₂H₄ and NaH₂PO₂ MH electrodes demonstrate sharp anodic peaks, which means oxidation reaction of H₂ on the MH electrode proceeded smoothly. These facts indicate that the surface modification improved the electrochemical activity of oxidation reaction of H₂ on the AB₅ MH electrode surface. In addition, NaH₂PO₂ based electroless plating bath had better performance than the N₂H₄ based electroless plating bath.

4.4.7 Impedance Analysis of AB₅ Type Alloy Immersed in Pd Electroless Plating Bath Derived from N₂H₄ and NaH₂PO₂ Reducing Agents

EIS was employed in the investigation to examine the effect of surface modification of the AB₅-type electrodes with Pd derived from N₂H₄ and NaH₂PO₂ based electroless plating bath. In addition, the impedance was used in the analysis to look at the improvements in electrochemical activity on the electrodes surface and decrease in the charge transfer resistance as the result of

4: Chapter Four

surface modification of the AB₅ alloy electrodes. **Figure 4.15** a) and b) illustrates the impedance images of AB₅-N₂H₄-Pd and AB₅-NaH₂PO₂-Pd alloy electrodes.

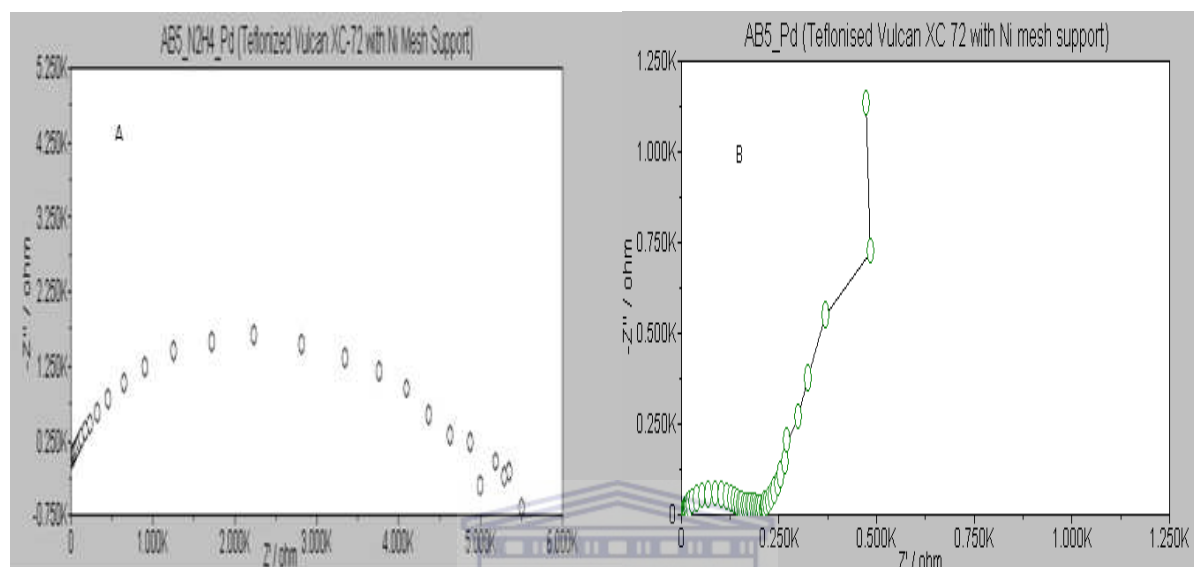


Figure 4.15: Shows EIS spectra of a) AB₅-N₂H₄-Pd and b) AB₅-NaH₂PO₂-Pd

The EIS images show that the AB₅-N₂H₄-Pd electrode has one semicircle at high frequency region, and it is not depressed. This behavior is obtained since the electrode was immersed in Pd electroless plating bath using N₂H₄ as reducing agent. The fact that the electrode exhibited only one semicircle was not understood, because according to some researchers the EIS spectrum shows that at high frequencies the plot start as a semicircle and, as the frequency decreases, it changes to a straight line [107].

AB₅-NaH₂PO₂-Pd image shows that at high frequencies the plot starts as a semicircle and, as the frequency decreases, it changes to a straight line. This behavior is similar to our earlier findings and other researchers [107]. **Figure 4.15** a) the semicircle for the AB₅-N₂H₄-Pd electrode gave high resistance of 97.8619Ω. This behavior has been attributed to the presence of a passive film oxide on the particle surface in the discharged material.

4: Chapter Four

Figure 4.15 b) shows that the semicircle in high frequency regions for the $AB_5_NaH_2PO_2_Pd$ modified and the resistance was 12.1061Ω . As can be seen from the results, the $AB_5_N_2H_4_Pd$ electrode has shown higher resistance than $AB_5_NaH_2PO_2_Pd$ electrode. This behavior occurs because the contact resistance decreased after surface modification. It is evident that the electrode modified by immersion in Pd electroless plating bath employing NaH_2PO_2 reducing agent had better performance than N_2H_4 electroless plating bath.

4.5 Summary of Effect of Different Reducing Agent Used for Electroless Pd Plating on the AB_5 MH Surface

The influence of the type of reducing agent (*i.e.*, N_2H_4 and NaH_2PO_2) on the morphological and kinetic properties of the AB_5 alloy, surface modified with Pd was investigated. The film microstructure was characterized by XRD, SEM, EDS, and AAS techniques. The electrochemical behaviour of the prepared electrodes was studied with galvanostatic charge/discharge cycles, CV and EIS. Based on the results, it was concluded that Pd electroless plated using NaH_2PO_2 reducing agent had better performance compared to one containing N_2H_4 as reducing agent.

As seen from the results, the surface modifications considerably decrease the charge transfer resistance and activation enthalpy of the electrode reaction on the surface. The modifications make the alloy form an Ni-rich layer surface with electrocatalytic activity on the surface and increase the larger specific area of the electrode. Hence, the activation for dissociation of H_2O is decreased. CV and EIS results indicate that the surface modifications apparently improve electrochemical activity on the electrodes surface and decrease the charge transfer resistance and activation of MH electrode reaction [107].

4: Chapter Four

4.6 Surface Functionalization In Palladium Electroless Plating on AB₅ MH alloys using Aminosilane

As was previously discussed, Pd coatings deposits on the surface of the AB₅ MH alloy using electroless plating were discontinuous in nature. This phenomenon was stated by Doyle et al. [111], stipulating that 80-100% of surface modified alloy particles may house discontinuous metal coatings after PGM depositions [111]. A pre-treatment technique was previously developed by Williams et al. [112] to pre-functionalize the surface of the alloy electrode prior to electroless deposition, to improve the deposition of Pd on the MH electrode surface. Employing a similar method, continuous layers of the Pd catalyst can be deposited on the AB₅ MH alloy for the purpose of further enhancing the kinetics of hydrogenation, enhancing the quality of coating, and increasing the plating efficiency in the electroless plating of Pd layers. In addition, preventing the decomposition of precious metal plating bath.

The attractiveness of functionalization method, in electroless plating of metal layers was thus demonstrated. As mentioned in the literature review, this can be realized by the treatment of the substrate material with an aqueous solution of amino silane (*e.g.*, γ -amisopropyltriethosilane or γ -APTES). The pre-treated AB₅ alloy electrode with γ -APTES was characterized with XRD, SEM, EDS, AAS and electrochemically characterized with galvanostatic charge/discharge cycles, CV and EIS. The results are demonstrated below.

4: Chapter Four

4.6.1 Structural characterization of γ -APTES functionalized AB₅ type alloy

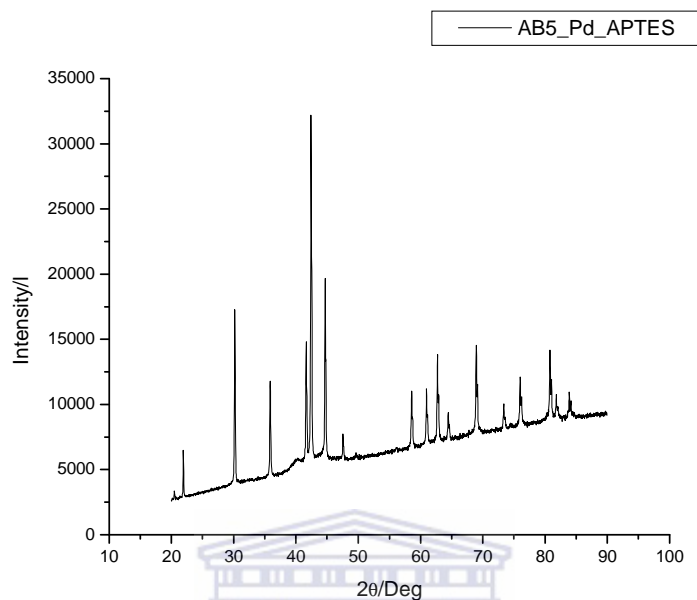


Figure 4.16: XRD Diffractogram of AB₅ γ -APTES_Pd

A microstructure of the AB₅ MH alloy coated in a NaH₂PO₂ based Pd electroless plating bath, after surface pre-functionalization with aqueous γ -APTES, was investigated. **Figure 4.16.** shows that the electrode has the same structure as the parent material CaCu₅ type with symmetry P6/mmm. No extra phases were detected and lattice parameters did not increase. No Pd particles were detected on the surface of the AB₅ alloy. The results were not expected since pre-treatment with γ -APTES increases the deposition of Pd on the surface of the electrode.

4: Chapter Four

4.6.2 Determination of Pd Content on the AB₅ Alloy Functionalized with γ -APTES

The determination of Palladium on the surface modified AB₅ MH alloy with application of NaH₂PO₂ as reducing agents pre-functionalized with γ -APTES was determined by EDS. **Figure 4.17** demonstrate the image of the modified AB₅ type alloy with Pd catalyst, using NaH₂PO₂ reducing agents with pre-functionalization with γ -APTES.

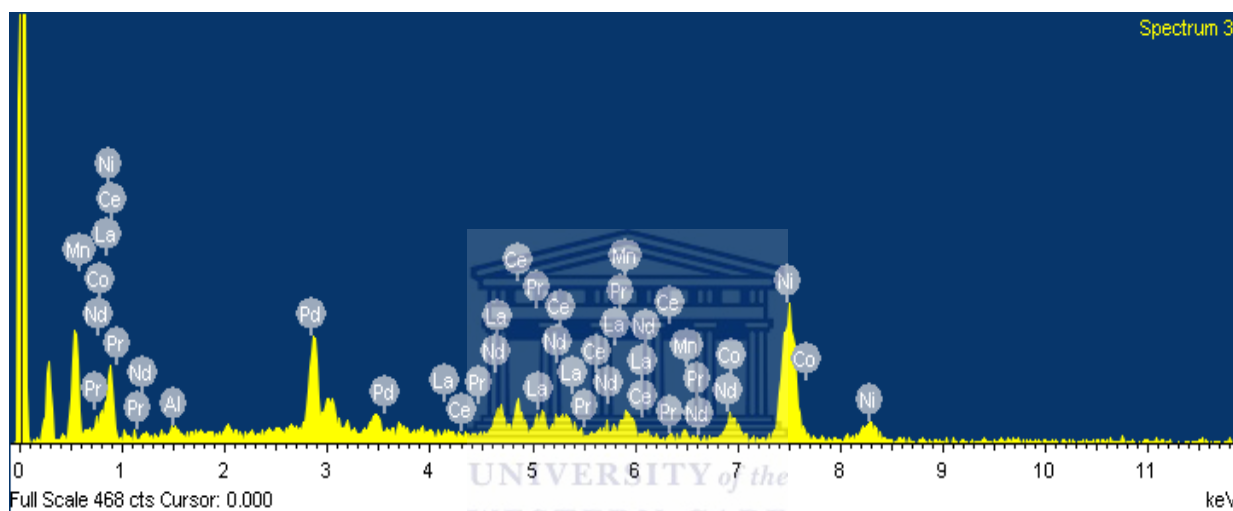


Figure 4.17: Shows EDS Spectrum for AB₅- γ -APTES-Pd

Table 4.3: Compares the total loading of AB₅ metal hydride alloy pre-functionalized with γ -APTES prior Pd electroless deposition using NaH₂PO₂ reducing agent and one without pre-functionalization. Several readings were taken and they were averaged to give the results shown in table below. It can be seen that Pd electroless plating using NaH₂PO₂ based bath without pre-functionalization had high weight % compared to the Pd electroless plating employing NaH₂PO₂ based bath pre-functionalized with γ -APTES.

4: Chapter Four

Table 4.3: EDS Data for $AB_5_NaH_2PO_2_Pd$ without Functionalization and $AB_5_NaH_2PO_2_Pd$ with Functionalization with γ -APTES

Element	Reducing agent	Weight %	Atomic %
Pd	NaH_2PO_2	31.08	1.95
Pd	NaH_2PO_2 with γ -APTES	10.24	7.57

4.6.3 Total Determination of Pd Content Deposited on the Surface of AB_5 MH Alloy Functionalized with γ -APTES Using AAS

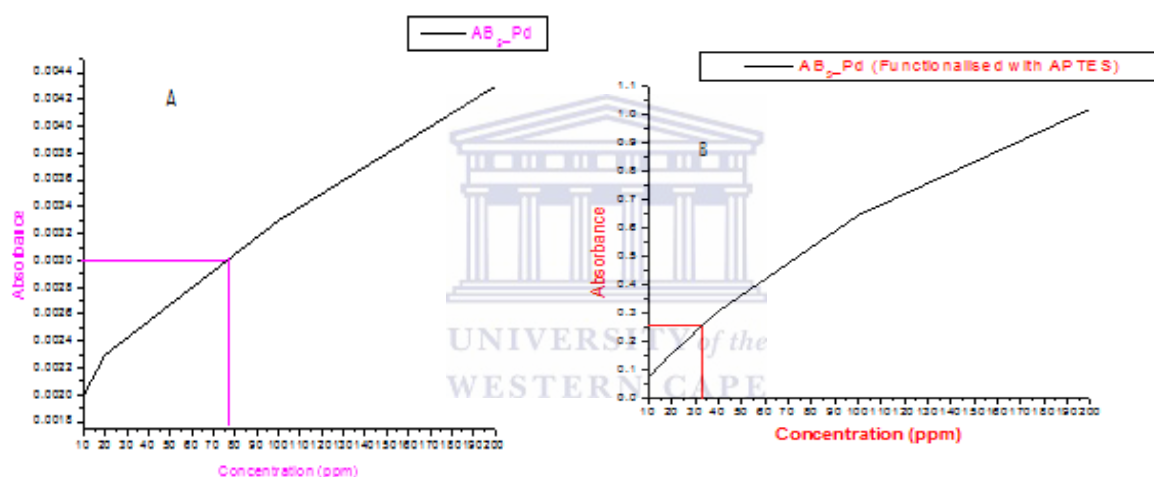


Figure 4.18: Shows AAS Spectrum of a) AB_5_Pd without functionalization and b) AB_5_Pd functionalized with γ -APTES

AAS was used to determine the total elemental content of the deposited layers Pd on the AB_5 alloy as a function of unit weight of the surface modified samples. Results obtained were plotted and extrapolated (see Appendix A3) and **Figure 4.18 a)** shows the total amount of Pd in the AB_5 sample without pre-functionalization ranged from 0.75wt% to 0.80wt%. **Figure 4.18 b)** shows the total amount of Pd in the AB_5 sample pre-functionalized with γ -APTES range between 0.30wt% to 0.35wt%.

4: Chapter Four

4.6.4 Surface Morphologies of AB₅ MH Alloy Functionalized with γ -APTES

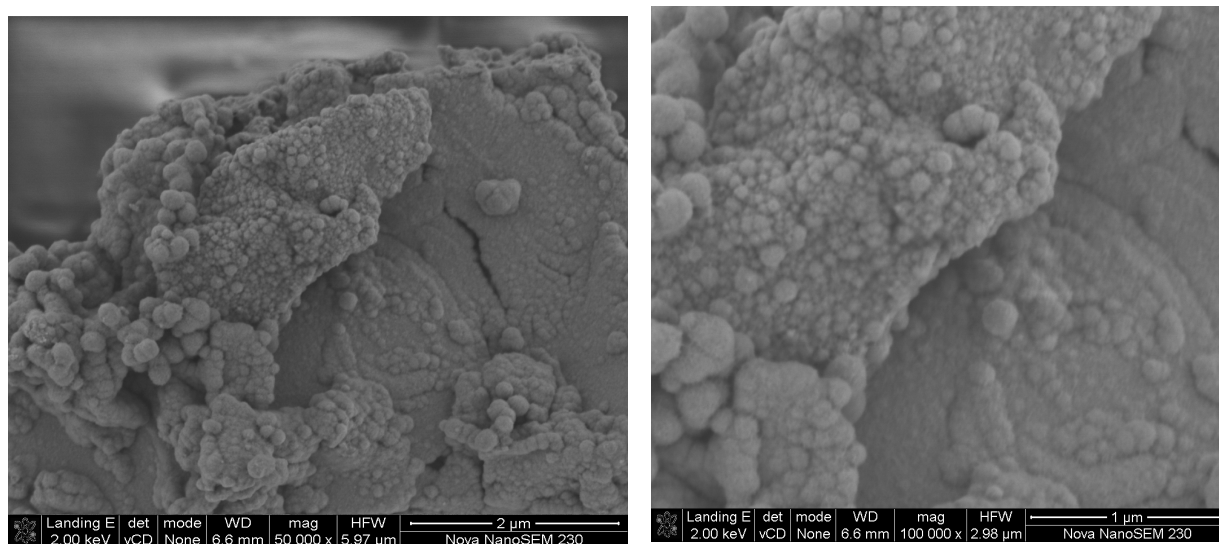


Figure 4.19: Show SEM images of AB₅_Pd (Functionalized with γ -APTES)

The quality of the Pd coatings after pre-functionalization in γ -APTES was compared to the Pd surface particles observed on AB₅ MH alloy surface modified without pre-functionalization (**Figure 4.19**). However, significant amounts of Pd agglomerates were observed after pre-functionalization in γ -APTES, which was not clearly seen in the sample modified without pre-functionalization. Interestingly, the dendrite structure previously observed between Pd particles where the alloy was pre-treated with γ -APTES, were not featured on the surface of the alloy without γ -APTES solution pre-functionalization. The pre-treated alloy with γ -APTES shows uniform deposition, showing that pre-functionalization with γ -APTES improved the deposition of Pd layers on the surface of the alloy electrode.

4: Chapter Four

4.6.5 Electrochemical Characterization of AB₅ MH Alloy Functionalized with γ -APTES using Galvanostatic Charging/discharging Cycles

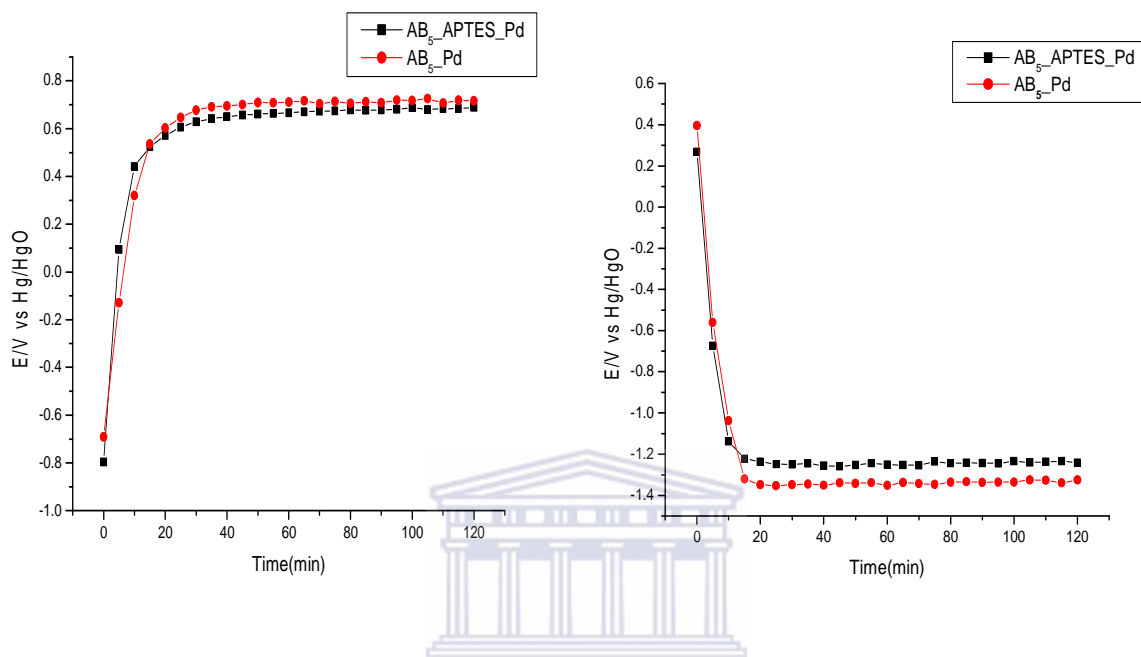


Figure 4.20: Shows 10th cycle for charge and discharge for AB₅NaH₂PO₂Pd without pre-functionalization and AB₅NaH₂PO₂Pd pre-functionalized with γ -APTES

Figure 4.20 shows charge/discharge potential versus time profiles obtained for the two electrodes at the 10th cycle. In each case, well defined charge/discharge plateaus are observed. The MH electrode without pre-functionalization with γ -APTES shows a high charge over-potential. While, the modified electrode pre-functionalized with γ -APTES presents lower discharge potentials values (i.e. more negative), implying a smaller discharge over-potential or higher specific power for the battery.

4: Chapter Four

4.6.6 Cyclic Voltammetry Characterization of $AB_5_NaH_2PO_2_Pd$ Functionalized with γ -APTES

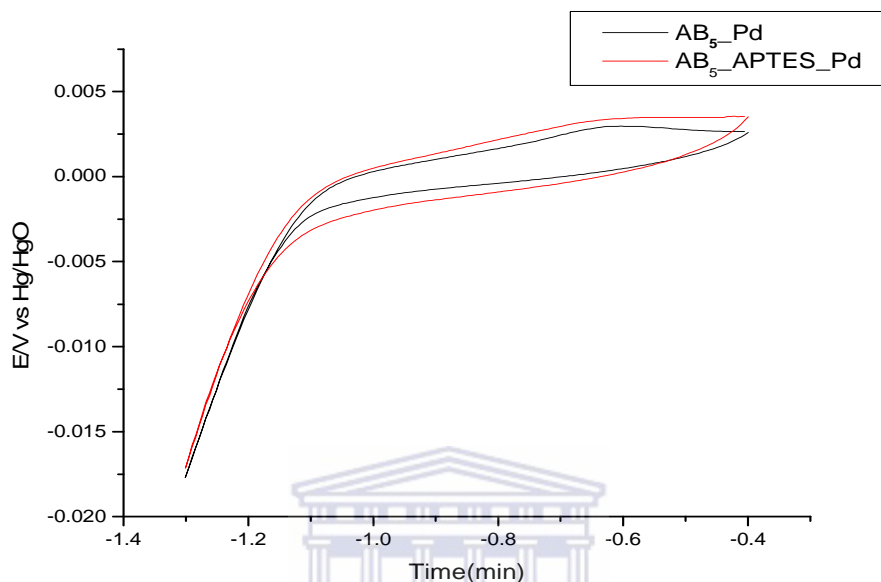


Figure 4.21: Show voltammograms of $AB_5_NaH_2PO_2_Pd$ without pre functionalization and $AB_5_NaH_2PO_2_Pd$ pre functionalized with γ -APTES

The voltammograms show that no electro-reduction current peak was observed, because there were no oxides present on the surface of the electrode, since the CV was applied after the activation of the electrode. Only, the current peaks related to the hydrogen electrode reaction could be detected. The anodic peaks were observed at around -0.65V vs Hg/HgO for the two electrodes as can be seen in **Figure 4.21**. However, the peak was higher for $AB_5_NaH_2PO_2_Pd$ pre-functionalized with γ -APTES compared to $AB_5_NaH_2PO_2_Pd$ without pre-functionalization with γ -APTES. Both electrodes demonstrate sharp anodic peaks, which means oxidation reaction of H_2 on the MH electrode proceeded smoothly. These facts indicate that the surface modification improved the electrochemical activity of oxidation reaction of H_2 on the AB_5 MH electrode surface.

4: Chapter Four

4.6.7 Impedance Characterization of AB₅ MH Electrode Functionalized with γ -APTES

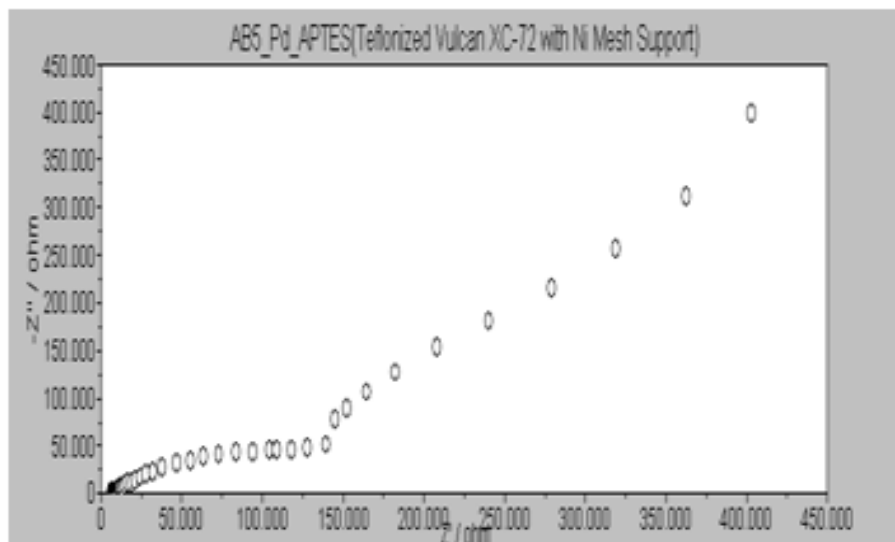


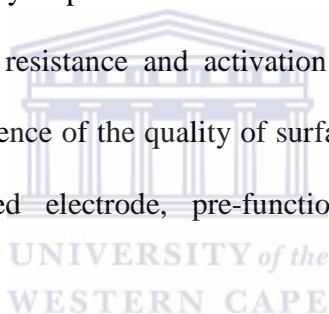
Figure 4. 22: Shows EIS image of AB₅_NaH₂PO₂_Pd pre functionalized with γ -APTES

In **Figure 4.22** the EIS images shows that the electrodes have depressed semicircles, and this may occur because the electrodes have high porosity. This behavior is similar to our earlier findings. The semicircle had resistance of 9.3128 Ω . Exhibiting that the semicircle in high frequency regions for the alloy electrode pre-functionalized with γ -APTES increased, compared to the modified electrode without γ -APTES pre-functionalization as can be seen (**Figure 4.8 c**))12.1061 Ω above. This behavior occurs because the contact resistance decreased after surface modification, because the modified alloy electrodes show less resistance. The resistance obtained from the impedance data was used to calculate the overpotentials and the results were found to be 0.2113V, showing lower values compared to modified electrode without pre-functionalization (c) 0.2724V).

4: Chapter Four

4.7 Summary of AB₅ MH Alloys Functionalized with Aminosilane

An aminosilane functionalization advance method was adopted in the deposition of Pd layers on the surface of AB₅ MH alloy. EDS and AAS showed that after γ -APTES functionalization the Pd surface loading did not increase, but rather decreased as compared to AB₅ without pre functionalization. SEM confirmed the deposition of continuous Pd layer on the surface of the AB₅ after functionalization in γ -APTES. Similarities were observed between the surface modified electrode with and without pre-treatment in γ -aminopropyltriethyosilane solution. In CV, both the alloys show similar anodic peaks around 0.65V. CV and EIS results indicate that the surface modifications apparently improve electrochemical activity on the electrodes surface and decrease the charge transfer resistance and activation of MH electrode reaction. These observations demonstrate the influence of the quality of surface modification on the H₂ sorption kinetics of the surface modified electrode, pre-functionalized with γ -APTES solution.



5: Chapter Five

5. Chapter Five

5.1 Conclusions and Recommendations

5.1.1 Conclusions

The vital purpose of the project was to study the feasibility of direct transformation of low potential heat into electricity, by the application of electrochemical hydrogen storage concentration cells with thermally managed metal hydride electrodes (e.g., Ni-MH battery). Ni-MH batteries have been developed because of the demand for power sources with high energy density, high capacity, long cycle life and excellent environmental compatibility. The characteristics of the battery depends mostly on the physical and chemical properties of the hydrogen storage alloy used as the anode.

In order to achieve MH alloy that exhibited better physical and chemical properties; a methodological advancement was due to successfully develop surface modified hydrogen sorption material, that meet the hydrogenation/dehydrogenation outputs considered to be the requirements for the practical applications of these materials in the electrochemical energy conversion. These requirements included easy activation, fast hydrogen absorption, stability at low temperatures and pressures, and low susceptibility to gaseous impurities.

The experimental assignment and a detailed examination work plan was formulated, in order to address the hypothesis and objectives of the investigation. The standard characterization tools were reviewed and used in the investigation of these materials, and these included Scanning Electron Microscopy (SEM), Energy Dispersive X-Ray Spectroscopy (EDS), Atomic Absorption Spectrometry (AAS), X-ray Diffraction (XRD), Galvanostatic charge/discharge rates, Cyclic Voltammetry (CV), and Electrochemical Impedance Spectroscopy (EIS).

5: Chapter Five

Firstly, AB₅ intermetallic hydrides were chosen as the best candidate materials because they show better hydrogen sorption performance, intermediate thermodynamic properties, and they can withstand exposure to gaseous impurities. The drawback to the use of the AB₅ intermetallic was that, they naturally form oxide film on their surfaces which hinders hydrogen uptake by the alloy material. Platinum group metals were deposited on their surfaces, since they are known to increase the electrocatalytic activity, activation, and improves the hydrogen sorption performance of the MH alloys. Platinum and Palladium catalyst were investigated, and the one which demonstrated better performance was chosen.

Electroless deposition technique was considered for plating the PGM catalyst on the surface of the AB₅ intermetallic material. This technique was chosen because, it posses the ability to plate metal surface layers on materials with irregular shape, ability to control the surface chemistry of the modified material and deposition of homogeneous coatings.

The effect of reducing agent on the surface of the MHE alloy was investigated, comparing hydrazine and sodium hypophosphite. Functionalization with γ -amisopropyltriethosilane prior electroless deposition of Pd on the surface of the AB₅ type intermetallic was also undertaken.

From the results collected in chapter 4, characterization of the surface modified sample material was completed and is summarized below:

1. Commercial AB₅ alloy obtained from Guangzhou Research Institute for Non-Ferrous Metals, China with composition La_{0.4} Ce_{0.48} (Nd, Pr)_{0.16} Ni_{3.34} Co_{0.64} Al_{0.63} Mn_{0.58} trade mark DH₄ was employed as the parent material for the investigation. The results showed that the alloy presents hexagonal CaCu₅ –type structure of symmetry P6/mmm. No extra phases were observed evidencing that the structure is a single phase. The lattice

5: Chapter Five

parameters were measured and found to be $a=4.9966$ and $c=4.0473$. AB_5 alloys surface modified with Pt and Pd and other pre-functionalized without γ -APTES, showed that the crystal symmetry was the same for these material as with the master alloy. The position of the diffraction peaks for the modified material did not significantly change. The lattice parameters were also the same. Presence of the PGM on the alloy surfaces was not observed.

2. Direct determination of the Pd particles distribution on the surface of the AB_5 MH alloy was conducted using SEM. Micrographs collected for the AB_5 -type alloys surface modified with Pt and Pd using NaH_2PO_2 electroless plating baths, showed crystalline Pd layers on the AB_5 -type alloy surface were found to be discontinuous. A rich coating of Pd was clearly observed compared to the Pt on the surface of AB_5 modified alloy.

Investigating the effect of N_2H_4 and NaH_2PO_2 reducing agents on the deposition quality. The results also showed that Pd layers were discontinuous on the surface of the alloy, and NaH_2PO_2 based bath gave fairly good dispersion on the surface of the AB_5 -type alloy compared to N_2H_4 based bath.

The quality of the Pd coatings after pre-functionalization in γ -APTES was compared to the Pd surface particles observed on AB_5 MH alloy surface modified without pre-functionalization. The pre-treated alloy with γ -APTES shown uniform deposition, showing that pre-functionalization with γ -APTES improved the deposition of Pd layers on the surface of the alloy electrode.

5: Chapter Five

3. Quantitative determination of the surface loading of the of metal catalyst was done using EDS. Alloy surface modified with Pd catalyst exhibited better deposition weight % as compared to Pt modified, results are as follows Pt (13.41wt%) and Pd (31.08wt%), respectively. The results were confirmed with AAS, Pt ranged(0.11-0.15wt%), Pd (0.75-0.80wt%).

Determination of Pd on the surface of AB₅ MH alloy modified with application of N₂H₄ and NaH₂PO₂ reducing agents, displayed that the use of NaH₂PO₂ gave better loading with AB₅_N₂H₄_Pd showing very small amounts 0.83wt%, compared to 31.08wt% of AB₅_NaH₂PO₂_Pd alloy. With AAS results were AB₅_N₂H₄_Pd (0.10-0,15wt%) and AB₅_NaH₂PO₂_Pd (0.75-0.80wt%) showing similar results to the above findings.

Lastly, comparing the total loading of AB₅ alloy pre functionalized with γ -APTES prior Pd electroless deposition and one without pre functionalization. The results demonstrated that Pd deposition without pre-functionalization had high weight % compared the alloy pre functionalized with γ -APTES.

4. Electrochemical characterization of the AB₅ alloy material was performed to investigate the effect of the addition of polycrystalline Pd and Pt powders into the hydride forming metal alloys electrode, effect of using different reducing agents for Pd electroless plating on the surface of the electrode, and functionalization of the alloy surface with γ -APTES prior Pd electroless deposition on the alloy surface. The investigation was based on the activation, cycle stability, and H₂ sorption characteristics of the alloy. These factors were

5: Chapter Five

examined employing charge/discharge galvanostatic, cyclic voltammetry and impedance spectroscopy characterization techniques.

Based on the results, it was concluded that electroless plated Pd and Pt MH alloy electrodes had better performance compared to AB₅ MH electrode. However, Pd showed more interesting results compared to Pt. Pd and Pt coated alloy electrodes represented lower discharge overpotentials, which is important to improve the battery performance. It was found that deposition of Pd and Pt improved the catalytic activity of charge/discharge, a dynamic exclusively connected to a higher active area of the coated layer, since the values of the apparent activation energy are higher for the coated samples. Pd was chosen as the better catalyst for the modification of AB₅ alloy.

Influence of reducing agent (*i.e.*, N₂H₄ and NaH₂PO₂) on the morphological and kinetic properties of the AB₅ alloy, surface modified with Pd was investigated. As seen from results surface modification significantly decreased the charge transfer resistance and activation of the electrode reaction on the surface. Modification increased the larger specific area of the electrode, and made the alloy form a Ni-rich layer surface with electrocatalytic activity on the surface. Consequently, the activation for dissociation of H₂O was decreased. CV and EIS findings specified that the surface modifications apparently improved electrochemical activity on the electrodes surface and decreased the charge transfer resistance and activation of MH electrode reaction. Based on the results, it was concluded that Pd electroless plated using NaH₂PO₂ reducing agent had better performance than electroless plating using N₂H₄ as reducing agent.

5: Chapter Five

Aminosilane functionalization method was adopted in the deposition of Pd layers on the surface of AB₅ MH alloy. CV and EIS results indicate that the surface modifications apparently improved electrochemical activity on the electrodes surface and decreased the charge transfer resistance and activation of MH electrode reaction. These observations demonstrated the influence of the quality of surface modification on the H₂ sorption kinetics of the surface modified electrode, pre-functionalized with γ -APTES solution.

In conclusion, surface modification of the AB₅ alloy with PGMs improved electrochemical activity on the electrodes surface and decreased the charge transfer resistance and activation of MH electrode reaction. The following observations were made: Pd exhibit better performance than Pt catalyst, NaH₂PO₂ is a better reducing agent for Pd electroless deposition than N₂H₄, and electrodes surface modified with γ -APTES pre functionalization displayed inconsistent results. The effect of pre functionalization with γ -APTES needs to be further investigated. As can be seen from the results, alloy electrode surface modified with Pd employing NaH₂PO₂ as reducing agent, gave better performance than all other alloys, and in conclusion it was found as a suitable anode for Ni-MH batteries.

5.2 Recommendations

Based on the analysis and conclusions of the study, a number of suggestions regarding priorities for the future search areas of investigation are given below.

Ni-MH battery development should achieve high power output and, long term stability is important for practical application. Optimization of the MH alloy preparation and surface

5: Chapter Five

modification procedure will be required for successful commercialization of the alloy in the battery industry. From this fundamental point of view it would be interesting to produce MH surfaces with smaller particle size, so that one can explore the effect of:

- deposition time (e.g., AB₅(DH₄)Pd-P - 1 to 30 minutes)
- catalyst concentration (e.g., AB₅(DH₄)Pd-P deposited for 30min – 0.1 to 2g/L), and
- reducing agent concentration (i.e., NaH₂PO₂).

These effects stated above can be investigated employing electrochemical characterization techniques Galvanostatic charging/discharging, Cyclic Voltammetry and Electrochemical Impedance Spectroscopy.



6: Bibliography

Bibliography

1. J. Miliken, F. Joseck, M. Wang, E. Yuzugulla, *Journal of Power Sources* 172(2007)131-31.
2. B. Choi, S. Lee, K. Kawai, C Fushimi, A Tsutsumi, *International Journal of Hydrogen Energy* 34(2009)2058-2061.
3. http://healthmad.com/health/nuclear_energy_and_health_hazards/
4. P.P. Edwards, V.L. Kuznetsov, W.I.F. David, *Philosophical Transactions of the Royal Society*, A 365(2007)1043-1056.
5. http://en.wikipedia.org/wiki/Primary_cell.
6. http://en.wikipedia.org/wiki/Rechargeable_battery.
7. Gates Energy Products. *Rechargeable Batteries Application Handbook*, Butterworth-Heinenenn Publishers (1998).
8. J. C. Salamone, *Concise Polymeric Materials Encyclopedia*, CRC Press (1998)88.
9. E. Baker, H. Chon, J. Keisler, *Technological Forecasting and Social Change* 77(2010)1139-1146.
10. G. Deng, Y. Chen, M. Tao, C. Wu, X. Shen, H. Yang, M. Lui, *International Journal of Hydrogen Energy* 34(2009)5568-5573.
11. X. Yuan, N. Xu, *Journal of Alloys and Compounds* 316(2001)113-117.
12. N. Furukawa, *Current Opinion in Solid state and Material Science* 1(1999)378-382.
13. D. Chartouni, F. Meli, A. Zuetzel, K. Gross, L. Schalpback, *Journal of Alloys and Compounds* 241(1996)160.
14. N. Kuriyama, T. Sekai, H. Miyamura, I. Uehara, H. Ishikawa. *Journal of Alloys and Compounds*.

6: Bibliography

15. F.A. Ghafir, M.F.M. Batcha, V.R. Raghvan, *International Journal of Hydrogen Energy* xxx(2008)2.
16. M. Suilma, F. Valverde, *Hydrogen as Energy Source to Avoid Environmental Pollution* 41(2002)223.
17. <http://www.h2-economy.com/compressed-hydrogen.html> (2005).
18. V.P. Utgikar*, T. Thiesen. *Technology in Society* 27(2005)315-320.
19. L. Becker. *Hydrogen Storage* (2001).
20. http://kuzwe.com/images/hydrogen_cycle.gif. (2008).
21. Dr. B. Darren, *Hydrogen Storage Materials and the Characterization of their Hydrogen Sorption Properties*, SciTopics Research Summaries by experts (2009).
22. I.P. Jain, *International Journal of Hydrogen Energy* (2009)5.
23. F. Bittner, C.C Badcock, *Journal of the Electrochemical Society* 130(1983)193C.
24. J.J.G Willemse, K.H.J. Buschow, *Journal of the Less-Common Metals* 129(1987)14.
25. K.J. Gross, K.R. Carrington, S. Barcelo, A. Karkamkar, Purewal, P. Parilla, *Recommended Best Practices for the Characterization of Storage Properties of Hydrogen Storage Materials* (2009) v2-64 U.S.D.O.E. Hydrogen Program document.
26. J. J. Vajo, F. Mertens, C .C. Ahn, R.C. Bowman, Jr., B. Fultz, *Physical Chemistry*, B108(2004)13977-13983.
27. C. Ku. *Carbon Nanotubes for Hydrogen Storage* (2002).
28. Technical University of Denmark (<http://www.w.materiale.kemi.dtu.dk/hydrider>).

6: Bibliography

29. P.P. Edwards, V.L. Kuznetsov, W.I.F. David, N.P. Brandon, *Energy Policy* 36(2008)4356-4362)
30. L.O. Valoen, *Metal Hydrides for Rechargeable Batteries*, Ph.D. Thesis, Norwegian University of Science and Technology, Norway (2000)19.
31. T.J. Carter, L.A. Cornish, *Engineering Failure Analysis* 8(2001)113-121.
32. T. N. Veziroglu, S. Y. Zaginaichenko, D.V. Schur, B. Baranowski, A.P. Shpak and V.V. Skorokhod, *Hydrogen Material Science and Chemistry of Carbon Nanomaterials* 172(2003)88.
33. A. Zuttel, Materials for Hydrogen Storage, *Materials Today* (2003)24-3.
34. G. Sandrock, series E: *Applied Science Hydrogen-Metal System* 295(1994).
35. M. Kanda, M Yamatoto, K Kanno, Y. Satoh, H. Hayashida, M. Suzuki, *Journal of the Less-Common Metals* 172-174(1991)1227.
36. T. Sakai, H Miyamura, N Kuriyama, H Ishikawa, I Uehara, *Journal of Physical Chemistry* Z.183(1994)333.
37. A. Anani, A. Visintin, S. Srinivasan, A.J. Apleby, H.S. Lim, *Journal of Electrochemical Society*.139(1992)985.
38. B. Paxton, J Newman, *Journal of Electrochemical Society* 144(1997)3818.
39. G. Benczur-Urmossy, B. Dom, K. Wiesener, C.F. In: Holmes, A.R. Landgrebe, *Batteries for portable applications and electric vehicles*. The Electrochemical Society proceeding series NJ: Pennington. 18 (1997)97.
40. C. Orion, MI. *Considerations for the Utilization of Ni-MH Battery technology in Stationery Applications*.
41. P.R. Gifford, M.A. Fetccenco, S. Venkatesan, D.A. Corringan, A. Holland, S.K. Dhar, S.R. Ovisinky, In. P.D. Bennet, T. Sekai, Ed, *The electrochemical Society Incorporation* 94-27(1994)353-369.

6: Bibliography

42. F. Feng, M. Geng, D.O. Northwood, *International Journal of Hydrogen Energy* 26(2001)726.
43. M. Latroche, J. Rodriguez-Carvajal, A. Pecheron-Guegan, F. Bouree-Vigneron, *Journal of Alloys and Compounds* 18(1995)63.
44. B.A Kolachev, *Properties of Hydrogen Storage Alloys*. No6 26(1990)38.
45. M. Fahmi, A. Ghafir, M.F.M. Batcha, V.R. Raghvan, *International Journal of Hydrogen Energy* (2008)2.
46. Y. Yurum, *Hydrogen Energy System: Production and Utilization of Hydrogen and Future Aspects*, Atlantic Treaty Organization, Scientific Division.
47. S. Futjitani, I. Yonezu, T. Saito, N. Furukawa, E. Akiba, H. Hayakawa, S. Ono, *Journal of the Less-common Society* 172-174(1991)220.
48. J.L. Murray. *Binary Alloy Phase Diagrams*, 2nd Edition, T.B. Massalski, ASM International, Materials Park , Ohio. 3(1990)2615-2617.
49. Y.Y. Pan, P. Nash, *Binary Phase Diagrams*, 2nd Edition, T.B. Massalski, ASM International, Material Park, Ohio 3(1990)2406-2408.
50. V.A. Robert, C.Tomasz, Zbgneiw, *Nanomaterials for Solid State Hydrogen Storage*, Springer(2008)13.
51. T. Vogt, J.J. Reilly, J.R. Johnson, C.D. Adzic, J. McBreen, *Journal of Electrochemical Society* 146(1999).
52. J.J. Willems, *Philips Research Journal of Reports* 39(1984) Suppl 1.
53. F. Meli, A. Zuttel, L. Schlapbach, *Journal of Alloys and Compounds* 17(1992)19.
54. J.F. Lynch, J. J. Reilly, *Journal of Less-common Metals*, 87(1982)225-226.
55. D. Noreus, L. G. Olsson, P. –E. Werner, *Journal of Physics F*, 13F(1983)715-727.
56. H. Kaiya, T. Ookawa, *Journal of Alloys and Compounds* 231(1995)598-603

6: Bibliography

57. A. Durairajan, B.S. Haran, B.N. Popov, R.E. White, *Journal of Power Sources* 83(1999)114
58. S. Srinivasan, *Fuel Cells: from fundamentals to applications*, Springer (2006)162
59. B. Laura, *Hydrogen storage* (2001)
60. S. Billur, F. Lamari-Darkim, H. Michael, *International Journal of Hydrogen Energy* (2007)32
61. D.B. Willey, I.R. Harris, A.S. Pratt, *Journal of Alloys and Compounds* 293-295(1999)613-620.
62. A.S. Pratt, D.B. Willey, I.R. Harris, *Platinum Metals Review* (2)43(1999)50-58.
63. L. Zaluski, A. Zaluki, P. Tessier, J.O Strom-Olsen, R. Schultz, *Journal of Alloys and compounds* 217(1995)295.
64. X. Xu, C. Song, *Applied Catalysis A: General* 300(2006)130-138.
65. C.R.K. Rao, D.C. Trivedi, *Coordination chemistry Reviews* 249(2005)613-631.
66. G.O. Mollory, J.B. Hajdu. *Electroless Plating- Fundamentals and Applications*, New York, William Andrew Publishing/Noyes 16(1990)1.
67. W. Riedel. *Electroless Nickel Plating*, ASM International/Finishing Publications Ltd(1991)14.
68. P. Steinmetz, S. Alperine, A. Friant-Contantine, P.Josso, *Surface and Coatings Technology* 43/44(1990)500-510.
69. L.Xu, J.Liao, L.Huang, D.Ou, Z. Guo, H. Zhang, C. Ce, N. Gu, J. Liu, *Thin Solid Films* 434(1-2)(2003)121-125.
70. M. Williams, A.N. Nechaev, M.V. Lototsky, V.A. Yartys, J.K. Solberg, R.V. Denys, C. Pineda, Q. Li, V. M. Linkov, *Material Chemistry and Physics* 115(2009)136-141.

6: Bibliography

71. D Barsellini, A. Visintin, W.E. Triaca, M.P. Soriaga, *Journal of Power Sources* 124(2003)309-313.
72. X. Changrong, G. Xiaoxia, L. Fanqing, P. Dingkun, M. Guangyao, *Colloids and Surfaces A: Physicochemical and Engineering Aspects* 179(2001)229-235.
73. D.H. Cheng, X.Y. Xu, Z.Y. Zhang, Z.H. Yiao, *Metal Finishing* (1997)
74. D.F. Shriver, P.W. Atkins. *Inorganic Chemistry*, New York, W.H. Freeman and Co.
75. http://serc.carleton.edu/research_education/geochemsheets/techniques/XRD.html.
76. P.W. Atkins. *Physical Chemistry New York*, Freeman and Co.
77. G. Perego, *Catalysis Today* 41(1998)251-259.
78. http://en.wikipedia.org/wiki/Scanning_electron_microscope.
79. I.A.S. Edwards. *Structure in Carbons and Carbon Forms*. In Marsh, H(Ed) Introduction to Carbon Science. London. Butterworths (1989).
80. <http://www.sdm.buffalo.edu/scic/sem-eds.html>.
81. <http://www.semitracks.com/index.php/en/reference-material/failure-and-yield-analysis/materials-characterization/eds>.
82. http://en.wikipedia.org/wiki/Energy_dispersive_X-ray_spectroscopy.
83. <http://www.highbeam.com/doc/1G2-3448300210.html>.
84. http://wiki.answers.com/Q/Principle_of_atomic_absorption_spectroscopy.
85. B. Welz, M.R. Sperling. *Atomic Absorption Spectrometry*, Chichester, Wiley-VHC(1999).

6: Bibliography

86. L. Ebdon, E.H. Evans. *An Introduction to Analytical Atomic Spectrometry*, Chichester, Wiley (1998).
87. J.M. Blackman. *High Pressure Hydrogen Storage on Carbon Materials for Mobile Applications* (Thesis) April 2005 University of Nottingham.
88. A.J. Bard, L.R. Faulkners. *Electrochemical Methods, Fundamentals & Applications*, Wiley. NY(2001)227.
89. A.J. Bard, L.R. Faulkners. *Electrochemical Methods, Fundamentals & Applications*, Wiley. NY(2001)227.
90. I. Paseka, *Applied Catalyst*, A. Gen 207 (2001) 254.
91. T. Kambara, I. Tachi. *Chronopotentiometry-Stepwise Potential-Time Curves for an Arbitrary number of Reducible Species* 61(1957)1405-1407.
92. <http://iopscience.iop.org/0022-3735/3/1/316/pdf/jev3ip69.pdf> An Apparatus for cyclic-chronopotentiometry in non-aqueous solvents 1970 Journal of Physics.E:Sci.Instrum3 69.
93. P.J. Lingane, D.G. Peters, *Critical Reviews in Analytical Chemistry* 1(4)(1971)587-634.
94. K. Tsukada. F. Kobayshi, H. Arai, T. Kiwa, *Electrochemistry Communications* 10(2008)938-942.
95. http://en.wikipedia.org/wiki/Cyclic_voltammetry.
96. A.S. Hamdy, E. El-Shenawy, T. El-Bitar, *International Journal of Electrochemical Sciences* 1(2006) 171-1.
97. L.O. Valoen, R. Tunold, *Journal of Alloys and Compounds* 330-332(2002)810-815
98. http://acs.expoplanner.com/files/acsspringlo/ExhibFiles/1037.2796_EIS300.pdf.

6: Bibliography

68. P. Steinmetz, S. Alperine, A. Friant-Costantine, P. Josso. *Surface Coatings technology* 43/44(1990)500-510.
99. <http://mse.iastate.edu/microscopy/whatsem.html>, (2005).
100. A. Visintin, C.A. Tori, G. Garaventa, W.E. Triaca, *Journal of Electrochemical Society* 145(1998)4169.
101. M.V.C. Sastri, B. Viswanathan, S.S. Murthy, *Metal Hydrides. Fundamentals and Applications*, Springer Verlag, Berlin (1998).
102. A. Visintin, W.E. Triaca, A.J. Arvia, H. Peretti, J.C. Bolcich, W. Zhang, S. Srinivasan, A.J. Appleby, Investigation of a new modified AB₅ type alloy for nickel-metal hydride batteries, Hydrogen Energy Progress XI, Proceedings of the 11th. World Hydrogen Energy Conference, Stuttgart, Germany, 23-28 June 1996, (Eds. T.N. Veziroglu, C.J. Winter, J.P. Baselt and G. Kreysa, IAHE), 2(1996)1983-1988.
103. R.C. Ambrosio, E.A. Ticianelli, *Surface & Coatings Technology* 197(2005)215-222.
104. A. Visintin, E.B. Castro, S.G. Real, W.E. Triaca, C. Wang, M.P. Soriga, *Electrochimica Acta* 51(2006)3658-3667.
105. M. Raju, M.V. Ananth, L. Vijavaraghan. *Electrochimica Acta* 54(2009)1368-1347.
106. A. Visintin, C.A. Tori, G. Garaventa, W.E. Triaca, *Journal of the Brazilian Chemical Society* 8(2)(1997)125-129.
107. S. Cheng, J. Zhang, M. Zao, C. Cao, *Journal of Alloys and Compounds* 293(1999)814-820.
108. X. Shan, J.H. Payer, J.S. Wainright, *Journal of Alloys and Compounds* 430(2007)262-268.
109. L. Zaluski, A. Zaluska, P. Tessier, J.O. Strum-Olsen, R. Schulz, *Journal of Alloys and Compounds* 217(1995)295-300.
110. A. S. Pratt, D.B. Willey, I.R. Harris, *Platinum Metals Review* 43(2)(1999)50-58.

6: Bibliography

111. M.L. Doyle, I.R. Harris, A.S. Pratt, D.B. Willey, *United States Patents* (2000)6,165,643.

112. M. Williams, C. A. Pineda-Vargas, E.V. Khataibe, B. J. Bladergroen, A.N. Nachaev, V.M. Linkov, *Applied Surface Science* 254(2008)3211-3219.



7: Appendix

Appendix A

1: Atomic Absorption Spectroscopy (AAS) Results (AB₅_NaH₂PO₂_Pt)

Absorbance	Concentration (ppm)
0.001	1
0.002	5
0.003	10
0.004	20
0.015	50
0.040	100

Sample (AB₅_NaH₂PO₂_Pd) = 0.002

2: Atomic Absorption Spectroscopy (AAS) Results (AB₅_NaH₂PO₂_Pd)

Absorbance	Concentration (ppm)
0.0020	10
0.0023	20
0.0033	100
0.0043	200

Sample (AB₅_NaH₂PO₂_Pd) = 0.003

7: Appendix

3: Atomic Absorption Spectroscopy (AAS) Results ($AB_5-N_2H_4-Pd$)

Absorbance	Concentration (ppm)
0.075	10
0.156	20
0.305	40
0.645	100
1.018	200

Sample ($AB_5-N_2H_4-Pd$) = 0.084

($AB_5-NaH_2PO_2-Pd$) pre-functionalized with γ -APTES = 0.251

